UNIVERSITY OF CRETE

DEPARTMENT OF CHEMISTRY

GENERAL POSTGRADUATE PROGRAMME

LABORATORY OF BIOINORGANIC CHEMISTRY

In collaboration with:

Laboratoire de Chimie et Biologie des Métaux,
SolHyCat Group, Université Grenoble Alpes
GRENOBLE, FRANCE

Master of Science Thesis

Synthesis and physicochemical characterization of new catalysts and photosensitizers

Giannoudis Emmanouil

Supervisor: Athanassios G. Coutsolelos

Heraklion, June 2017

ΠΑΝΕΠΙΣΤΗΜΙΟ ΚΡΗΤΗΣ
ΤΜΗΜΑ ΧΗΜΕΙΑΣ

ΓΕΝΙΚΟ ΜΕΤΑΠΤΥΧΙΑΚΟ ΠΡΟΓΡΑΜΜΑ

ΕΡΓΑΣΤΗΡΙΟ ΒΙΟΑΝΟΡΓΑΝΗΣ ΧΗΜΕΙΑΣ

Σε συνεργασία με:
Εργαστήριο Χημείας και Βιολογίας Μετάλλων,
Ομάδα SolHyCat, Πανεπιστήμιο Γκρενόμπλ-Αλπέων

ΜΕΤΑΠΤΥΧΙΑΚΟ ΔΙΠΛΩΜΑ ΕΙΔΙΚΕΥΣΗΣ

Σύνθεση και φυσικοχημικός χαρακτηρισμός νέων καταλυτών και φωτοευαισθητοποιητών

Γιαννούδης Εμμανουήλ

Υπεύθυνος καθηγητής: Αθανάσιος Κουτσολέλος

Ηράκλειο, Ιούνιος 2017

Examination Committee

Athanassios G. Coutsolelos
Professor, Department of Chemistry, University of Crete

Constantinos J. Milios
Professor, Department of Chemistry, University of Crete

Murielle Chavarot-Kerlidou
CNRS Senior Scientist, LCBM, Université Grenoble Alpes

To my beloved ones….

Acknowledgments

This master thesis began in the laboratory of Bioinorganic Chemistry of Chemistry Department at the University of Crete under the supervision of Professor Athanassios G. Coutsolelos. I would like to thank him for his continuous support during the 2 years that I was in his group. His encouragement, his advice strengthened me to complete this thesis in success. He gave me the opportunity to interact with amazing people during all these years.

Part of this thesis was carried out in Grenoble, France and particularly in the SolHyCat group at the Laboratoire de Chimie et Biologie des Métaux, under the supervision or Dr. Murielle Chavarot Kerlidou. I am really grateful for everything that you did for me the 3 months that I was working with you. You were always by my side. Almost every day, we had discussion about my project and always with smile you tried to fix my problems. I will never forget your help that made my staying in Grenoble an unforgettable experience. I owe a big thanks to Dr. Vincent Artero for accepting me to work in his group and the assistance that he gave me to complete my project. I hope that in the future we will collaborate again.

Also, I owe a big thanks to Assistant Professor Pascal Guillo from the University of Toulouse, who synthesized the cobalt and nickel complexes and for the interaction that we had during this project.

I would like to acknowledge Assistant Professor Constantinos J. Milios for approving to be part of my examination committee and his valuable comments on this thesis.

I would like also to thank the members of Bioinorganic group for their support, friendship and great moments that we had. Altogether, we have created a pleasant working environment. I believe that we will have the same relationship throughout the years.

I could not forget the members of SolHyCat group for welcoming me in their team. They made me feel like my home with their company and backing. I hope that we will meet again in Greece or in their home countries.

Last but not least, I would like to thank my parents, my brother and my friends for their love, encouragement and support during all these years. Without them, I could not have the chance to complete this thesis. Thank you for everything and for being with me all these years.

Abstract

It is well known that our environment is changing day by day. The human activity has caused enormous environmental problems, especially the last decades. Pollution of air, water, global warming are some examples of the problems that have been created and the impact on humans are catastrophic (healthy issues, etc.). Energy is the most important tool of modern communities in order to facilitate their daily life. Energy is incident to fossil fuels that cause most of the environmental problems. This fact along with their depletion due to their continuous use has forced the scientific community to find clean and abundant sources of energy. Although hydrogen has some drawbacks such as its storage, it could be a solution and especially its production using water and sunlight. The splitting of water produce hydrogen and oxygen. Nature is able to do this, using sunlight as energy source, a natural process called photosynthesis. Scientists try to mimic the basic mechanisms of photosynthesis, a field of research called artificial photosynthesis, and apply them to catalysis in order to produce hydrogen from water and sunlight. Photocatalysis is one of the most promising ways to produce clean hydrogen. The photocatalytic hydrogen production from aqueous protons constitutes the reductive side of water splitting. Each photocatalytic system, contains three essential components. A photosensitizer that absorbs light, a catalyst that receives the excited electron from the photosensitizer, a sacrificial electron donor that feeds the photosensitizer with electrons and many times an electron relay that facilitates the electron transfer.

In the present study, we report novel photocatalytic systems for hydrogen evolution. The first systems consist of tin porphyrins as photosensitizers and cobaloximes as catalysts. Porphyrins are excellent chromophores due to their high stability, high absorption in the visible region and their long life time in their excited states. Cobaloximes are molecular catalysts that are easy to prepare and their cost is low (noble

metal free). In the second part we present systems consisting of triethanolamine (TEOA) as sacrificial electron donor, TiO_2 nanoparticles, porphyrins $[ZnTMPyP^{4+}]Cl_4$ (P1), ZnPCNCOOH (P2) and ZnP(SP)CNCOOH (P3) as photosensitizers and cobaloximes CoN-Methyl-imidazole (C1), CoCNCOOH (C2) and Co(SP)CNCOOH (C3) as catalysts. In the third one, we tested two novel nickel and two novel cobalt complexes as catalysts for hydrogen evolution and make a comparison among them as far as their catalytic activity concerns. We tried to optimize the conditions, using different photosensitizers (fluorescein, $[Ir(ppy)_2(bpy)](PF_6)$, $[ZnTMPyP^{4+}]Cl_4$, $[Ru(bpy)_3]Cl_2$ and different sacrificial electron donors (TEOA, TEA and ascorbic acid). We obtained results for all the complexes using Ir-PS, as SED TEA and mixed aqueous-organic media.

Keywords: porphyrins, cobaloximes, nickel and cobalt complexes, hydrogen evolution, photocatalysis, artificial photosynthesis

Περίληψη

Είναι ευρέως γνωστό ότι το περιβάλλον μας αλλάζει μέρα με τη μέρα. Η ανθρώπινη δραστηριότητα έχει προκαλέσει τεράστια περιβαλλοντολογικά προβλήματα, ιδίως τις τελευταίες δεκαετίες. Η μόλυνση του αέρα, του νερού και το φαινόμενο του θερμοκηπίου είναι μόνο μερικά παραδείγματα προβλημάτων που έχουν δημιουργηθεί και ο αντίκτυπός τους στον άνθρωπο είναι καταστροφικός (προβλήματα υγείας, κτλ.). Η ενέργεια είναι το κυριότερο όργανο των σύγχρονων κοινωνιών ούτως ώστε να διευκολύνουν την καθημερινότητά τους. Η ενέργεια είναι συνυφασμένη με τα ορυκτά καύσιμα που αποτελούν κύρια πηγή των περιβαλλοντολογικών προβλημάτων. Το γεγονός αυτό σε συνδυασμό με την εξάντλησή τους λόγω της υπερβολικής τους χρήσης έχει αναγκάσει την επιστημονική κοινότητα να βρει καθαρές και ανεξάντλητες πηγές ενέργειας. Παρόλο που το υδρογόνο έχει μειονεκτήματα κυρίως λόγω της αποθήκευσής του, θα μπορούσε να αποτελέσει μία λύση και ειδικότερα η παραγωγή του από νερό και ηλιακή ενέργεια. Η διάσπαση του νερού παράγει υδρογόνο και οξυγόνο. Η φύση έχει τη δυνατότητα να το κάνει αυτό χρησιμοποιώντας ηλιακή ακτινοβολία ως πηγή ενέργειας, μια φυσική διαδικασία που ονομάζεται φωτοσύνθεση. Οι επιστήμονες προσπαθούν να μιμηθούν τους βασικούς μηχανισμούς της φωτοσύνθεσης, μια διαδικασία που ονομάζεται τεχνητή φωτοσύνθεση, και να τους εφαρμόσουν στην κατάλυση για την παραγωγή υδρογόνου από νερό και ηλιακή ακτινοβολία. Η φωτοκατάλυση είναι ένας από τους πλέον ελπιδοφόρους τρόπους για παραγωγή καθαρού υδρογόνου. Η φωτοκαταλυτική παραγωγή υδρογόνου από υδατικά πρωτόνια αποτελεί το αναγωγικό κομμάτι της διάσπασης του νερού. Κάθε φωτοκαταλυτικό σύστημα αποτελείται από τρία απαραίτητα συστατικά. Ένα φωτοευαισθητοποιητή που απορροφά το φως, ένα καταλύτη που δέχεται τα διεγερμένα ηλεκτρόνια του φωτοευαισθητοποιητή, ένα θυσιαζόμενο δότη ηλεκτρονίων που τροφοδοτεί με ηλεκτρόνια το φωτοευαισθητοποιητή και πολλές φορές μία αλυσίδα ηλεκτρονίων για να διευκολύνει τη μεταφορά των ηλεκτρονίων.

Στην παρούσα μελέτη, αναφέρουμε νέα φωτοκαταλυτικά συστήματα για παραγωγή υδρογόνου. Τα πρώτα συστήματα αποτελούνται από πορφυρίνους κασσιτέρου ως φωτοευαισθητοποιητές και κοβαλοξίμες ως καταλύτες. Οι πορφυρίνες είναι εξαιρετικά χρωμοφόρα λόγω της υψηλής σταθερότητας, της ευρείας απορρόφησης στην ορατή περιοχή και το μεγάλο χρόνο ζωής της διεγερμένης κατάστασης. Οι κοβαλοξίμες είναι μοριακοί καταλύτες, εύκολοι στην παραγωγή και με χαμηλό κόστος (δεν περιέχουν ακριβά μέταλλα). Στο δεύτερο μέρος παρουσιάζουμε συστήματα αποτελούμενα από τριεθανολαμίνη (TEOA) ως δότης ηλεκτρονίων, νανοσωματίδια οξειδίου του τιτανίου, πορφυρίνες $[ZnTMPyP^{4+}]Cl_4$ (P1), ZnPCNCOOH (P2) και ZnP(SP)CNCOOH (P3) ως φωτοευαισθητοποιητές και κοβαλοξίμες CoN-Methyl-imidazole (C1), CoCNCOOH (C2) και Co(SP)CNCOOH (C3) ως καταλύτες. Στο τρίτο μέρος, εξετάζουμε δύο νέα σύμπλοκα του κοβαλτίου και δύο του νικελίου ως καταλύτες για παραγωγή υδρογόνου και πραγματοποιούμε σύγκριση μεταξύ τους όσον αφορά τη δραστικότητά τους. Έγινε προσπάθεια βελτιστοποίησης των συνθηκών, χρησιμοποιώντας διαφορετικούς φωτοευαισθητοποιητές (fluorescein, $[Ir(ppy)_2(bpy)](PF_6)$, $[ZnTMPyP^{4+}]Cl_4$, $[Ru(bpy)_3]Cl_2$ και διαφορετικούς δότες ηλεκτρονίων (TEOA, τριαιθυλαμίνη-TEA και ασκορβικό οξύ). Είχαμε αποτελέσματα για όλα τα σύμπλοκα χρησιμοποιώντας ως φωτοευαισθητοποιητή το Ir-PS, ως δότη ηλετρονίων TEA σε μίγμα οργανικών και υδατικών διαλυτών.

Λέξεις κλειδιά : πορφυρίνες, κοβαλοξίμες, σύμπλοκα νικελίου κοβαλτίου, παραγωγή υδρογόνου, φωτοκατάλυση, τεχνητή φωτοσύνθεση

Table of Contents

ABBREVIATIONS

PS	Photosensitizer
Cat	Catalyst
m	multiplet
s	singlet
d	doublet
ε	molar absorptivity
eq	equivalents
^{1}H NMR	proton nuclear magnetic resonance
^{13}C NMR	carbon nuclear magnetic resonance
MALDI	matrix assisted laser spray desorption ionization
MW	molecular weight
TOF	time-of-flight
UV-Vis	ultraviolet/visible
ZnP	zinc porphyrin
SnP	tin porphyrin
HEC	hydrogen evolution catalyst
AP	artificial photosynthesis
TON	turnover number
GC	gas chromatography
SED	sacrificial electron donor
Ir-PS	$[Ir(ppy)_2(bpy)](PF_6)$

Chapter 1- Introduction

1. Hydrogen

1.1 Overview

Hydrogen is a chemical element with chemical symbol H with just one proton and one electron and it is the most abundant chemical substance in the universe. The molecule of hydrogen is generally nontoxic, colorless, tasteless and odourless gas. Its name arises from the Greek words hydro for "water" and genes for "forming". Hydrogen makes up more than 90 percent of all of the atoms, which equals three quarters of the mass of the universe.[1] In ionic compounds, hydrogen can take the form of a negative charge (i.e., anion), known as a hydride, or as a positively charged (i.e., cation) species, called proton and denoted by the symbol H^+. Hydrogen plays an important role in acid–base reactions, because most of them involve the exchange of protons between soluble molecules. Hydrogen is essential for life, and it is present in nearly all the molecules in living organisms. The element also occurs in the stars and powers the universe through the proton-proton reaction and carbon-nitrogen cycle.

Although it is the most common element in the universe, it is really rare to be found under the form of dihydrogen H_2 (named hydrogen in the following of the report) in nature. Preferably it is bonded to other elements, such as to oxygen in order to form the most important good of our life, water (H_2O) and many more common compounds such as ammonia (NH_3), methane (CH_4), table sugar ($C_{12}H_{22}O_{11}$), hydrogen peroxide (H_2O_2) and hydrochloric acid (HCl). Obviously hydrogen should be produced from various sources. The first attempt to produce artificially hydrogen was made in the early 1500s by the alchemist Paracelsus that he noted that the bubbles given off when iron filings were added to sulfuric acid were flammable. In 1671 Robert Boyle made the same observation with Paracelsus. Although they both were the first one that produce hydrogen, none took the credits for this discovery. It was Henry Cavendish that first recognized hydrogen as a discrete substance in 1766–81. He later on discovered that hydrogen produces water when burned. Hydrogen took his name by the French chemist Antoine. One more really important discovery was made many years after (1931) by Harold Urey and his colleagues at Columbia University in the USA. In their laboratory

they managed to detect a second, rarer, form of hydrogen. This new type has twice the mass of normal hydrogen, and they named it deuterium.

1.2 Hydrogen as fuel

Our planet is facing many challenges as the years go by. Climate change and rising global demands have created serious environmental problems. Current environmental problems make us vulnerable to disasters and tragedies, now and in the future. The planet is in an emergency and without a change in our way of life the future consequences will be really damaging and probably irreversible. Some of the most significant environmental problems are: pollution, global warming, overpopulation, natural resource depletion, waste disposal, loss of biodiversity, deforestation, ozone layer depletion, acid rain, water pollution. It is undeniable that most of them are caused by human activity. Our goal ought to be a general change in our daily life in order to improve the environment that we live and we will live for centuries. Energy is the most important tool of modern communities in order to facilitate their daily life. Energy is incident to fossil fuels that cause most of the environmental problems. The fact that they will be brought to completion within the next years and the environmental problems that they create due to their combustion (high amounts of CO_2 production), force the scientific community to search for renewable energy sources.[2] Although many efforts have been made, a clean and abundant source of energy that will replace or reduce fossil fuels has not been yet developed. Molecular fuels offer an important option. The most significant characteristic that makes these fuels attractive is the high energy density that can be concentrated within chemical bonds. Hydrogen is considered the fuel of the future.[3,4] The first one that believed that hydrogen could be used as a fuel was not a scientist but a novelist, Jules Verne in his novel ‘L'Île mystérieuse’(**Fig. 1**).

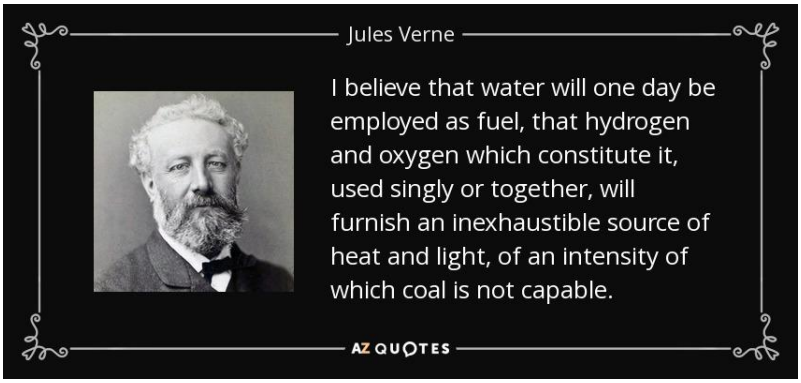

Fig. 1 Jules Verne for use of hydrogen as a fuel.

Hydrogen has many feedbacks as a fuel. The oxidation of hydrogen, by either fuel cell or combustion produces only water. It is practically clean energy source. Basically, H_2 has a high energy density of 120 $MJ.kg^{-1}$ and 1 kg of hydrogen generates three times more energy than 1 kg of gasoline (energy density of 44.4 $MJ.kg^{-1}$), therefore it is much more efficient compared to other energy sources. The most important drawbacks are the storage of hydrogen, the fact that is highly flammable (safety reasons) and it is, until today, expensive to produce hydrogen with the processes that are used.

1.3 Uses of hydrogen

In our days, hydrogen is almost exclusively used for industrial purposes in chemicals and refining. In the figure below (**Fig. 2**) we can see the most common uses of hydrogen. It is observed that almost 80% of hydrogen produced today is used to make ammonia, a crucial ingredient in fertilizer, methanol, a really common solvent with numerous of applications and to remove sulfur from fuel in petroleum refining operations (hydrodesulfurization process). The remainder is used for other chemical processes, for certain glassmaking processes and in the production of plastics and printed circuit boards. It is also widely used for the hydrogenation of vegetable and animal oils and fats. Hydrogen also finds uses in the metallurgy field because of its ability to reduce metal oxides and prevent oxidation of metals in heat treating certain metals and alloys. Liquefied hydrogen has been used primarily as a rocket fuel for combustion with oxygen or fluorine, and as a propellant for nuclear-powered rockets and space vehicles. Because of its lightness, 14 times lighter than air, hydrogen is generally used in weather

balloons by meteorologists. These balloons are fitted with equipment to record information necessary to study the climate.

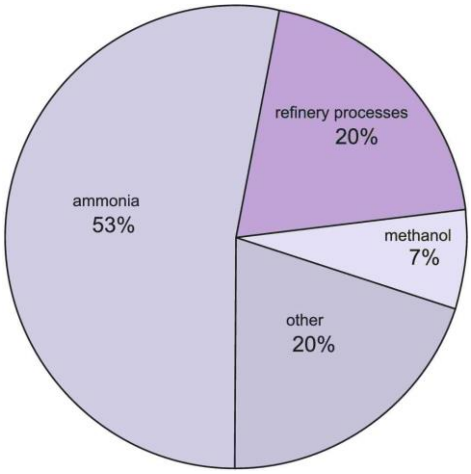

Fig. 2: Most common uses of hydrogen

1.4 Production of hydrogen

Hydrogen can be produced by many different ways.[5] In **Fig. 3** there are the most common sources for hydrogen evolution: natural gas, hydrocarbon, coal, electrolysis and biomass. Thermochemical processes use heat and chemical reactions to release hydrogen from organic materials such as fossil fuels and biomass. Water (H_2O) can be split into hydrogen (H_2) and oxygen (O_2) using electrolysis or solar energy. Microorganisms such as bacteria and algae can produce hydrogen through biological processes.

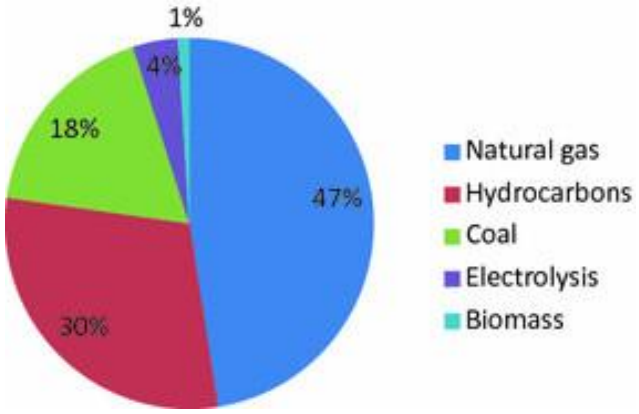

Fig. 3: Sources for hydrogen production

The cheapest source of production of hydrogen until today is from natural gas. The general procedure consists of heating the gas in the presence of steam and a nickel catalyst. The methane molecules are broken up by the exothermic reaction that takes place and then we have the formation of carbon monoxide CO and hydrogen H_2. A following water shift reaction for carbon monoxide takes place that has as a result the production of greater amount of hydrogen. Although the production of hydrogen with this method is really common, the environmental problems that are caused because of the byproducts (CO, CO_2 and other greenhouse gases) makes this process an issue of controversy for the scientific community.

Another common process is charcoal gasification. Charcoal consists mainly of carbon and water. The procedure is realized in a reactor at very high temperatures of almost 1,500 °C. As a result, the charcoal releases gas that separates and reforms to produce hydrogen (H_2) and carbon monoxide (CO). This source of hydrogen is advantageous compared to natural gas since its main product is coal-derived gas which can be used for fuel and many scientific groups try work on this issue.[6,7]

Nowadays, the scientific community tries to find ways friendly for our environment in order to produce hydrogen. The most common processes are from biomass and electrolysis of water. Biomass gasification[8-11] is a technology pathway that uses a controlled process involving heat, steam, and oxygen in order to convert biomass to hydrogen and other products, without combustion as it seems in the reaction below. Because growing biomass removes carbon dioxide from the atmosphere, the net carbon emissions of this method can be low, especially if coupled with carbon capture, utilization, and storage in the long term.

Simplified example reaction

$C_6H_{12}O_6 + O_2 + H_2O \rightarrow CO + CO_2 + H_2$ + other species

1.5 Artificial photosynthesis

This approach has gained important attention the last decades, because through this technique it is avoided the necessity of using electric energy in order to split water. Much more research should be done in order to improve the efficiency of this technique. The use of renewable resources, such as water and sunlight, in order to produce energy

for our demands is a challenging solution. Solar energy that reaches the surface of the Earth each year is almost twice the amount of all non-renewable resources, including fossil fuels and nuclear uranium.[12,13] It is obvious that it is crucial to try to convert solar energy into energy bonds. The conversion of solar energy into chemical energy through the light-driven water splitting produces oxygen and hydrogen, that can be converted into electricity thanks to the fuel cells. Nature is an inspiration of how to make it possible. One of the most famous natural processes, photosynthesis, realizes this conversion daily. The effort to mimic the natural photosynthesis, called 'artificial photosynthesis' has gained great attention for the scientific community, but still remains impossible to achieve the efficiency of natural photosynthesis.[14-16] In nature, there are many organisms that can perform photosynthesis. Algae, cyanobacteria and plants are named photosynthetic organisms or photoautotrophs. It means that they are able to synthesize food directly from carbon dioxide and water using energy from light. They use the photogenerated electrons in order to reduce carbon dioxide and produce their biomass, carbohydrates, lipids, proteins. In addition, there are some microorganisms that can photosynthesize hydrogen as well. All these transformations are realized thanks to an amazing biologic machinery, presented schematically in **Fig. 4**, consisting of two large protein complexes, the photosystem I (PS I) and the photosystem II (PS II), assisted by various redox cofactors, and a unique enzyme, the hydrogenase.

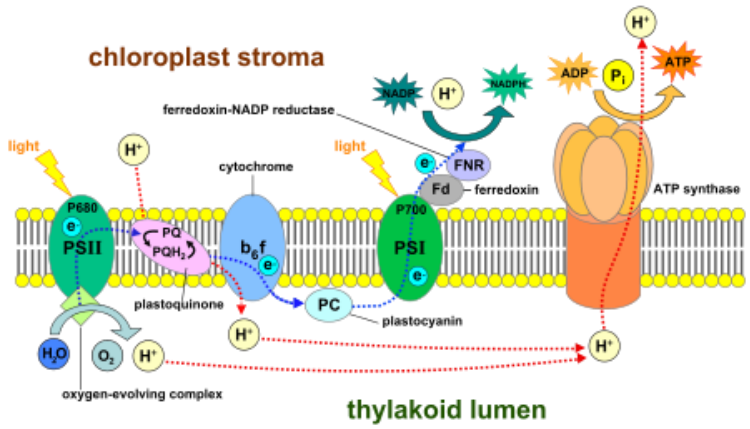

Fig. 4 Natural photosynthesis

The photosynthetic process can be divided into three distinct steps:

- initial light-harvesting process and local charge separation in PS I and II

- proton-coupled electron transfers between redox cofactors along the photosynthetic chain, allowing further spatial charge separation

- multielectronic redox catalysis generating hydrogen and oxygen at remarkable enzymatic sites such as dinuclear metal clusters in hydrogenases

The general concepts of natural photosynthesis can be used in order to produce hydrogen from renewable sources. Especially, it is significant to mimic the activity of the hydrogenase, the enzyme that catalyzes the reduction of protons. Hydrogenases are classified into three different types (**Fig. 5**) based on the active site metal content: iron-iron hydrogenase, nickel-iron hydrogenase, and iron hydrogenase.[17-20]

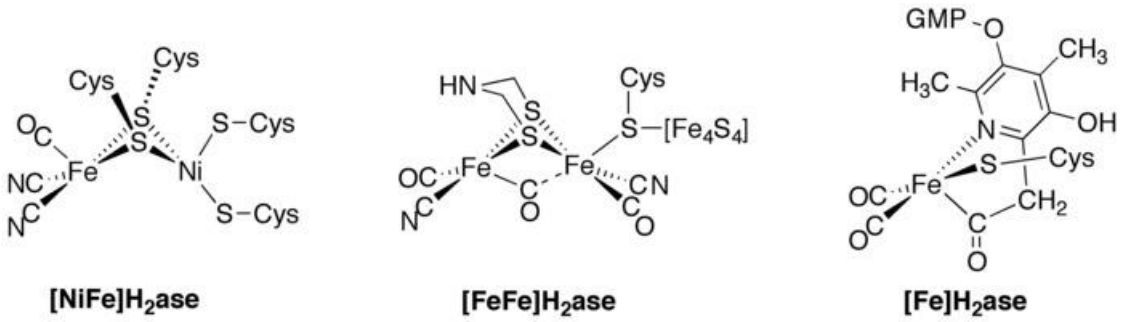

[NiFe]H_2ase **[FeFe]H_2ase** **[Fe]H_2ase**

Fig. 5: Three different types of hydrogenases

Hydrogenases are considered to have important catalytic activity. The metals that consists their catalytic center can be found easily in nature. The researchers try to synthesize complexes that mimic these catalytic centers. Great effort has already been done to this field of research with catalysts that contain Fe, Co and Ni with same functional and structural characteristics with the hydrogenases.[21-24] In order to mimic the hydrogen evolution from hydrogenases as effective as possible, it is essential to understand the mechanism for the proton reduction. There are many proposed mechanisms that could explain the hydrogen evolution. In the figure below (**Fig. 6**), it is shown the proposed mechanism for the reduction of protons by [Fe-Fe] hydrogenase, one of the most accepted mechanisms.[25-27]

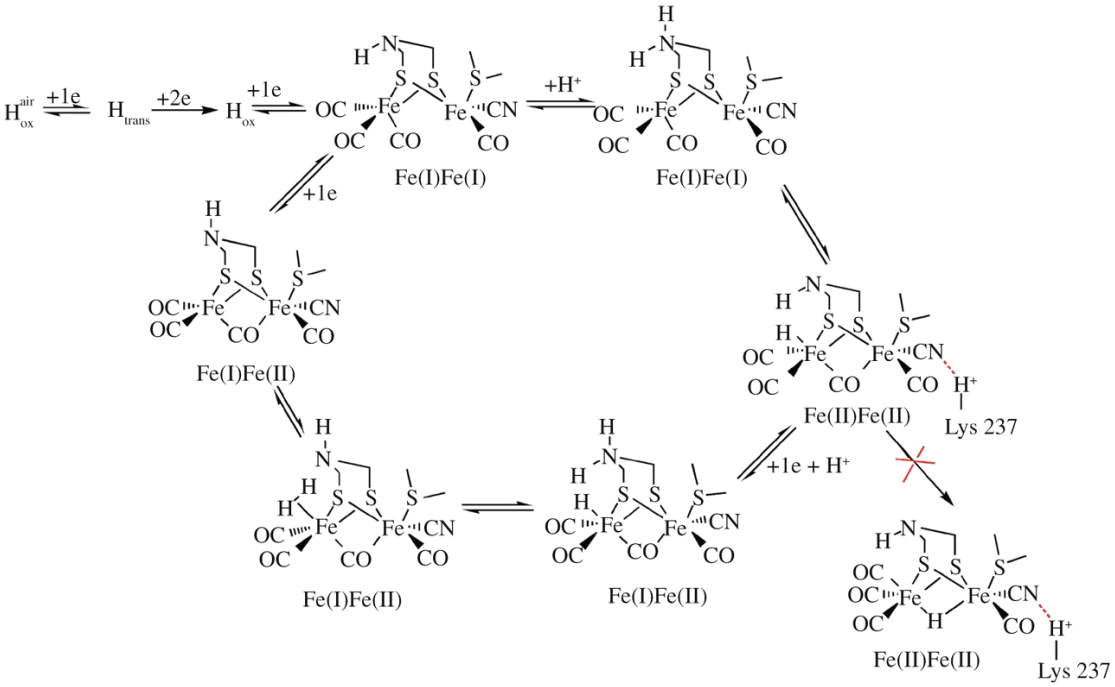

Fig. 6 Proposed mechanism for hydrogen evolution by [Fe-Fe] hydrogenase.

1.5.1 Electrocatalytic hydrogen evolution

Electrolysis is generally considered as an encouraging option for hydrogen production from renewable resources exploiting the artificial photosynthesis.[28] It is an electrochemical process in which electrical energy is the driving force of chemical reactions. Compounds are decomposed, when a current passes through them. The first scientists that observe this phenomenon were Nicholson and Carlisle in 1800. From then, there was a revolution in this field of science and by the beginning of the 20th century there were already 400 industrial water electrolysis units in use. The general procedure for electrolysis of water is shown in **Fig. 7**.

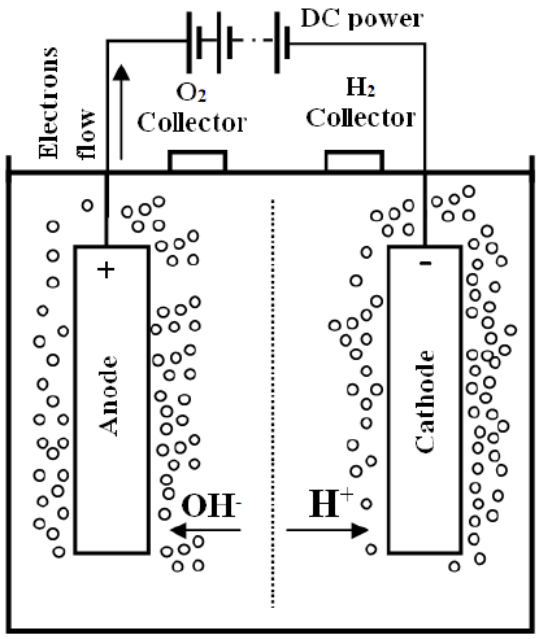

Fig. 7: Electrolysis of water

In water, there is always a certain percentage found as ionic species. The equilibrium equation that represents this phenomenon is:

$H_2O\ (l) \leftrightarrow H^+\ (aq) + OH^-(aq)$

As mentioned before, water is decomposed to hydrogen and oxygen, by passing a current through it in the presence of suitable substances, called electrolytes. On the one hand, electric current causes positively charged hydrogen ions to migrate to the negatively charged cathode, where a reduction takes place in order to form hydrogen atoms. The atoms formed then combine to form gaseous hydrogen molecules (H_2) as it seems in the equation:

electrode (cathode): $2H^+\ (aq) + 2e^- \leftrightarrow H_2\ (g)$

On the other hand, oxygen is formed at the other electrode (the positively charged anode). The stoichiometry of the reaction is two volumes of hydrogen to one volume of oxygen:

electrode (anode): $4OH^- \leftrightarrow 2H_2O + O_2 + 4e^-$

The most important issue of the construction of electrolysis units is to use adequate electrodes to avoid unwanted reactions, which could produce impurities in the hydrogen

gas. The electrodes should be resistant to corrosion, have a good electric conductivity, exhibit good catalytic properties and show a suitable structural integrity. Most of them today are Pt and platinoids that are really expensive and prevents the development of electrolysis-based technologies at a large scale. This makes a necessity to develop bio-inspired catalysts based on first row transition metal (Fe, Co, Ni) as alternatives. Furthermore, the electrodes should not react with the electrolyte.[29] Another crucial component of such a unit is a separating membrane that allows the passage of ions, or electrons and not oxygen, or hydrogen atoms. This membrane allows the gases to be kept separate in order to avoid the risk of an explosive mixture being formed in the electrolysis unit.

Electrolysis, nowadays, is considered as the cleanest way to produce hydrogen, if the required electricity is derived from renewable energy sources. Renewable sources that could be used for supplying electrolysis units are solar, aeolic and geothermal energy.

1.5.2 Photocatalytic hydrogen evolution

As it was referred above, the water splitting can be divided into two half reactions, the reductive and oxidative. The reductive site of water splitting is the generation of hydrogen from aqueous protons. The basic structure of the AP systems remains the same, although there is much research in this scientific field.[30,31] The three most important components are:

1. A chromophore to absorb light
2. A catalyst to reduce protons and generates hydrogen (HEC).
3. A sacrificial electron donor to supply electrons and regenerate the chromophore

Many times are used compounds as electron relays in order to transfer efficiently the electrons from the photosensitizer to the catalyst or compounds that can regenerated the sacrificial electron donor, which is constantly oxidized.

The basic concept of the photocatalytic hydrogen evolution is shown in **Fig. 8**. The process of converting sunlight into H_2 from H_2O comprises the harvesting of sunlight

by a photosensitizer (PS). When a PS absorbs light, i.e. one photon, one electron from the ground state is promoted into an excited state (which generates PS*). The excited PS* species possesses different electronic structure and redox potentials compared to the ground state of the PS as it is both a better oxidant and a better reductant, which confers its specific properties to initiate photoinduced electron transfer processes. Subsequently, there are two paths:

a) reductive quenching of PS* by a sacrificial electron donor (which generates PS^-), then electron transfer from PS^- to the hydrogen evolution catalyst (HEC), followed by protonation/hydride formation and H_2 evolution,

b) oxidative quenching of the PS by the HEC and the formation of the oxidized species of PS, PS^+, followed by protonation/hydride formation and H_2 evolution. Finally, the oxidized PS is regenerated by the sacrificial electron donor (scheme 3)

It is obvious from the mechanism below that two successive light-induced electron transfers are required to supply the catalytic centre with two electrons that are needed for the reduction of protons to hydrogen.

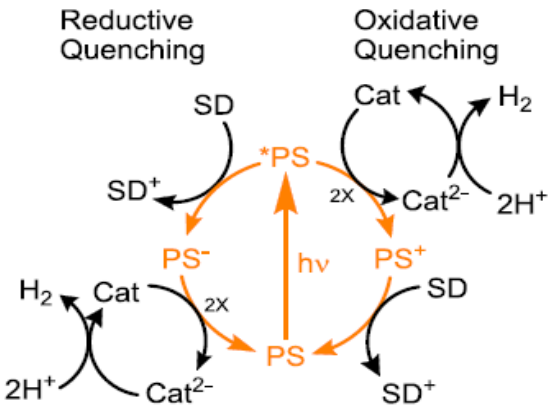

Fig. 8: Reductive and oxidative quenching mechanisms of photocatalytic hydrogen evolution

The relative viability of each of these two mechanisms is determined by the rates of the respective electron transfers and the relative stabilities of PS*, PS^+, PS^-.

Examples of photocatalytic systems for hydrogen production based on noble-metal free catalysts will be given in section 3.

2. Porphyrins

2.1 Overview

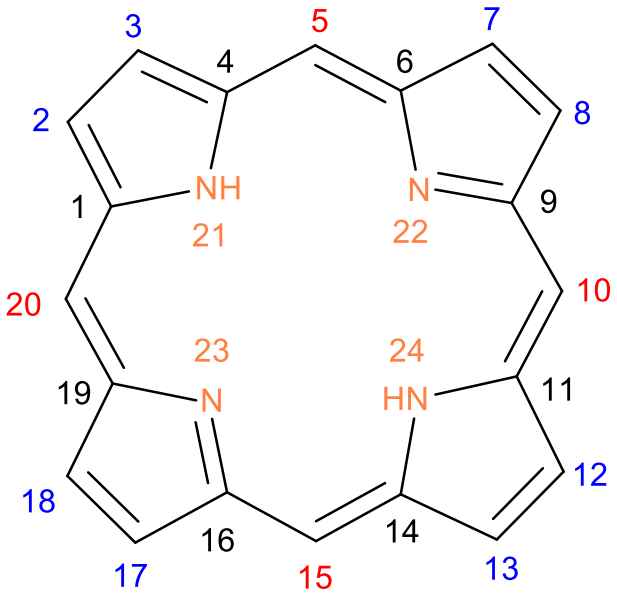

Fig. 9: Numbering of the atoms of the porphyrin ring according to Corwin

Porphyrins are a group of heterocyclic macrocycle organic compounds, composed of four modified pyrrole subunits interconnected at their α carbon atoms via methine bridges (=CH−). They are one of the most important class of biological systems in nature and they have gained the scientific attention since the 19th century due to their biological significance and photophysical properties. The parent porphyrin is porphin, and substituted porphines are called porphyrins. Above is the numbering of the atoms of the porphyrin and the distinction between the pyrrole rings, according to Corwin (**Fig. 9**).[32]

The porphyrin ring structure is aromatic, with a total of 26 electrons in the conjugated system. Various analyses indicate that not all atoms of the ring are involved equally in the conjugation or that the molecule's overall nature is substantially based on several smaller conjugated systems. One result of the large conjugated system is that porphyrin molecules typically have very intense absorption bands in the visible region and may be deeply colored.

Furthermore, porphyrins are aromatic compounds that obey the Hückel rule (4n+2). They have 18 π electrons which are delocalized over the entire circumference of the porphyrin ring. Generally, porphyrins participate in electrophilic and radical reactions due to the aromatic nature of the porphyrin ring. Meso- positions have higher electron density, so they are more reactive. However if meso- positions are occupied, β-positions can participate in electrophilic reactions.[33]

2.2 Laboratory synthesis of porphyrins

The most common synthesis in the lab is based on work by Paul Rothemund.[34] His techniques underpin more modern synthesis such as those described by Adler and Longo.[35] The Rothemund synthesis is a condensation and oxidation starting with pyrrole and an aldehyde (**Fig. 10**). In solution-phase synthesis, acidic conditions are essential; formic acid, acetic acid, and propionic acid are typical reaction solvents, or *p*-toluenesulfonic acid or various Lewis acids can be used with a non-acidic solvent. A large amount of side-product is formed and is removed, usually by recrystallization or chromatography and generally the yields that are obtained are relatively small.

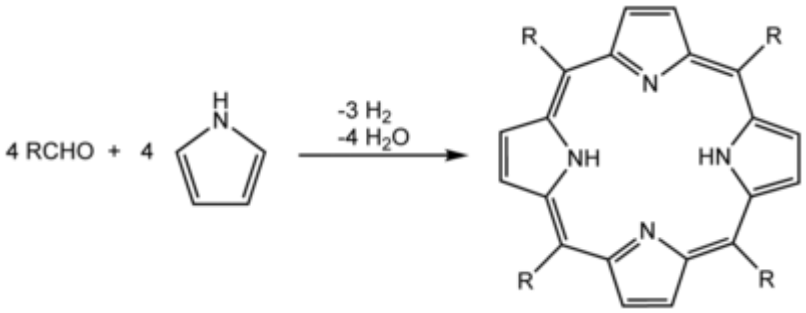

Fig. 10: General reaction for the synthesis of porphyrins

2.3 Metallation of porphyrins

Porphyrins are unsaturated tetradented macrocyclic ligands which can bind divalent metal ions that behave as Lewis acids, such as Pd^{2+}, Pt^{2+}, Zn^{2+}, Fe^{2+} . The introduction

of metal ions is an easy process including the departure of the two acidic protons which are coordinated to two out of four nitrogen atoms of the porphyrin core **(Fig. 11).**

Fig. 11: Metallation of porphyrins

2.4 Porphyrins: essential molecules

Porphyrins are considered molecules with great interest, because they possess some remarkable features that makes them essential for many living organisms. The most important of them are the following:

- The stability of the ring that can adopt different geometric conformations (planar or twisted structure).[36] Carbon atoms as well as nitrogen atoms participating in the porphyrin skeleton have sp^2 hybridization. As a result, all the bond lengths range from 134-145 pm and angles from 107º-126º. As tetra-dented chelating substituents, tetra-pyrrole rings are able to be assemble in order to stabilize "unstable" metal ions or metal ions with unusual oxidation states.
- Macrocyclic ligands show selectivity with respect to the size of the bound metal ion. This also applies to the porphyrin rings and gives them a significant stability, due to the conjugation of double bonds. Structural studies and computational models showed that ions with spherical radius of 60-70 pm are located in the central cavity of the tetrapyrrole ring. In case of a bigger radius, like in lanthanides (85-106pm), ions are located out of the plane defined by the four nitrogens of the porphyrin ring[37,38] (**Fig. 12**).

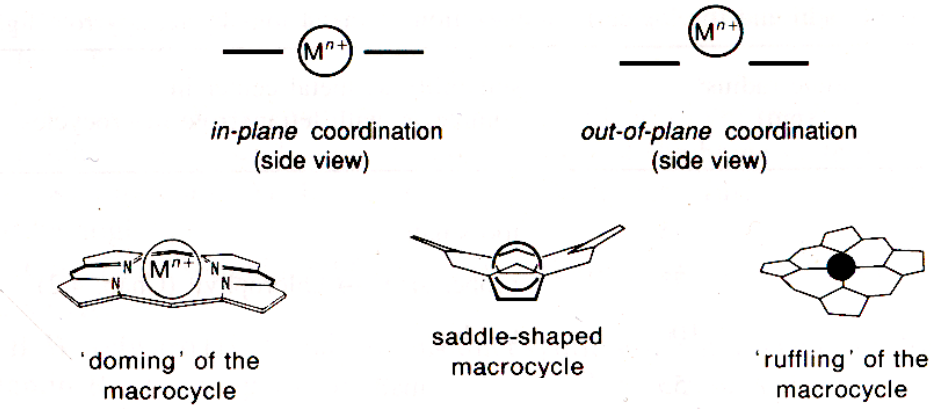

Fig. 12: Typical geometric configuration of tetrapyrrolic complexes

- These molecules prefer an almost planar configuration when attached (linked) to a metal ion. This feature, provided that the coordination number is 6 in octahedral geometry, leaves two empty coordination sites X, Y in axial positions allowing in that way *trans* substitution to occur in various reactions (**Fig**. **13**).

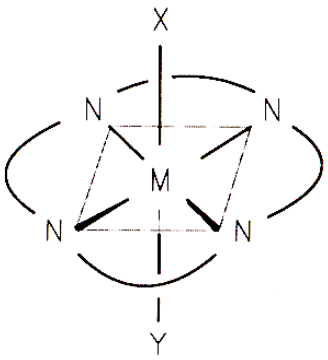

Fig. 13: Axial positions X, Y at six coordinated complexes

- Porphyrins are capable of "taking" and "giving" electrons, so the processes of the first oxidation and the first reduction are taking place with great ease. The formed anions or cations, respectively, are quite stable.

Therefore, the absorption of light and the easy redox processes make these tetrapyrrole molecules the most important energy convertors in biological systems.

2.5 Methods of characterization

A complete study and an adequate characterization of the derivatives of porphyrins is made by taking the NMR spectrum (^{13}C, ^{1}H), mass spectrum, cyclic voltammogram, UV-Vis spectrum and fluorescence spectrum. Important method is also the X-ray crystallography that provides information on the location of the compound atoms in the space and on how the molecules interact with each other.

Ultra violet–visible spectroscopy

UV-Vis spectroscopy refers to absorption spectroscopy in the ultraviolet-visible spectral region. This means it uses light in the visible and neighboring ranges. It provides information on the structure of the compounds after studying the spectrum of the basic and excited state. The wavelength of the radiation varies between 200-800nm. UV-Vis spectroscopy uses the Beer-Lambert law[39], according to which radiation absorption from a sample is proportional to its concentration. More specifically: $A = \varepsilon \times b \times C$,

where A is the absorption

ε is the molar absorptivity

b is the cell thickness

C is the concentration of the sample

Porphyrins exhibit intense absorption of wavelength radiation that lies in the area of the UV-Vis. This is due to the intense 18p conjugates that appear. The porphyrin spectra consist of a number of bands which are characteristic of each porphyrin because the spectrum depends on the nature of the substitutes but also on the central metal. The absorbing bands that are displayed are separated into two groups.

In the porphyrin spectrum, there are the Soret[40] and the Q bands. The Soret is a band with high absorption and appears in the area 380-420 nm. The Q bands consist of four low absorption bands for the free base porphyrin (with no central metal). For metal

porphyrins 2 bands appear, because their symmetry is larger relative to the proportion of the free base porphyrin. This means that there are fewer possible transitions, that means fewer bands. The Q bands appear in the 500-700nm area.

In order to obtain a UV-Vis spectrum, we used the spectrometer below (**Fig. 14**), which is a PharmaSpect UV-1700. The basic function of a spectrometer is to take in light, break it into its spectral components, digitize the signal as a function of wavelength, and read it out and display it through a computer.[41]

Fig. 14: The spectrometer of our experiments.

Mass spectroscopy MALDI-TOF[42]

The mass spectroscopy is characterized as a sensitive technique for the qualitative analysis of chemical compounds. It relies on separating the masses of charged particles (mainly cations) with the aid of a suitable arrangement (for example flight time) and finding the correspondence of the masses of the obtained ions with the structure of the precursor compound. Generally, it calculates the m/z for each ion.

For our experiment we used MALDI-TOF (**Fig. 16**), which is a methodology consisting of a three-step process (**Fig. 15**). At first, the sample is mixed with a suitable matrix material (important to protect the sample from decomposition) and applied to a metal plate. Second, a pulsed laser irradiates the sample, triggering ablation and desorption of the sample and matrix material. The analyte

molecules are ionized by being protonated or deprotonated in the hot plume of ablated gases, and can then be accelerated into the flight tube in order to be separated and analysed.

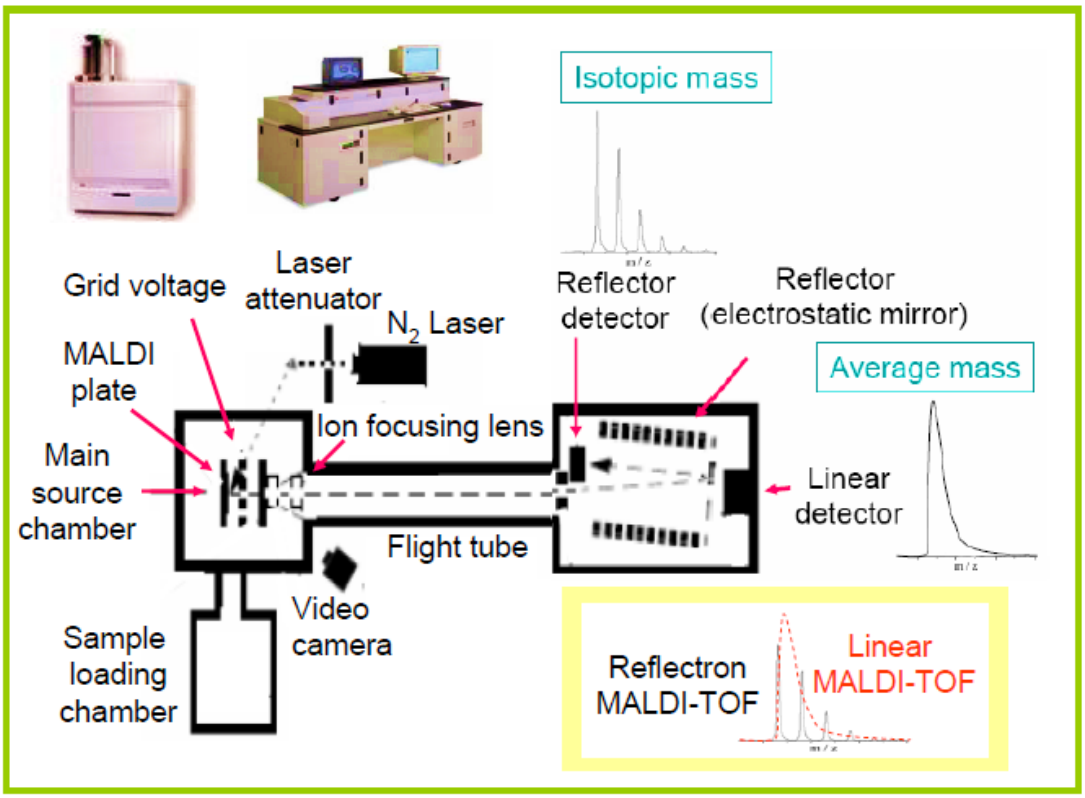

Fig. 15: The basic parts and the operating principle of the MALDI-TOF.[43]

Fig. 16: The MALDI-TOF equipment employed to characterize the compounds synthesized in the Laboratory of Bioinorganic Chemistry.

Nuclear magnetic resonance spectroscopy (NMR)

Nuclear magnetic resonance is a form of absorption spectroscopy where the sample is located in the direction of its own spin (spin or self-rotating) within a magnetic field absorbing electromagnetic radiation at frequencies that characterize it. Absorption depends on the observed nucleus.[44] NMR spectrum is composed of a plurality of peaks that are tuned at different frequencies.

The NMR spectrophotometers that are used today are separated into two groups:

- Continuous wave NMR spectrometers and
- pulse fourier transform NMR spectrometers (FT-NMR)

The key ingredients for all high resolution capacitance spectrophotometers are an electromagnetic radiation source in the radio frequency range with which the sample is bombarded and a strong magnet that must have a high degree of stability and homogeneity.[45]

During scanning, each nucleus of the sample (proton, carbon) is brought to the resonance stage, absorbs energy from the radiation oscillator and as the nucleus returns to its original state, the emitted energy is collected from the detector coil (which is wrapped around the sample) is amplified and recorded.

X-ray crystallography

X-ray crystallography is a technique used for determining the atomic and molecular structure of a crystal, in which the crystalline atoms cause a beam of incident X-rays to diffract into many specific directions. By measuring the angles and intensities of these diffracted beams, a crystallographer can produce a three-dimensional picture of the density of electrons within the crystal. From this electron density, the mean positions of the atoms in the crystal can be determined, as well as their chemical bonds, their disorder, and various other information.

2.6 Porphyrins in nature

Porphyrins are molecules that can be found easily in nature. They are considered the most important macrocycle ring of nature. They take part in some of the most important biological processes, such as biosynthesis and the transportation of oxygen in human body.

In human body, we can find three types of porphyrins:

1. Protoporphyrin (PROTO) (**Fig. 17**)
2. Uroporphyrin (URO) (**Fig. 18**)
3. Coproporphyrin (COPRO) (**Fig. 19**)

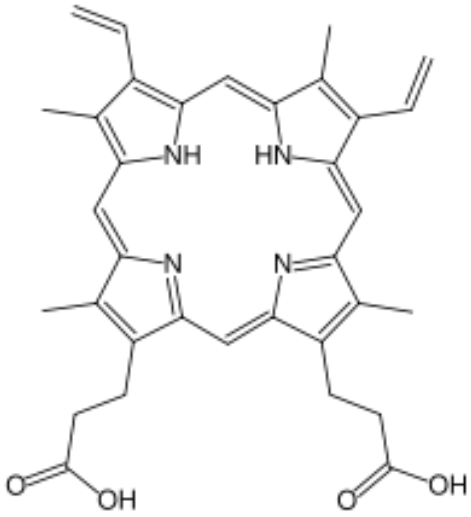

Fig. 17: Protoporphyrin

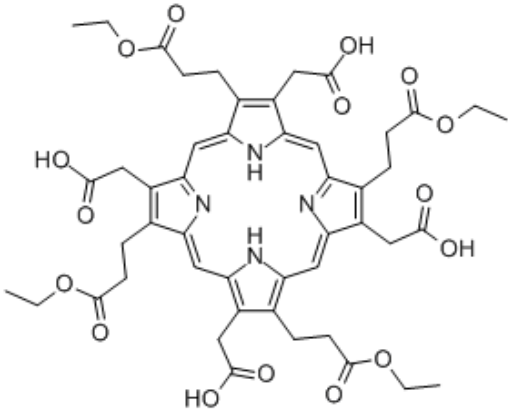

Fig. 18: Uroporphyrin

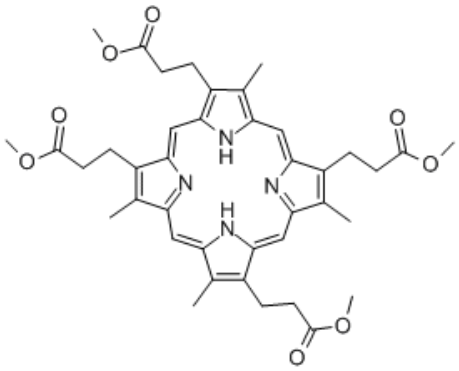

Fig. 19: Coproporphyrin

Hemes molecules, they called the chromophores of life, are type of porphyrins that can be found in human body. They are coordinated with iron and they are the active sites of proteins hemoglobin (**Fig. 20**) and myoglobin (**Fig. 21**), which are responsible for the transportation and elimination of oxygen in organisms.[46]

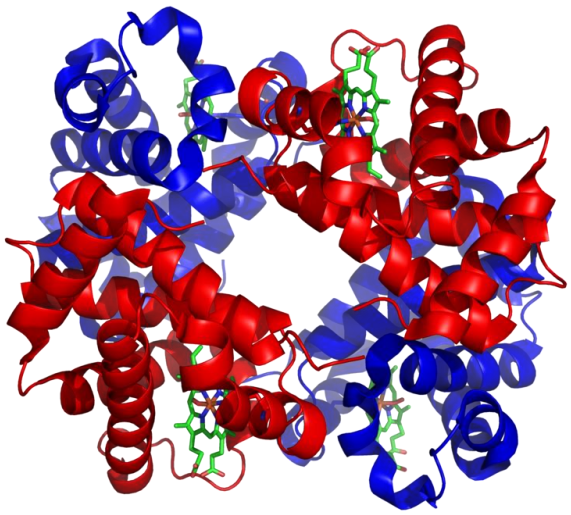

Fig. 20: Structure of human hemoglobin. The proteins α and β subunits are in red and blue, and the iron-containing heme groups in green.

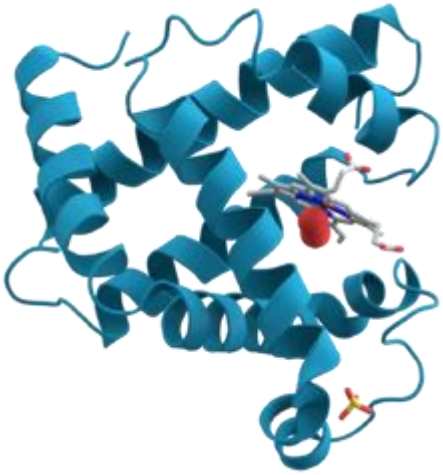

Fig. 21: Structure of myoglobin.

Derivatives of porphyrins are essential molecules for photosynthesis. Chlorins are derivatives of porphyrins that are made when one of the groups of pyrrole has been reduced. Magnesium-containing chlorins are called chlorophylls, which are the most important components of photosynthesis. They ensure photosynthesis in plants by triggering photochemical electron transfer events. The photosynthesis takes place in the chloroplast. There are five main types of chlorophylls: chlorophylls *a*, *b*, *c* and *d*, plus a related molecule found in prokaryotes called bacteriochlorophyll. In

plants, **chlorophyll *a*** ***(*Fig. 22*)*** and **chlorophyll *b*** are the main photosynthetic pigments.

Structurally, chlorophyll molecules include a hydrophobic ("water-fearing") tail that inserts into the thylakoid membrane and a porphyrin ring head (a circular group of atoms surrounding a magnesium ion) that absorbs the light. Although both chlorophyll *a* and chlorophyll *b* absorb light, chlorophyll *a* plays a unique and crucial role in converting light energy to chemical energy. All photosynthetic plants, algae, and cyanobacteria contain chlorophyll *a*, whereas only plants and green algae contain chlorophyll *b*, along with a few types of cyanobacteria.

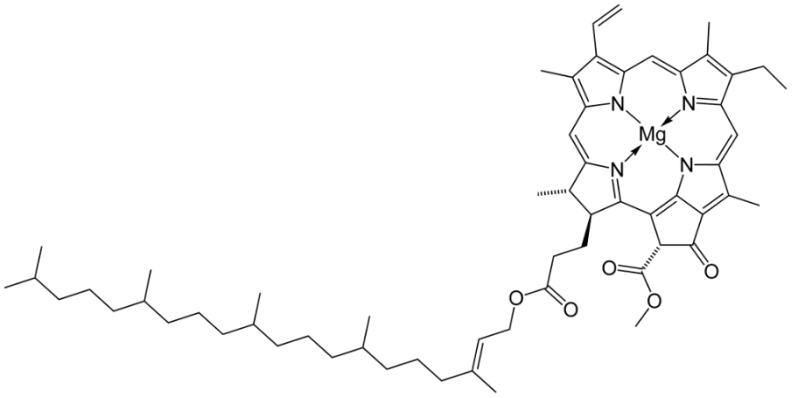

Fig. 22: Structure of chlorophyll a.

2.7 Applications of porphyrins

Porphyrins and their derivatives, due to their stability under high temperature and different pH, their photophysical properties, their low toxicity, are used in many different applications, such as medicine, biomimetic catalysis, molecular electronics, supramolecular chemistry, organic geochemistry, toxicology.

In medicine, porphyrins have been used in photodynamic therapy. Generally, for the treatment of cancer are used the radiotherapy and the chemotherapy. The biggest drawback for these techniques are the dangerous side effects due to their indiscriminately destruction of both normal and tumor tissues. Photodynamic therapy (PDT) is a new technique for the treatment of various types of malignant tumors. PDT

is based on the ability of some photosensitizers, such as porphyrins and porphyrin-like chromophores to be accumulated selectivity in tumor tissues; tumor necrosis can be obtained by irradiation of the neoplastic area with light of the appropriate wavelength. Until now a few thousand patients have been successfully treated by PDT worldwide.

In molecular electronics, they are used for the development of DSSCs (dye-sensitized solar cells) that can be applied to photovoltaic systems. Their main role is again to absorb the solar radiation and convert it into electric energy.

Porphyrins and metal porphyrins are generally used as light harvesting molecules due to their ability to absorb light. Consequently, they have been used as photosensitizers in photocatalytic hydrogen evolution systems, where a PS is essential in order to absorb solar radiation and begin the redox reactions that will regenerate hydrogen.

3. Photocatalytic systems for hydrogen evolution

The interest for using hydrogen as fuel has increased from 1970, almost one century after the prediction of Jules Verne. As it was mentioned in previous chapters, one of the most attractive ways to produce hydrogen is photocatalytic. Various photocatalytic hydrogen evolution catalysts, with a specific interest on the use of noble-metal free catalysts and different photosensitizers (dyes) have been extensively studied as it is analysed below.

Among, the catalysts that have been used so far, cobaloximes are particularly attractive due to their high activity and easy preparation.[47-51] As photosensitizers, they have used organic dyes, but the most common are $[Ru(bpy)_3]^{2+}$, $[ReX(bpy)(CO)_3]$, $[Ir(ppy)_2$-$(diimine)]^+$ or [PtX(terpy)] types.[52-54] The most important drawback of them is their cost, because are noble metal complexes and their efficiency is not the expected one. Organic dyes are used especially by the scientific group of Eisenberg[55,56], but their instability in the conditions of hydrogen evolution is an important issue that ought to be faced. Porphyrins and metalporphyrins due to their similarity with chlorophylls have been examined in details for hydrogen evolution. More specifically, various metalloporphyrins such as Zn(II), Al(II), Sn(IV), Mg(II), Pt(II), Pd(II) have been extensively used as photosensitizers for H_2 production. The redox center in

metalloporphyrins is the porphyrin ring where the electrochemical potential is sensitively influenced by the kind of central metal ions. Among a series of metalloporphyrins tin(IV)-porphyrin derivatives have already been used as mimics for the photocatalysis of light-driven water-oxidation and proton-reduction.[57]

Lehn and co-workers reported first the homogeneous photogeneration of hydrogen using $[Co(dmgH)_2(OH_2)_2]$ (where dmgH = dimethylglyoximate) as a catalyst with $[Ru(bpy)_3]^{2+}$ (bpy = 2,2′-bipyridine) as photosensitizer and triethanolamine (TEOA) as a sacrificial electron donor in a DMF solution.[58] Eisenberg and co-workers have shown that $[Co(dmgH)_2(pyridine)(Cl)]$ catalyzes H_2 evolution with a platinum(II) terpyridyl phenylacetylide complex, $[Pt(ttpy)(CtCPh)]^+$(ttpy) 4′-p-tolylterpyridine), as photosensitizer and TEOA as a donor in 3:2 (v/v) CH_3CN/H_2O solutions between pH 7 and pH 12.[59] At pH 8.5 with 0.27 M TEOA, 1000 turnovers were achieved after 10 h irradiation (λ > 410 nm). Systems also have been reported in which organic chromophores replaced noble metal photosensitizers.[60] In 12 h of irradiation (λ > 450 nm), 900 turnovers were achieved using the eosin Y photosensitizer with $[Co(dmgH)_2(pyridine)(Cl)]$, TEOA, and 3 mM free dimethylglyoxime in 1:1 CH_3CN/H_2O at pH 7. Degradation of the photosensitizer/catalyst system was minimized with added dimethylglyoxime. Fontecave and co-workers have tested multicomponent photosystems for H_2 evolution with $[Co(dmgBF_2)_2L]$ and both $[Ir(ppy)_2phen)]^+$(ppy=2-phenylpyridine, phen=phenanthroline) and $[ReBr(CO)_3(phen)]$ as photosensitizers in acetone. Both a sacrificial donor and a proton source was used (Et_3N/Et_3NH^+).[61,75]

To perform the photocatalytic production of hydrogen in homogeneous media, a sacrificial electron donor (SD) is required in order to provide the system with the electrons. Most common SDs are aliphatic tertiary amines such as triethanolamine (TEOA), triethylamine (TEA), ethylenediaminetetraacetic acid (EDTA) and sodium ascorbate (NaHA), the deprotonated form of acid ascorbic (vitamin C).[62]

Catalysts for the conversion of electrical energy to fuels and for the reverse process, the conversion of fuels to electricity, will have a significant impact on future renewable energy systems. Nickel catalysts, such as nickel thiolate and bis(diphosphine), have received special attention in recent years because they mimic the [Fe-Ni]-hydrogenase

active site. In the following table (**Table 1**) there is a brief summary of literature data for the reported nickel catalysts. We selected suitable photocatalytic conditions to evaluate the novel nickel catalysts, according to these data.

Table 1: Photocatalytic systems with nickel catalysts

PS	Catalysts	ED	Solvent	TONs	pH	References
RuP	NiP(phosphonate)	Ascorbate	Aqueous	723(2h)	4.5	[63]
Carbon-QDs	Ni-bis-(diphosphine)	EDTA(0.1M)	Aqueous	64(4h)	6	[64]
$Ru(bpy)_3^{2+}$	Ni-phosphine	Ascorbic acid(05M)	CH_3CN-H_2O(1/1)	2700(150h)	2.25	[65]
Eosin Y	Ni-phosphine	Ascorbic acid(0.5M)	CH_3CN-H_2O(1/1)	1.1ml(8h)	2.25	[65]
Carbon nitride	Ni-bis-(diphosphine)	-	Aqueous phospate	425,4(24h)	4.5	[66]
Carbon-QDs	NiP(phosphonate)	TCEP/AA	aqueous	1094 (24h)	5	[67]
Fluorescein	$Ni(MBD)_4$	TEOA(5%)	CH_3CN-H_2O(1/1)	320(10h)	10.5	[68]
Fluorescein	$Ni(pyS)_3^-$	TEA(5%)	EtOH-H_2O(1/1)	5500(24h)	12.12.5	[69]
Erythrosin Y	NiL_2	TEOA(15%)	aqueous	3.2mmol(24h)	8.5	[70]

Erythrosin B	Ni-thiolate complex	TEOA	aqueous	12.3mmol (24 h)	8.5	[71]
g-C_3N_4	$[Ni(TEOA)_2Cl_2$	TEOA(10%) (MeOH)	aqueous	57(8h)	10.5	[72]
Fluorescein	Ni-pyridinethiolate (4c)	TEA(0.36M)	EtOH-H_2O(1/1)	7300(30h)	11.5	[73]
Cd-Se nanocrystals	Ni^{2+}-DHLA(20*)	Ascorbate(0.5)	aqueous	4.5(360h)	>600000	[74]

Aim of this thesis

This thesis was inspired by previous literature references and previous work of our scientific group. The thesis is divided in three parts. In the first one, we report photochemical hydrogen evolution systems consisting of various cobalt based catalysts[75], metallated Sn porphyrins[76] as photosensitizers, triethanolamine as sacrificial electron donor in acetonitrile/H_2O (1:1) solution. Upon visible irradiation hydrogen production was detected with the best result obtained at pH 7 with turnover number (TON) of 124, after 48 hours in the presence of catalyst N-methyl imidazole cobaloxime and tin-5, 10, 15, 20-tetrakis-(4-carboxyl–methyl-phenyl) porphyrin.

In the second one we present for the first time, photocatalytic systems for hydrogen production in aqueous solutions. The systems consist of a triethanolamine (TEOA) as sacrificial electron donor, TiO_2 nanoparticles, porphyrins **[ZnTMPyP^{4+}]Cl$_4$** (**P1**), **ZnPCNCOOH** (**P2**) and **ZnP(SP)CNCOOH** (**P3**) as photosensitizers and cobaloximes **CoN-Methyl-imidazole** (**C1**), **CoCNCOOH** (**C2**) and **Co(SP)CNCOOH** (**C3**) as catalysts. Porphyrins **P2**, **P3** and cobaloximes **C2** and **C3** contain a cyano-carboxylic acid anchoring group for their attachment onto TiO_2 nanoparticles. In the case of **porphyrin P2** and cobaloxime **C2** the anchoring groups

are directly linked to the *meso* position of the macrocycle or pyridine ligand, respectively, while in case of **P3** and **C3** there is a π spacer group (SP) in between. Upon visible irradiation hydrogen production was detected with the best result obtained at pH 7 with porphyrin **P1** ($C = 4.0 \times 10^{-5}$ M) and catalyst **C2** ($C = 4.9 \times 10^{-4}$ M) with a TON of 240, after 23 hours. In the case of photosensitizer **P1** ($C = 4.0 \times 10^{-5}$ M) and catalyst **C3** ($C = 4.9 \times 10^{-4}$ M) a TON of 60 was measured after the same irradiation time.

In the third one, part of the experiments took place in Grenoble during Erasmus programme, we tested two novel nickel catalysts and two novel cobalt complexes. A bibliographic study (**Table 1**) was essential in order to define the best experimental conditions for the photocatalytic tests. Then, we performed a screening of various experimental parameters in order to assess the catalytic activity of these complexes under fully aqueous and mixed aqueous-organic media. An optimization of the conditions were made under visible irradiation and using different photosensitizers (fluorescein, Ir-PS, $[ZnTMPyP^{4+}]Cl_4$, $[Ru(bpy)_3]Cl_2$ and different sacrificial electron donors (TEOA, TEA and ascorbic acid). Based on the literature we obtained the best results for all the complexes using as PS Ir-PS, as SED TEA and mixed aqueous-organic media. In order to make a comparison between nickel complexes and cobalt complexes, we test the cobalt complexes with the same structure with nickel complexes. All of the catalysts were synthesized by collaborators of the laboratory and we synthesized the porphyrin and part of the Ir-PS.

Chapter 2 - Experimental Section

Materials and Techniques. Reagents and solvents were purchased as reagent grade from usual commercial sources and used without further purification, unless otherwise stated. Thin layer chromatography was performed on silica gel 60 F_{254} plates, while chromatographic separations were carried out using silica gel 60, SDS, 70–230 mesh ASTM. ^{1}H NMR and ^{13}C NMR spectra were recorded on Bruker AMX-500 MHz and Bruker DPX-300 MHz spectrometers, as solutions in deuterated solvents by using the solvent peak as the internal standard. High-resolution mass spectra were recorded on a Bruker ultrafleXtreme MALDI-TOF/TOF spectrometer, using trans-2-[3-(4-tert-butylphenyl)-2-methyl-2-propenylidene]malononitrile as matrix. Elemental analysis were performed with a Perkin–Elmer 240B elemental analyzer.

Photophysical Measurements. UV-Vis absorption spectra were measured on a Shimadzu UV-1700 spectrophotometer using 10 mm path-length cuvettes. The emission spectra were measured on a JASCO FP-6500 fluorescence spectrophotometer equipped with a red-sensitive WRE-343 photomultiplier tube (wavelength range 200-850 nm).

Hydrogen evolution experiments. Due to the fact that the experiments have done in two different laboratories, the equipment in each one was different. Hence, both equipment will be described in details below.

SolHyCat group, Grenoble: Each sample was prepared in a schlenk tube. Before sample preparation, an aqueous solution of TEOA, TEA or ascorbate was prepared, adjusted to the required pH using conc. HCl or NaOH and finally degassed for 15 minutes with nitrogen. The organic solvent was degassed for 15 minutes with nitrogen. The components (PS and Cat) were weighted and transferred in the schlenk tube under N_2 atmosphere. 5 mL of the solvent mixture were added and the schlenck was sealed with a Suba-seal septum and placed at a fixed distance of 19 cm of the lamp. The solution was stirred and irradiated with a 150 W Xenon lamp using a water filter (elimination of IR irradiation) and a UV cut-off filter (λ < 400 nm). Under these conditions, the power density (measured at the schlenk position) is 2 suns. Extra care was taken to prevent stray UV light from reaching the sample by covering the area around the filter assembly with a large carton.

The amounts of hydrogen evolved were determined by gas chromatography, with a Perkin Elmer *Clarus 580* instrument, equipped with a Porapack Q 80/100 column (6' 1/8'') thermostated at 40 °C and a TCD detector thermostated at 100 °C; N_2 was used as carrying gas (gas flow: 20 mL.min^{-1}) (name of the method used: "injection directe H_2 O_2 20mL/min 32°C (sans FID)").

For control experiments with Hg, a drop of Hg was added to the solution and irradiation was performed under vigorous stirring to investigate if metallic nanoparticles or colloids could be responsible for the observed H_2 evolution.

Bioinorganic group, Heraklion: The procedure for a typical photocatalytic experiment is as follows. Each sample was prepared in vials. The components (PS and Cat) were weighted and transferred in the vials. Before sample preparation, an aqueous solution of TEOA and TEA was made. The pH was determined by pH meter and adjusted to the required pH using conc. NaOH or HCl and finally degassed for 10 minutes with nitrogen. 10 mL of the solvent mixture was added in each vial. The sample was sealed and placed at a fixed distance from the white LED lights (handmade photoreactor), which are shown in the **Fig. 23**. The solution was stirred and irradiated. After irradiation, 100 μL samples were taken from the headspace and injected immediately into the GC.

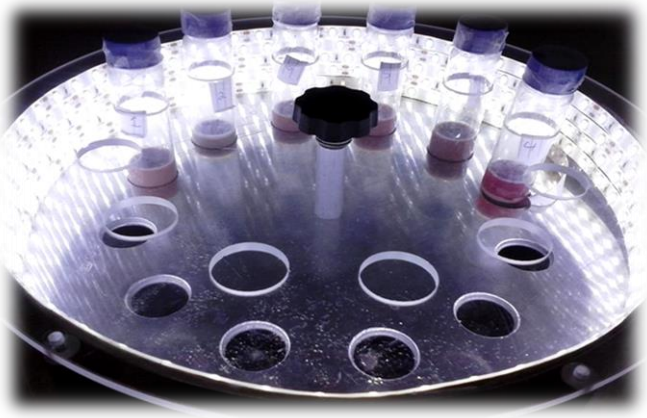

Fig. 23: Handmade photoreactor with white led lights

The amounts of hydrogen evolved were measured by gas chromatography (external standard technique) using a Shimadzu GC-2010 plus chromatograph with a TCD detector and a molecular sieve 5 Å column (30 m - 0.53 mm). Control experiments were performed under the same conditions as the hydrogen evolution experiments with removal of one of the components of the hydrogen generating system (PS, catalyst and/or sacrificial electron donor).

Mercury poisoning experiments were performed by adding an excess of mercury (ca. 40 equiv.) to our solution in order to examine the possibility of formation of metallic nanoparticles or colloids during hydrogen evolution.

Synthesis of the compounds

Synthesis of 5,10,15,20-tetrakis-(4-carboxyl–methyl-phenyl) porphyrin (1)

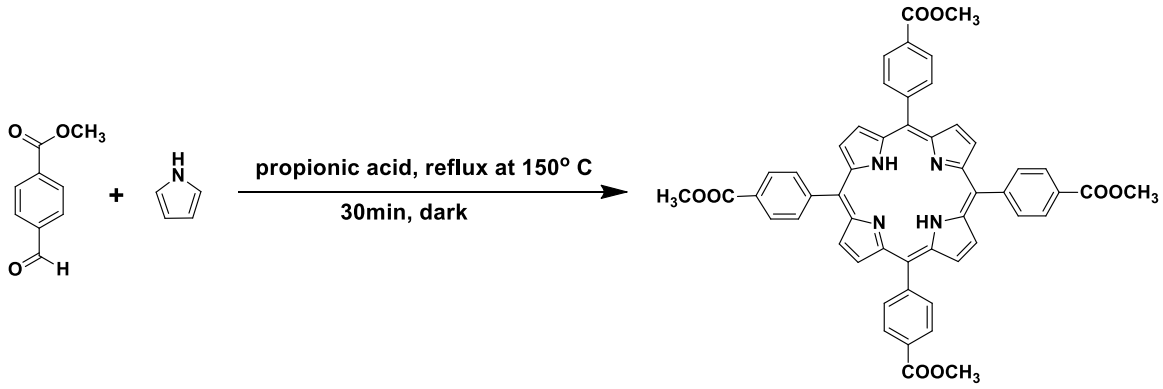

(1)

A solution of methyl-p-formylbenzoate (3.3g, 20.1mmol) and pyrrole (1.5mL, 21.6mol) in propionic acid (75mL) was refluxed at 150°C in a flask protected from light for 30min. As soon as the mixture cooled to room temperature, the mixture was washed with distilled water, cold MeOH and Et_2O. The crude product was purified by silica column chromatography eluting with CH_2Cl_2 – EtOH (98:2 v/v). Yield: 733mg (4.3%).

Synthesis of 5,10,15,20-tetrakis-(4-carboxy–phenyl) porphyrin (2)

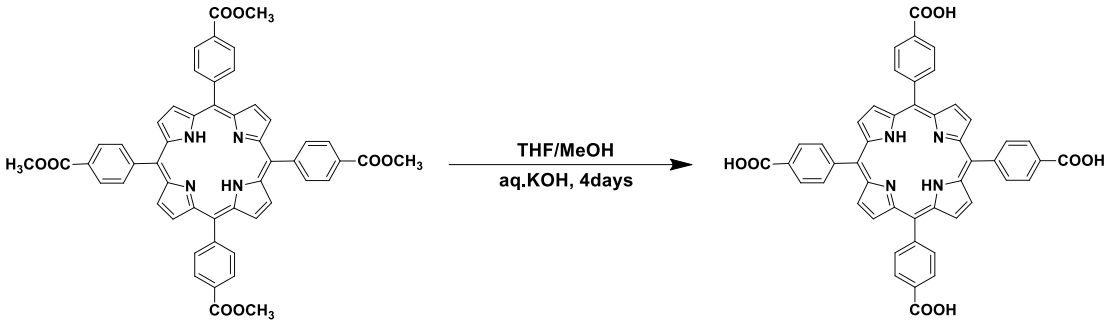

(1) (2)

In a 250mL round bottom flask, a solution of porphyrin (1) (200mg, 0.24mmol) was in THF (70mL) and MeOH (30mL) was mixed with a solution of KOH (2gr, 35.64mmol) in distilled water (36mL). The reaction mixture was stirred at room temperature for 4 days. The solvents, THF and MeOH, were completely removed on a rotary evaporator. The rest of the mixture was acidized with HCl 1M (pH 5). The precipitate was filtered and washed with distilled water many times. Yield: 126mg (66%).

Synthesis of Tin-5,10,15,20-tetrakis-(4–carboxyl–methyl-phenyl) porphyrin (3)

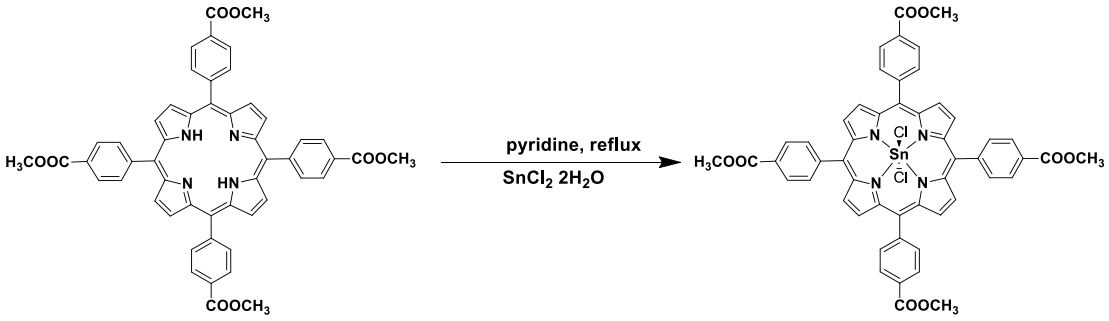

(1) (3)

In a round bottom flask porphyrin (1) (137mg, 0.162mmol), $SnCl_2$ (307mg, 1.62mmol), pyridine (30ml) were added and refluxed for 9 hours. The solvent was evaporated under vacuum. The solid was dissolved in dichloromethane and was filtered with celite. Yield: 100mg (65%).

Synthesis of Tin-5,10,15,20-tetrakis-(4–carboxyl–phenyl) porphyrin (4)

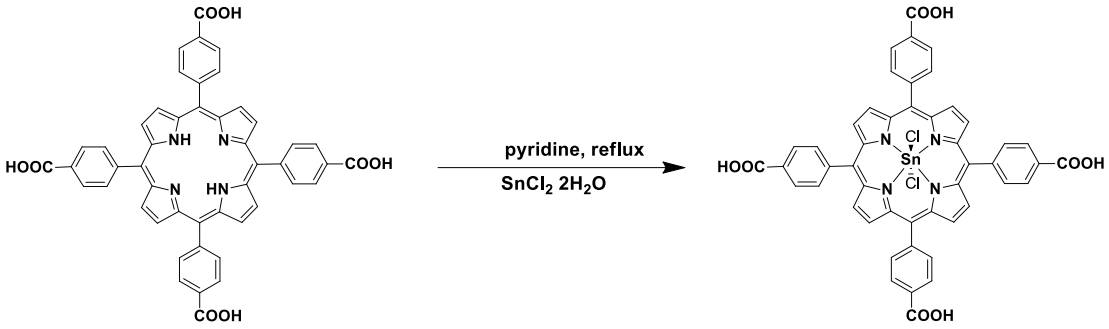

(1) (4)

In a round bottom flask porphyrin (2) (128mg, 0.162mmol), $SnCl_2$ (307mg, 1.62mmol), pyridine (30ml) were added and refluxed for 9 hours. The solvent was evaporated under vacuum. The solid was dissolved in dichloromethane and was filtered with celite. Yield: 90mg (65%).

Synthesis of diethyl–4–aldehydephenylphosphonate (5)

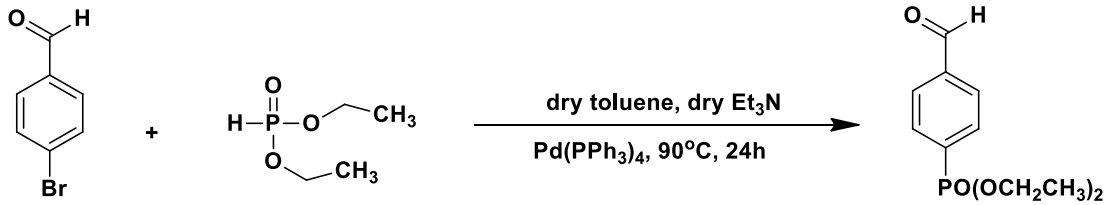

(5)

4-bromobenzaldehyde (500mg, 2.70mmol) was taken in a 100mL two-necked bottom flask. To this solution, dry toluene (4mL), dry Et_3N (4mL) and diethylphosphite (0.4mL, 6 mmol) were added and purged with Ar gas for 2min. Finally, $Pd(PPh_3)_4$ (155mg, 0.135mmol) was added and the reaction mixture heated to 90°C for 24h under Ar atmosphere. The reaction mixture was cooled to room temperature and the solvent evaporated to dryness under vacuum, re-dissolved in CH_3Cl (35mL), washed with distilled water (3 × 50mL), followed by brine solution (50mL), and finally dried over with Na_2SO_4. The crude product was purified on a silica column chromatography using CH_3Cl – EtOAc (70:30, v/v) as the eluent. Yield: 300mg (47%).

Synthesis of 5,10,15,20-tetrakis-(4-di-ethyl-phosphonate-phenyl) porphyrin (6)

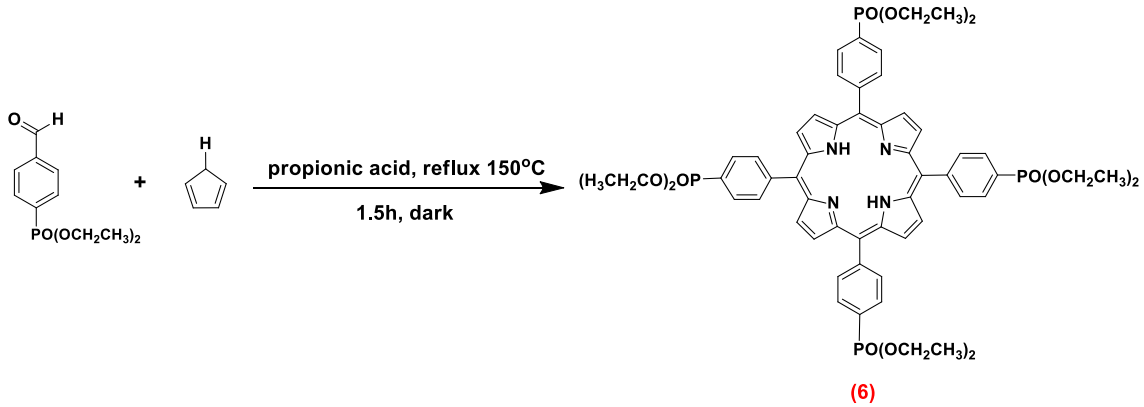

(6)

A solution of aldehyde (5) (280mg, 1.18mmol) and pyrrole (0.080mL, 1.15mol) in 10mL of propionic acid was refluxed at 150°C in a flask protected from light for 1.5h. The mixture was evaporated to dryness, and purified by column chromatography on neutral alumina eluting with CH_2Cl_2 – MeOH (99:1, v/v). Yield: 92.4mg (6.7%).

Synthesis of 5,10,15,20-tetrakis-(4-phosphonato-phenyl) porphyrin (7)

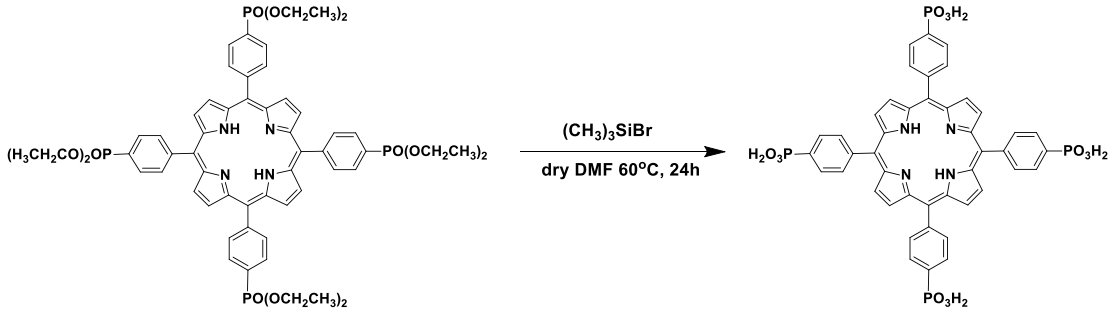

(6) (7)

In a two-necked bottom flask, a solution of porphyrin (6) (20mg, 0.0172 mmol) and CH_3SiBr (0.1mL, 0.76mmol) in dry DMSO (4mL) was heated under Ar atmosphere at 60° C for 24h. The solvent was evaporated under vacuum and the green solid residue was dissolved in MeOH and stirred at room temperature for 1h. Et_2O was added until precipitation occurred, and the resulting solid was filtered off, washed with Et_2O and dried under vacuum. Yield: 16mg (99%)

Synthesis of tin 5,10,15,20-tetrakis-(4-di-ethyl-phosphonate-phenyl) porphyrin(8)

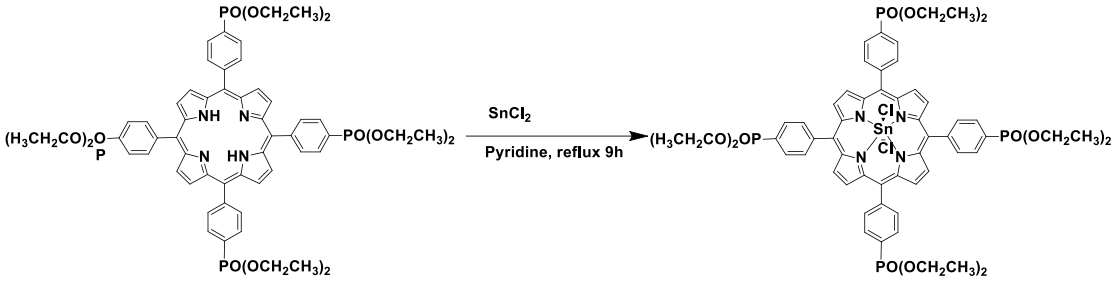

In a round bottom flask porphyrin (6) (188mg, 0.162mmol), $SnCl_2$ (307mg, 1.62mmol), pyridine (30ml) were added and refluxed for 9 hours. The solvent was evaporated under vacuum. The solid was dissolved in dichloromethane and was filtered with celite. Yield: 108mg (50%).

Synthesis of Tin 5,10,15,20-tetrakis-(4-phosphonato-phenyl) porphyrin (9)

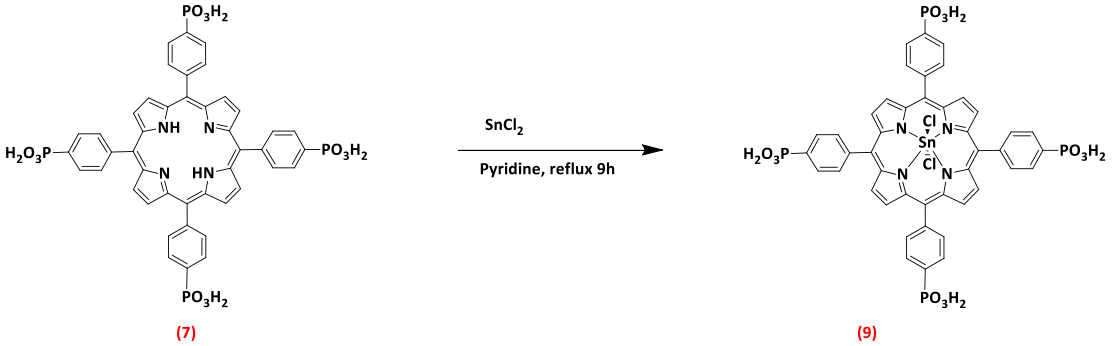

In a round bottom flask porphyrin (7) (151mg, 0.162mmol), $SnCl_2$ (307mg, 1.62mmol), pyridine (30ml) were added and refluxed for 9 hours. The solvent was evaporated under vacuum. We tried to dissolve the solid in dichloromethane but we couldnot. We couldnot obtain the porphyrin 9. We thought that probably tin was attached to phosphonato groups so we tried to use porphyrin 8 and to do hydrolysis using the same experimental conditions for the porphyrin 7 but again we couldnot obtain the porphyrin 9.

Synthesis of 5-(4-Methoxy-carbonyl-phenyl)-10,15,20-triphenyl porphyrin (10).

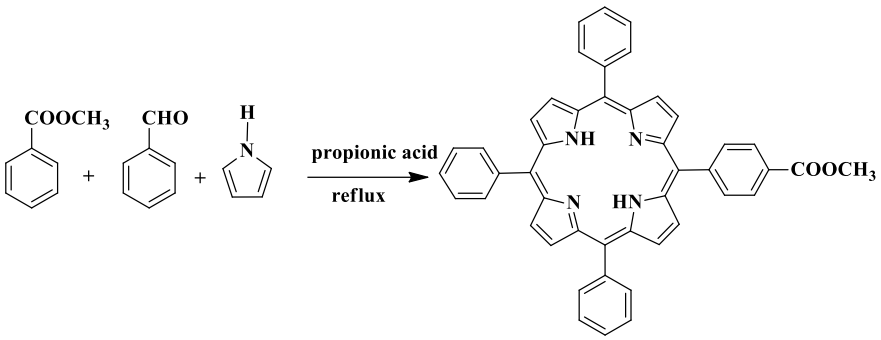

(10)

In a round bottom flask was added benzaldehyde (0.70 mL, 6.89 mmol), methyl-4-formaldehyde (377 mg, 2.30 mmol) and propionic acid (40.0 mL). The reaction mixture was heated to 100 °C and then pyrrole was added dropwise (616 mg, 9.20 mmol). The reaction mixture was refluxed under stirring for 3 hours, protected from light. The solution was cooled to room temperature and then was added CH_3OH and H_2O. The mixture was filtered and the precipitate was successively washed with water (50 mL) and CH_3OH (10 mL). The crude residue was purified by column chromatography (SiO_2, CH_2Cl_2 / Hexane 40 : 60) to obtain the porphyrin **10** as a dark purple solid. Yield: 170 mg (19 %). UV/vis (CH_2Cl_2) λ_{max}, nm (ε, $mM^{-1}cm^{-1}$): 419 (550.5), 516 (28.7), 550 (19.3), 590 (15.6), 642 (8.7). HRMS (MALDI-TOF): *m/z* calcd for $C_{46}H_{32}N_4O_2$: 672.2525 $[M]^+$. Found: 672.2520. Anal. Calcd. For $C_{46}H_{32}N_4O_2$: C, 82.12; H, 4.79; N, 8.33. Found: C, 82.19; H, 4.70; N, 8.35.

Synthesis of Zinc-5-(4-methoxy-carbonyl-phenyl)-10,15,20-triphenyl-porphyrin (11).

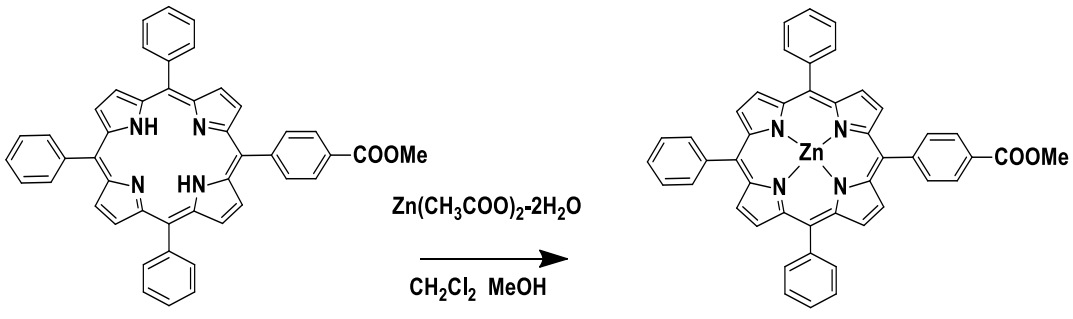

(11)

In a solution of porphyrin **10** (100 mg, 0.149 mmol) in CH_2Cl_2 (100 mL) in a round bottom flask, a solution of $Zn(CH_3COO)_2 \cdot 2H_2O$ (326 mg, 1.49 mmol) in CH_3OH (20 mL) was added and the reaction mixture was stirred at room temperature overnight. The

crude residue was purified by column chromatography (SiO_2, CH_2Cl_2) to obtain the porphyrin **11** as a purple solid. Yield: 107 mg (98 %). UV/vis (CH_2Cl_2) λ_{max}, nm (ε, $mM^{-1}cm^{-1}$): 415 (345.6), 535 (18.9), 580 (6.4). HRMS (MALDI-TOF): *m/z* calcd for $C_{46}H_{30}N_4O_2Zn$: 734.1660 $[M]^+$. Found: 734.1650. Anal. Calcd. For $C_{46}H_{32}N_4O_2Zn$: C, 75.05; H, 4.11; N, 7.61. Found: C, 75.11; H, 4.13; N, 7.58.

Synthesis of Zinc-5-(4-methyl-hydroxy-phenyl)-10,15,20-triphenyl-porphyrin (12).

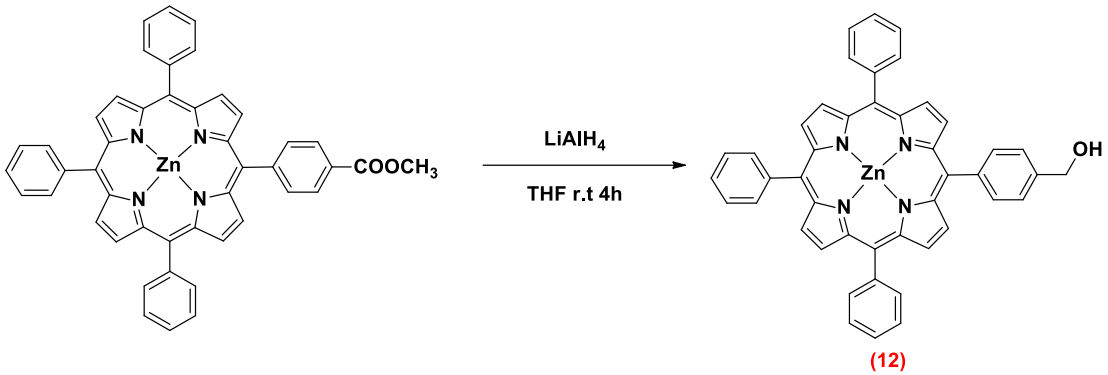

(12)

In a solution of 11 (71 mg, 0.096 mmol) in anhydrous THF (10 mL) in a round bottom flask, $LiAlH_4$ (18 mg, 0.485 mmol) was added and the reaction mixture was stirred at room temperature. After stirring for 30 min, H_2O and then aqueous solution of NaOH 15 % w/v was very carefully poured in the mixture in order to neutralize $LiAlH_4$. After extraction with CH_2Cl_2 / $NaHCO_3$ solvents were evaporated under reduced pressure and the product was purified by column chromatography (SiO_2, CH_2Cl_2) to obtain the porphyrin **12** as a red-purple solid Yield: 48 mg (70 %). UV/vis (CH_2Cl_2) λ_{max}, nm (ε, $mM^{-1}cm^{-1}$): 413 (563.5), 548 (27.4). HRMS (MALDI-TOF): *m/z* calcd for $C_{45}H_{30}N_4OZn$: 706.1711 $[M]^+$. Found: 706.1705. Anal. Calcd. For $C_{45}H_{30}N_4OZn$: C, 76.33; H, 4.27; N, 7.91. Found: C, 76.38; H, 4.21; N, 7.89.

Synthesis of Zinc-5-(4-formyl-phenyl)-10,15,20-triphenyl-porphyrin (13).

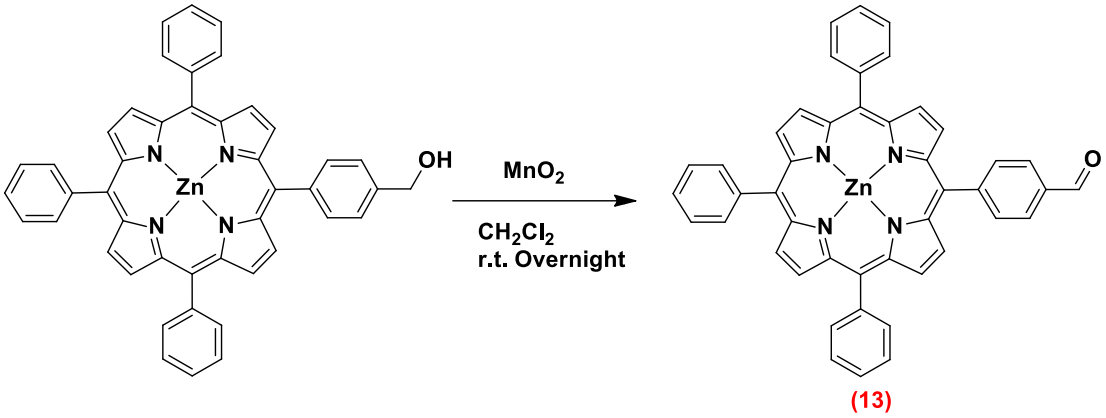

6 eq. of activated manganese oxide (22 mg, 0.25 mmol) was added to a solution of porphyrin **12** (30 mg, 0.042 mmol) in 2 mL chloroform under stirring. The heterogeneous mixture was stirred vigorously at room temperature. The reaction was monitored by thin layer chromatography (TLC) and when the alcohol was oxidized into the aldehyde, manganese dioxide was removed by filtration through Celite, washed three times with chloroform and the combined organic phases were concentrated and dried under vacuum. The crude residue was purified by column chromatography (SiO_2, CH_2Cl_2 / CH_3OH 99 : 1) to obtain the porphyrin **13** as a dark purple solid. Yield: 25.0 mg (83%). UV/vis (CH_2Cl_2) λ_{max}, nm (ε, $mM^{-1}cm^{-1}$): 426 (475.5), 549 (24.8), 587 (5.2). HRMS (MALDI-TOF): *m/z* calcd for $C_{45}H_{28}N_4OZn$: 704.1550 $[M]^+$. Found: 704.1555. Anal. Calcd. For $C_{45}H_{28}N_4OZn$: C, 76.54; H, 4.00; N, 7.93. Found: C, 76.50; H, 4.04; N, 7.97.

Synthesis of Zinc-5-(-Z-2-cyano-3-phenylacrylic acid)- 10,15,20-triphenyl-porphyrin (ZnPCNCOOH) (14).

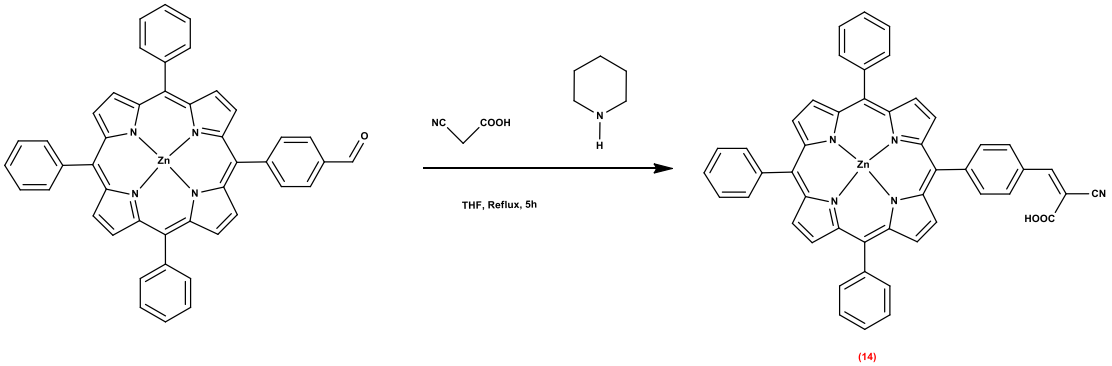

In a solution of porphyrin **13** (25 mg, 0.03 mmol) in THF (1 mL) in a three-necked round bottom flask, 2-cyanoacetic acid (12 mg, 0.14 mmol) and piperidine (1µL) was

added and the mixture was heated to 60 ^{o}C under N_2 atmosphere overnight. The solvents were evaporated under reduced pressure and the product was purified by column chromatography (SiO_2, CH_2Cl_2 / CH_3OH 97 : 3) to obtain the porphyrin **ZnPCNCOOH** as a green-purple solid Yield: 14 mg (56 %). ^{1}H NMR (300 MHz, DMSO): δ 8.80 (m, 8H), 8.53 (s, 1H), 8.42 (d, 2H), 8.37 (d, 2H), 8.18 (m, 6H), 7.80 (m, 9H). ^{13}C NMR (75 MHz, DMSO): δ 163.21, 157.90, 149.45, 149.34, 148.88, 142.71, 135.02, 134.22, 132.00, 131.74, 131.49, 128.72, 128.48, 127.59, 127.10, 126.68, 120.77, 120.58, 118.96. UV/vis (DMSO) λ_{max}, nm (ε, $mM^{-1}cm^{-1}$): 418 (637.0), 550 (25.3), 602 (5.6). Emission (DMSO, λ_{ex} = 540 nm) λ_{em}, nm: 596 (63), 659 (79). HRMS (MALDI-TOF): *m/z* calcd for $C_{48}H_{29}N_5O_2Zn$: 771.1613 $[M]^+$. Found: 771.1611. Anal. Calcd. For $C_{48}H_{29}N_5O_2Zn$: C, 74.57; H, 3.78; N, 9.06. Found: C, 74.61; H, 3.79; N, 9.00.

Synthesis of (Z)-2-cyano-3-(pyridin-4-yl) acrylic acid (15).

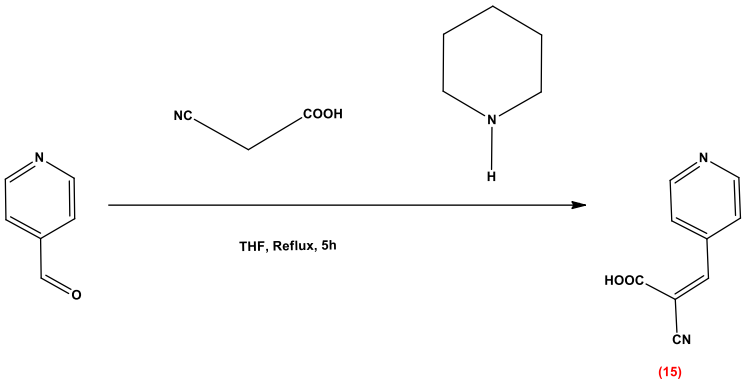

(15)

In a solution of isonicotinaldehyde (14 mg, 0.129 mmol) in THF (5 mL) in a three-necked round bottom flask, 2-cyanocetic acid (66 mg, 0.772 mmol) and piperidine (6μL) was added and the mixture was heated to 60 ^{o}C under N_2 atmosphere overnight. The solvents were evaporated under reduced pressure and the product was purified by column chromatography (SiO_2, CH_2Cl_2/CH_3OH 97:3) to obtain the product **15**. Yield: 15 mg (68 %). HRMS (MALDI-TOF): *m/z* calcd for $C_9H_6N_2O_2$: 174.0429 $[M]^+$. Found: 174.0425. Anal. Calcd. For $C_9H_6N_2O_2$: C, 62.07; H, 3.47; N, 16.09. Found: C, 62.11; H, 3.54; N, 16.00.

Synthesis of CoCNCOOH (C2)(16).

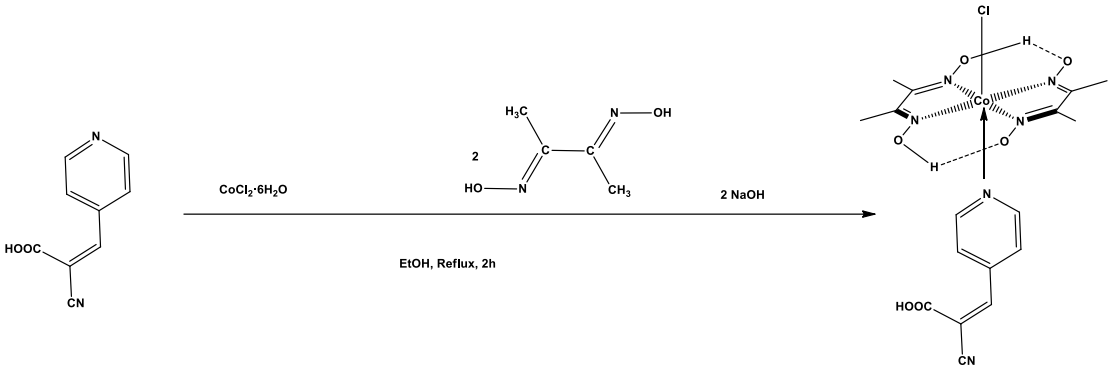

(16)

$CoCl_2 \cdot 6H_2O$ (500 mg, 2.15 mmol), dimethylglyoxime (551 mg, 4.70 mmol), and NaOH (86.0 mg, 2.15 mmol) were dissolved in 95% ethanol (20 mL) and heated to 70°C. Ligand **14** (374 mg, 2.15 mmol) was then added and the resulting solution cooled to room temperature. A stream of air was then passed through the solution for 30 min, which caused precipitation of a brown solid. The suspension was stirred for 1 h and filtered. The precipitate was successively washed with water (5 mL), ethanol (2 x 5 mL), and diethyl ether (3 x 5 mL). The product was then extracted with acetone. Removal of the solvent from the extracts yielded pure complex **C2**. Yield: 932 mg (87 %). HRMS (MALDI-TOF): *m/z* calcd for $C_{17}H_{20}ClCoN_6O_6$: 498.0465 $[M]^+$. Found: 498.0468. Anal. Calcd. For $C_{17}H_{20}ClCoN_6O_6$: C, 40.94; H, 4.04; N, 16.85. Found: C, 40.99; H, 4.00; N, 16.82.

Synthesis of meso-tetrakis-pyridyl porphyrin ($TPyPH_2$) (17)

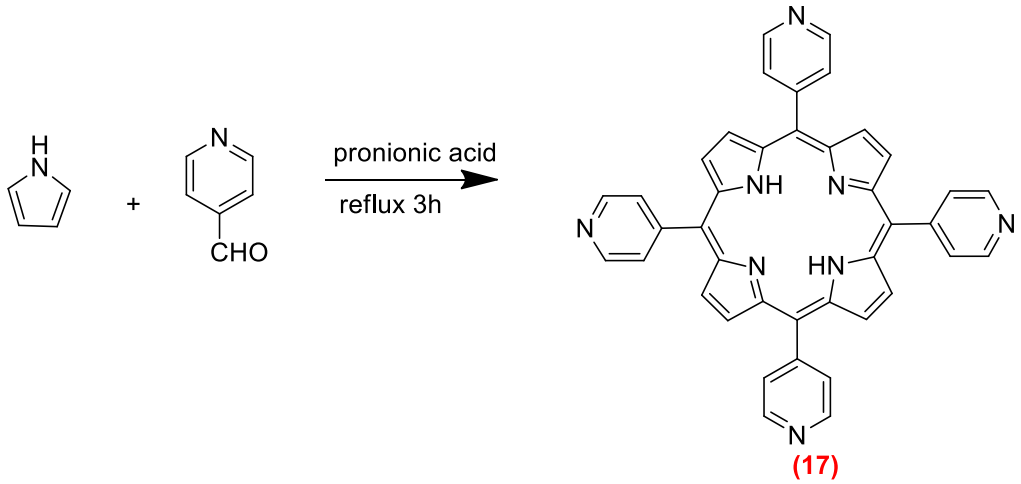

(17)

In a round bottom flask, 125 ml of propionic acid, 3.60 ml (37.7mmol) of pyridine-4-carboxy-aldehyde and 2.63 ml (37.9 mmol) of pyrrole was refluxed at 150°C in a flask

protected from light for 3h. The mixture was cooled to room temperature, was evaporated to dryness. In the flask was added 70 ml of DMF and the mixture was stored in the fridge overnight. The mixture was filtered and the precipitate was successively washed with cold DMF and diethyl ether to obtain the porphyrin (17). Yield: 2.035g (35%). UV–vis: θabs (DMSO) (ε, mM^{-1} cm^{-1}) 415 (256.4), 514 (12.2), 553 (11.2), 576 (4.0), 650 (6.8). HRMS (MALDI-TOF): m/z calculated [M] $C_{40}H_{26}N_8$ 618.2280, found 618.2210.

Synthesis of Zinc-meso-tetrakis-pyridyl porphyrin (ZnTPyP) (18)

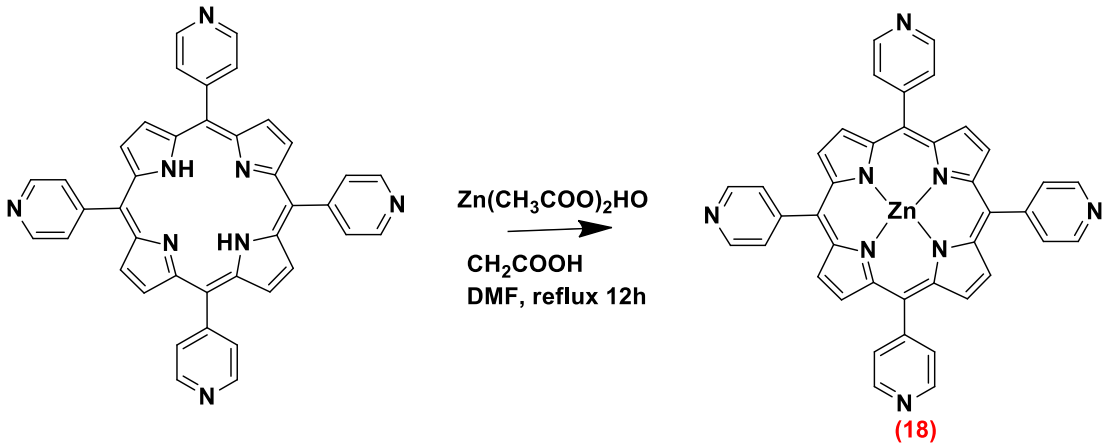

In a round bottom flask porphyrin 17 (240.0 mg, 0.388 mmol), $Zn(CH_3COO)_2 2H_2O$ (1.28 gr, 5.82 mmol), CH_3COOH (24 ml), DMF (24 ml) and a magnetic stirrer were added. The solution was refluxed at 140°C for 12h and was cooled to room temperature. After that, 40 ml of cold water was added and the solution was filtered and washed with cold water and diethyl ether and porphyrin 18 was obtained. Yield: 248.9 mg (94%). UV–vis: θabs (DMSO) (ε, mM^{-1} cm^{-1}) 417 (267.3), 511 (13.1), 574 (5.0). HRMS (MALDI-TOF): m/z theoretical [M] $C_{40}H_{24}N_8Zn$ 680.1415, found 680.1437.

Synthesis of Zinc-*meso*-tetrakis(1-methylpyridinium-4-yl)porphyrin iodine [ZnTMPyP^{4+}]I_4 (19)

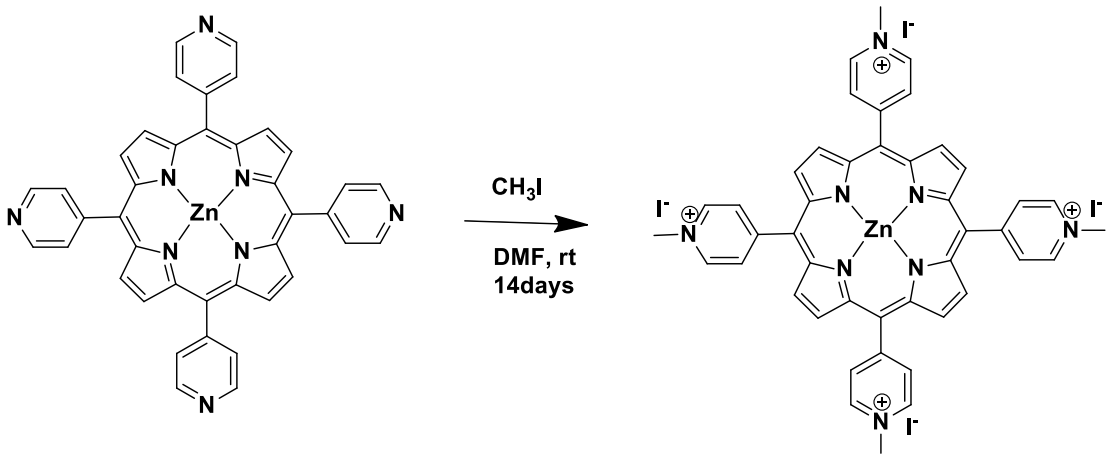

In a round bottom flask, porphyrin 18 (60.0 mg, 0.088 mmol), DMF (11 ml), CH_3I (11 ml, 167.7 mmol) were added. The flask was sealed and stirred at room temperature for 14 days. The reaction stopped and the mixture was transferred to a bottle and 50 ml of diethyl ether was added. The solution was filtered and washed with diethyl ether and porphyrin 19 was obtained. Yield: 107.8 mg (98%). UV–vis: θabs (H_2O) (ε, mM^{-1} cm^{-1}) 418 (266.1), 513 (14.2), 586 (5.5). HRMS (MALDI-TOF): m/z theoretical $[M-4I]^{+4}$ $C_{44}H_{36}N_8ZnI_4$ 740.2332, found 740.2316.

Synthesis of Zinc-*meso*-tetrakis(1-methylpyridinium-4-yl)porphyrin chloride [ZnTMPyP^{4+}]Cl$_4$ (20)

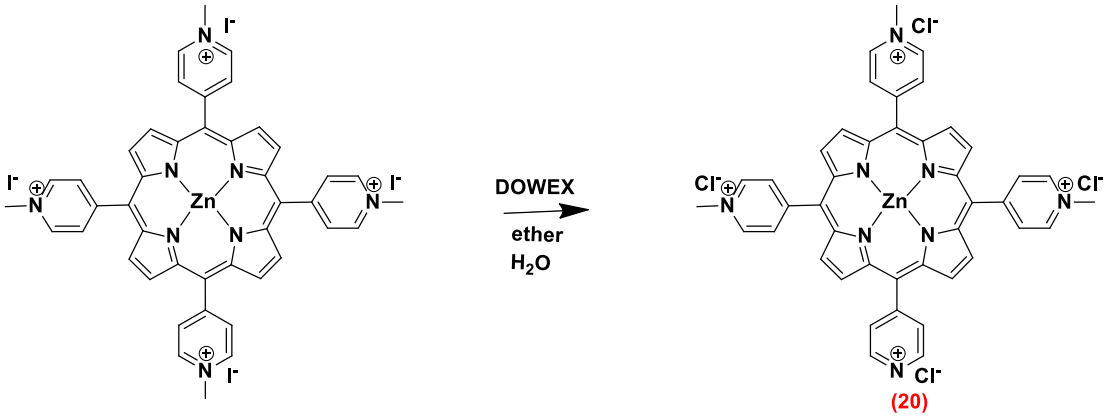

Porphyrin 19 (107.8 mg, 0.086 mmol) was transferred to a bottle with 50 ml of water. The solid was sonicated for a few minutes. A small amount of ion-exchange resin (Dowex) was added to the solution. The mixture passed through a column

chromatography (Dowex, water) and the solvents were evaporated in order to obtain porphyrin 20. Yield (61.1 mg, 96 %). UV–vis: θabs (H_2O) (ε, mM^{-1} cm^{-1}) 418 (268.1), 514 (14.7), 585 (5.7). HRMS (MALDI-TOF): m/z theoretical $[M-4Cl]^{+4}$ $C_{44}H_{36}N_8ZnCl_4$ 740.2338, found 740.2369.

Chapter 3-Results and discussion

I) Photocatalytic hydrogen evolution based on tin porphyrins derivatives and various cobaloximes as catalysts

In the first part of this thesis, we examined the catalytic activity for hydrogen evolution of four tin porphyrins, two water soluble (PS2, PS4) and two partly water soluble (PS1, PS3), and three cobaloximes, that have been previously used from our group as catalysts for similar photocatalytic systems. The porphyrins that were used are $SnTPP(COOMe)_4Cl_2$ (PS1), $SnTPP(COOH)_4Cl_2$ (PS2), $SnTPP(PO(OEt)_2)_4Cl_2$ (PS3), $SnTPP(PO_3H_2)_4Cl_2$ (PS4). The structure of PS and catalysts are shown in **Fig. 24**.

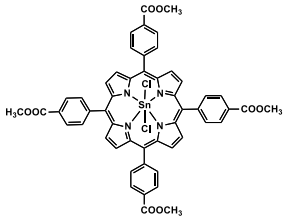

PS1

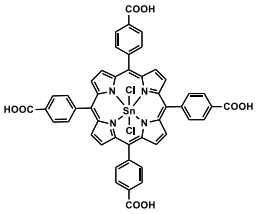

PS2

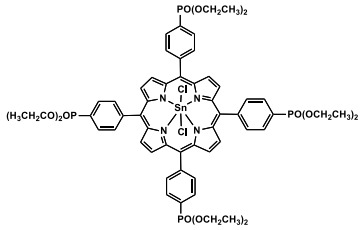

PS3

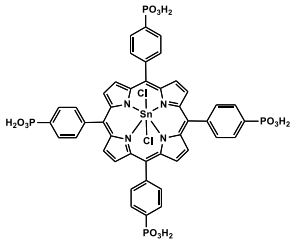

PS4

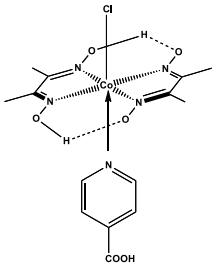

C1

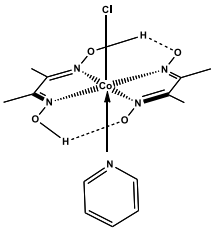

C2

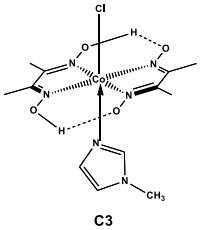

C3

Fig. 24: Structure of the four PS and the three cobaloximes that were used for the photocatalytic experiments.

The idea to test these complexes based on previous publications of our group. In one of them, the group reported photocatalytic systems for H_2 production in mixed aqueous/organic pH 7 solutions.[75] These systems consist of various cobaloxime catalysts $Co(dmgH)_2(L)Cl$ (L = nitrogen-based axial ligands) and a water soluble porphyrin as a photosensitizer. They were assayed in the presence of triethanolamine as sacrificial electron donor. In another publication, we reported a photocatalytic system consisting of different cobaloxime catalysts, a partly water soluble Sn-porphyrin based dye as photosensitizer, a TEOA as sacrificial donor in acetonitrile/H_2O solution.[76`] Tin(IV)-porphyrin derivatives have already been used as mimics for the photocatalysis of light-driven water-oxidation and proton-reduction[77] due to the fact that they have suitable redox potentials for water splitting. Also, these porphyrins are very stable as the large, highly-charged Sn^{4+} ion fits perfectly into the porphyrin ring system.[78] In addition, it has already been demonstrated that tin(IV) porphyrins can be used in combination with heterogeneous platinum-based hydrogen evolution reaction catalysts for photocatalytic H_2 production. In order to expand our research for tin porphyrins we thought to examine the porphyrins above (**Fig. 24**) using standard cobaloxime catalysts. We wanted to compare the water soluble (PS2, PS4) with the partly water soluble (PS1, PS3) porphyrins under exactly the same photocatalytic conditions for hydrogen evolution.

1°) Synthesis of the compounds

The porphyrins that were used have already been synthesized in our group but most of them have never been metallated with tin. We could also obtain the X-ray structure of PS1.

The catalysts were available in the lab and were used before from our group.[75]

The synthesis for the PS4 was a little bit difficult and we could not manage to obtain and characterise the final product.

2°) Photocatalytic tests

The initial experiments were made with the two water soluble porphyrins (PS2, PS4). In our present work, after 24 hours of irradiation no hydrogen was obtained using the

three cobaloximes as catalysts. It is obvious that under these experimental conditions the tin water soluble porphyrins cannot produce hydrogen, in full agreement with our previous work. We also add TiO_2 that can act as an electron relay in order to enchance the photocatalytic activity.[76] The attachment of TiO_2 to a component needs an anchoring group such as carboxyl.

In our previous publications the water soluble porphyrins were $[ZnTMPyP^{4+}]Cl_4$ and $[SnTMPyP^{4+}]Cl_4$. On the one hand, the water soluble zinc porphyrins were catallytically active for hydrogen evolution, but the water soluble tin porphyrin did not evolute hydrogen at all. On the other hand, the water insoluble zinc porphyrin did not produce hydrogen, but the partly water soluble tin porphyrin did.

In this thesis, when the partly water soluble porphyrins were used, we could observe hydrogen evolution/production for almost 48 hours with every cobaloxime (**Fig. 25**)

Fig. 25: Comparison of photocatalytic hydrogen evolution for PS3 (a) and PS1 (b) with the three different cobaloximes.

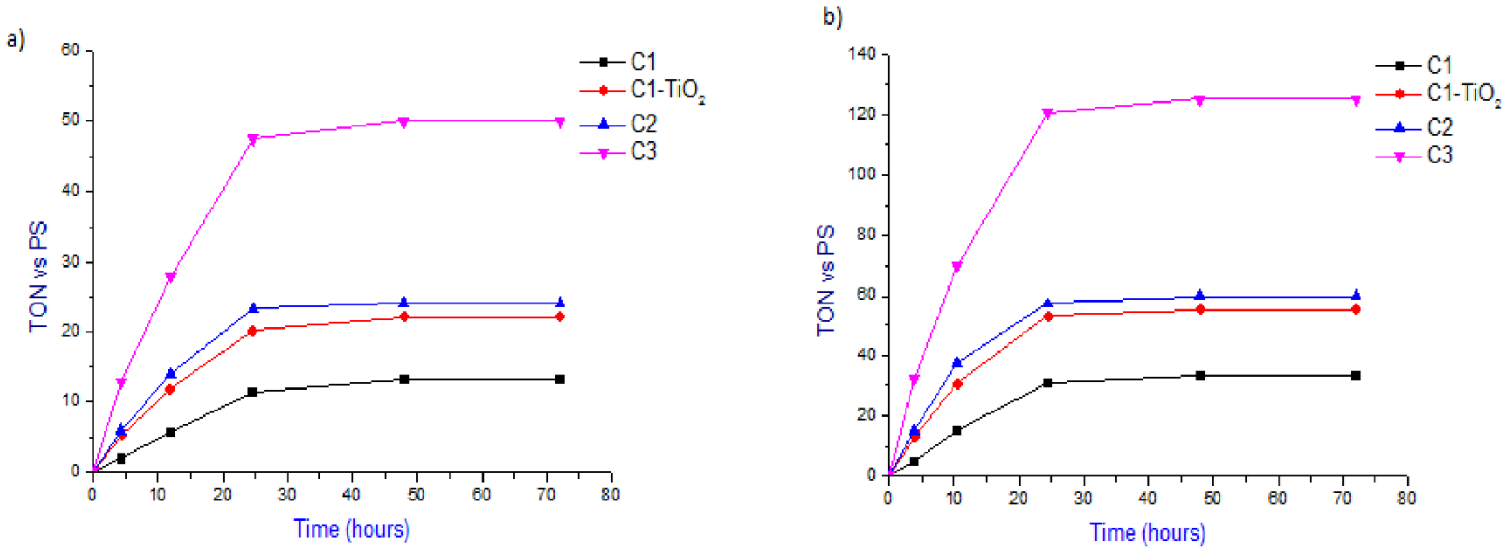

In order to understand why we have these changes among tin and zinc porphyrins, we sent samples to collaborators for further research and especially for transient absorption spectroscopy.

After a quick observation of the graphs, it is obvious that the most active PS is the Sn-TPP-$(COOMe)_4$. For both PS, the biggest TONs are obtained with the imidazole derivatives (C3) and the lowest with the carboxylatopyridine (C1). The optimal photocatalytic system is the one with PS1 and C3 and it reaches 128 TONs after 48 hours of irradiation. For C1, we managed to increase the TONs for both PS when TiO_2 nanoparticles were used due to the fact that this catalyst has anchoring group and can attached to TiO_2 that generally is considered to enhance the electron transfer rate. [76]All these observations are in complete agreement with a previous publication of our group, in which biggest turnover numbers are obtained with electron-rich axial ligands such as imidazole derivatives.[75] Lower stabilities are observed with various pyridine axial ligands, especially for those containing electron-acceptor substituents. Using pyridine ligands with electron donating groups as axial ligands yield highly effective catalysts. Such an activity can be explained on the basis of the basicity of these N-based aromatic ligands, resulting in various electron-donor ability, after binding to cobalt. The higher pKa of imidazole derivatives correlates well with the higher stability of the corresponding systems compared to pyridine-based ones. In addition, when the axial ligand is the para-carboxylatopyridine the activity of the system is increased in the presence of TiO_2 nanoparticles.

We obtain only some traces of hydrogen at pH 6 and 8 that means that our photocatalytic system is more active in pH 7, an observation that we have for most of similar photocatalytic systems.[75]

CONCLUSIONS

In summary, photocatalytic systems consisting of cobaloximes catalysts with Tin-porphyrins as photosensitizers, TEOA 5% v/v as sacrificial electron donor at pH 7 in CH_3CN/H_2O (1:1) solution, were reported. Upon visible irradiation, hydrogen production was detected with the best result obtained at pH 7 with dye **PS1** ($C = 4.0 \times 10^{-5}$ M) and the catalyst **C3** ($C = 4.9 \times 10^{-4}$ M) with a TON of 128, after 48 hours and

with dye **PS2** ($C = 4.0 \times 10^{-5}$ M) and catalyst **C3** ($C = 4.9 \times 10^{-4}$ M) with a TON of 48, after the same irradiation time. The presence of TiO_2 nanoparticles increased the photocatalytic activity when we used the **C1**. Further investigations are necessary to shed light on the electron transfer in photocatalytic systems that have been used in this study.

II) Photocatalytic hydrogen evolution based on Zinc porphyrins derivatives and cobaloximes with cyano-acetic acid anchoring groups

The aim of this work was to study the photocatalytic hydrogen production with cobaloximes complexes **C1**-**C3** as catalysts and water soluble dyes **P1**, **P2** and **P3** as photosensitizers bearing cyano carboxylate groups in the presence or not of TiO_2 nanoparticles. (**Fig. 27**)

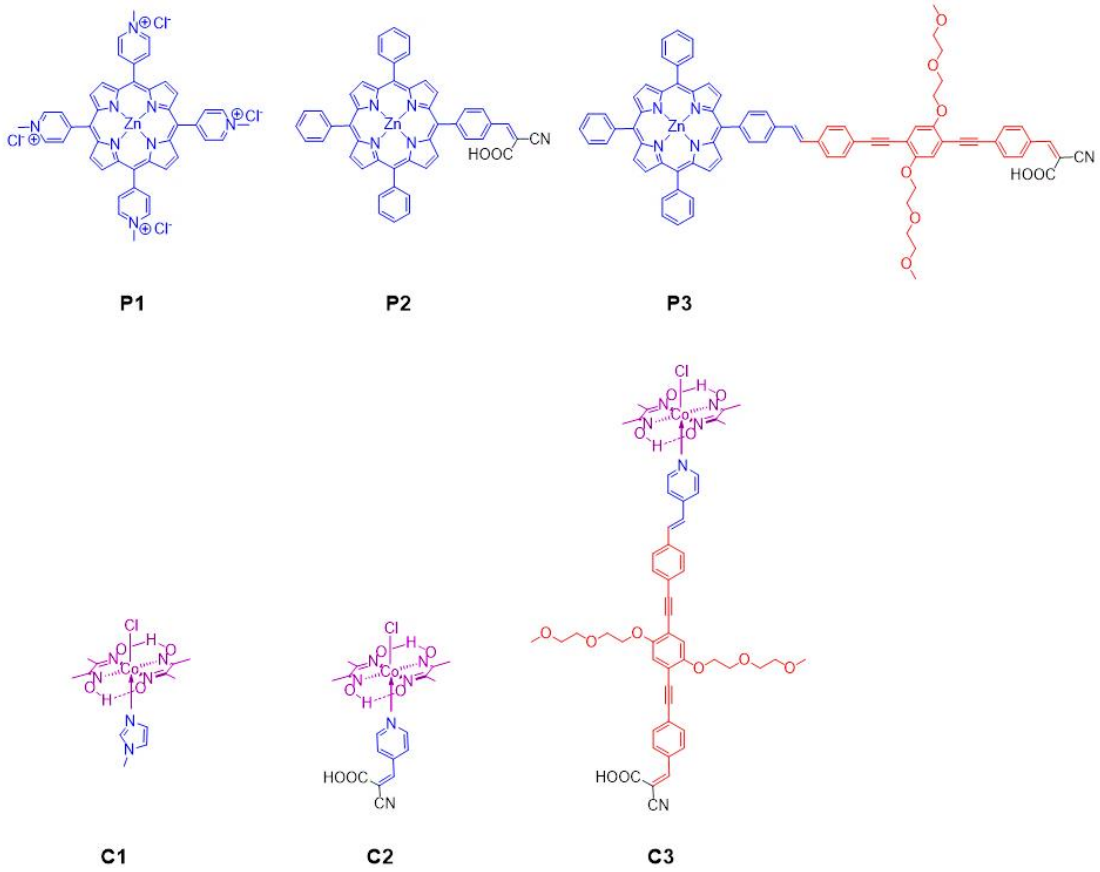

Fig. 27: The structure of PS and catalysts employed in this study

Therefore, our current study is based on our previous published work where a combination of Zn water soluble porphyrin **[ZnTMPyP]Cl_4** (**P1**) sensitizer, a cobaloxime catalyst **CoN-Methyl-imidazole** (**C1**) and TEOA at pH = 7 in 1:1 CH_3CN-H_2O solution.[75] In addition, the photochemical hydrogen production was studied using **C1**-**C3** as catalysts and **P1**, **P2** and **P3** as photosensitizers at different pH = 6, 7, 8 and 9 in the presence of 20 mg of TiO_2 nanoparticles.

Initial experiments were performed in order to produce hydrogen from the systems that contain **C2, C3** complexes as catalysts and **P2** and **P3** as as photosensitizers, respectively. In these cases, no hydrogen was observed after continuous irradiation of the samples. The same results were performed and when the combinations of the photosensitizer and catalyst were the following **C2**-**P3** and **C3**-**P2**, in various of different conditions. For this reason we wanted to examine which factors prevent the hydrogen production. According to our previous work catalyst **C1** was sufficiently efficient.[75] Therefore, catalyst C1 in combination of photosensitizers **P2** and **P3**, were studied. In neither case, no hydrogen evolution was performed after continuous irradiation of the samples. Therefore, it can be concluded that the porphyrins **P2** and **P3** were not efficient photosensitizers in these systems, because the cyano-acetic acid anchoring groups are electron acceptors reducing the rate of electrons which were transferred in the complexes of cobaloximes for proton reduction.

On the other hand, the systems containing porphyrin **P1** as photosensitizer and the cobaloximes **C2** and **C3**, respectively, showed quite well hydrogen production yields.

The best results for hydrogen production system were obtained when porphyrin **P1** and cobaloxime **C2** were used, as shown in Fig. . Upon irradiation of the system at pH 7, up to 240 turnovers of H_2 obtained after 23 hours of irradiation without the presence of TiO_2 nanoparticles. On the other hand, when TiO_2 nanoparticles were used under the same conditions the production of hydrogen was reduced to 210 turnovers of H_2.

Based on previous publications of our group, the use of TiO_2 nanoparticles increases the catalytic activity, however, in this case the cyano-acetic acid as anchoring group of

cobaloximes, maybe commit more easy the electron transfer from cobaloxime catalyst to TiO_2 nanoparticles. This process results in the decrease of catalytic efficiency.

Hydrogen production was studied at pH 6, 7, 8 and 9. In the case of pH 9 lower production of hydrogen was observed for all the systems. The pH value is an important factor in photochemical hydrogen production since the efficiency of the system depends on the concentration of the protonated and the non protonated form of the sacrificial donor. It is known that the optimum pH value is often close to the pKa value of the sacrificial electron donor, in our case the pKa of TEOA is 7.76. Therefore, at pH > pKa there is a low amount of SED that makes the quenching and regeneration of the photosensitizer less efficient. This can explain why the H_2 production at pH = 9 is low. Fairly important hydrogen evolution occurred for systems at pH 6, 7 and 8.[76]

More specifically, when **P1** was used as photosensitizer, and cobaloxime **C2** as catalyst the production of hydrogen recorded 147 TON at pH 6, 240 TON at pH 7, 32 TON at pH 8 and 20 TON at pH 9 after 23 hours of irradiation of the solutions in the absence of TiO_2 nanoparticles (**Fig. 28a**). In the presence of TiO_2 nanoparticles the photocatalytic H_2 production recorded 139 TON at pH 6, 210 TON at pH 7, 15 TON at pH 8 and 8 TON at pH 9 after 23 hours of irradiation of the solutions (**Fig. 28b**).

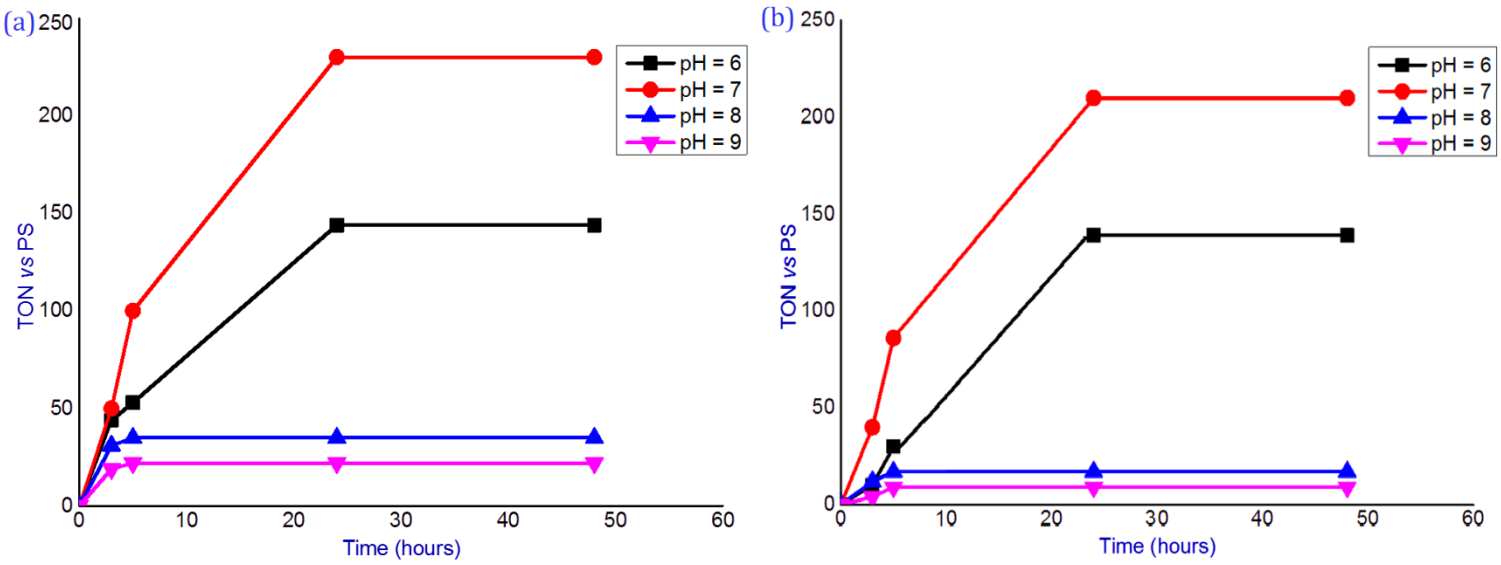

Fig. 28: Plots of hydrogen production upon irradiation (λ > 440 nm) of solutions (1:1 CH_3CN-H_2O) containing **P1** (C = 4.0 × 10^{-5} M), **C2** (C = 4.9 × 10^{-4} M) and TEOA 5%

v/v at pH 6, 7, 8 and 9, without TiO_2 nanoparticles (a) or with 20 mgr of TiO_2 nanoparticles in reaction's solutions (b).

In the photocatalytic system with photosensitizer **P1**, and cobaloxime **C3** as catalyst the production of hydrogen was recorded 49 TON at pH 6, 60 TON at pH 7, 22 TON at pH 8 and 8 TON at pH 9 after 23 hours of irradiation of the solutions without TiO_2 nanoparticles (**Fig. 29a**). In the presence of TiO_2 nanoparticles the photocatalytic H_2 production recorded 10 TON at pH 6, 15 TON at pH 7, 6 TON at pH 8 and 2 TON at pH 9 after 23 hours of irradiation of the solutions (**Fig. 29b**).

These results are in complete agreement with previous observations of the **P1**-**C2** system. And in this case, the presence of nanoparticles are reducing the photocatalytic activity. Also, the observations for the pH values are in agreemet with the litterature. Overall, this system is less effective in relation to **P1**-**C2** system. The use of π spacer group (SP) between the pyridine and the anchoring group on cobaloxime reduces the photocatalytic activity.[79-80] This observation can be explained by the fact of the effective electron transfer from the cobaloxime to the cyano-acetic acid anchoring group. For this reason, the presence of TiO_2 nanoparticles reduce rapidly the photocatalytic activity.

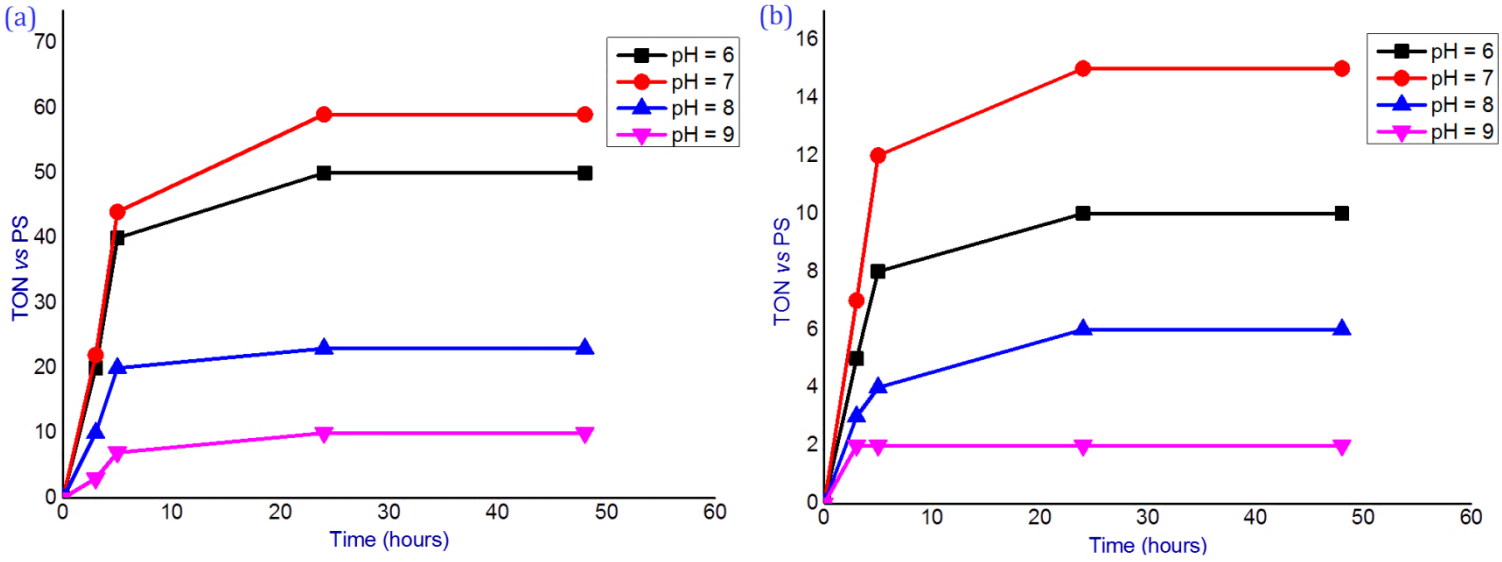

Fig. 29: Plots of hydrogen production upon irradiation (λ > 440 nm) of solutions (1:1 CH_3CN-H_2O) containing **P1** (C = 4.0×10^{-5} M), **C3** (C = 4.9×10^{-4} M) and TEOA 5% v/v at pH 6, 7, 8 and 9, without TiO_2 nanoparticles (a) or with 20 mgr of TiO_2 nanoparticles in reaction's solutions (b).

CONCLUSIONS

In summary, photocatalytic systems consisting of cobaloximes catalysts with Zn-porphyrins as photosensitizers, TEOA 5% v/v as sacrificial electron donor at pH 6, 7, 8 and 9 in CH_3CN/H_2O (1:1) solution, were reported. Upon visible irradiation (λ > 440 nm) hydrogen production was detected with the best result obtained at pH 7 with dye **P1** (C = 4.0×10^{-5} M) and the catalyst **C2** (C = 4.9×10^{-4} M) with a TON of 240, after 23 hours and with dye **P1** (C = 4.0×10^{-5} M) and catalyst **C3** (C = 4.9×10^{-4} M) with a TON of 60, after the same irradiation time. The presence of TiO_2 nanoparticles reduced the photocatalytic activity. The hydrogen evolution with dye **P1** (C = 4.0×10^{-5} M) and catalyst **C2** (C = 4.9×10^{-4} M) with TiO_2 was 210 TON, after 23 hours and with dye **P1** (C = 4.0×10^{-5} M) and catalyst **C3** (C = 4.9×10^{-4} M) with TiO_2 was 15 TON, after the same hours. Further investigations are necessary to shed light on the electron transfer in photocatalytic systems that have been used in this study.

III) Photocatalytic hydrogen production with novel nickel(II) and cobalt(II) aminopyridyl complexes

Control of the factors that govern the reactivity of a metal complex is crucial in homogeneous metal-based catalysis. It is usually assumed that the reactivity of a metal center is mainly dictated by the interaction between the metal center and its primary coordination sphere. In Nature, in addition to the first coordination sphere, the second coordination sphere also plays an important role. In oxygenase metalloenzymes, the local environment and notably hydrogen bond networks have an essential role in the generation of high-valent species in the catalytic cycle of these

enzymes. For example, proton delivery to the coordinated peroxo moiety in metal monooxygenase hydroxylase, a dinuclear nonheme iron enzyme, triggers O-O bond cleavage in the peroxo intermediate and affords a high-valent, diiron oxo intermediate, which is capable of hydroxylating methane.[81] In hydrogenase metalloenzymes the presence of proton relays are also essential for the efficient reduction of H^+ into H_2.[82] In the third part of this thesis, we are interested in developing new catalytic systems possessing in their second coordination sphere functional groups able to interact with different kind of substrates to enhance the catalytic activity of the targeted reactions. One collaborator of the SolHyCat group (Pascal Guillo, from the Laboratoire de Chimie de Coordination in Toulouse, France) designed ligands decorated in the second coordination sphere by hydroxyl groups that have CF_3 substituents in their proximity.[83] First row metal complexes (metal = manganese, iron, cobalt, nickel, copper and zinc) have been prepared and tested for proton reduction. For proton reduction, the fluoroalcohol groups might act as proton relays.

1°) Photocatalytic activity assessment of the Ni complexes

The goal of the third part was to examine if two novel nickel complexes (**Fig. 30**) possess any photocatalytic activity for hydrogen evolution.

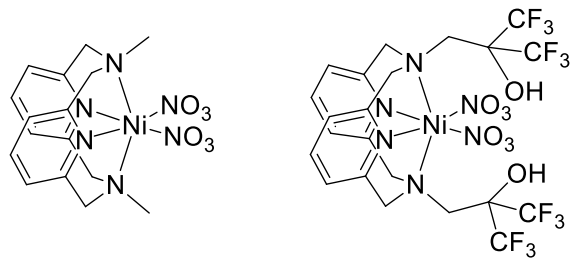

Fig. 30: Structure of the catalysts

After a detailed bibliographic study, we started to realise experiments using four different photosensitizers as shown in the figure below (**Fig. 31**)

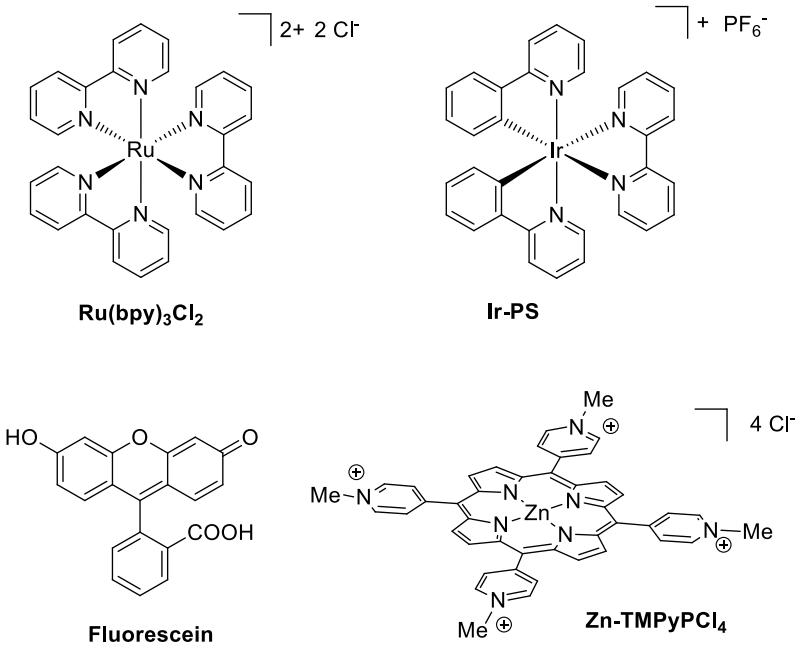

Fig. 31: Structure of the photosensitizers

In the table below (**Table 2**) is shown in details the experiments that took place in order to find the best experimental conditions.

Table 2: Experiments that have been done in order to assess the photocatalytic activity of the two novel nickel complexes

Catalyst	PS	Ratio (PS/cat)	Solvents	SED	pH	**TON vs Cat** (time when H_2 evolution stopped)
PGII-99	**$Ru(bpy)_3Cl_2$**	5:1	H_2O	TEOA	8	-
		5:1	H_2O	Ascorbate	4.5	0.3
		5:1	H_2O/CH_3CN (1:1)	Ascorbate	2.5	-
PGII-99	**$[ZnTMPyP]Cl_4$**	5:1	H_2O	TEOA	8.5	-
			H_2O/CH_3CN (1:1)	TEOA	7	-
PGII-99	**Fluorescein**	10:1	$EtOH/H_2O$ (1:1)	TEA	12.5	20.0 (20h)
						Hg => < 1
PGII-99	**Ir-PS**	5:1	**H_2O/CH_3CN (1:1)**	**TEA (5%)**	**10**	12.5 (5h)
						Hg => 8.0 (3h)
	″	1:5	″	″	″	3.4 (6h) (eq. to 17.2 vs PS)
	″	1:1	″	″	″	9.0 (7h)
	″	**10:1**	″	″	″	**28.0 (6h)**
						Hg => 23.2 (5h)
	″	10:1	″	″	″	13.3 (4h)
	″	10:1	″	″	11	14.4 (4h)
	″	10:1	″	″	9	16.6 (4h)
	″	10:1	″	TEA (10%)	10	18.2 (3h)
PGII-83	**$Ru(bpy)_3Cl_2$**	5:1	H_2O	Ascorbate	4.5	-
		5:1	H_2O/CH_3CN (1:1)	″	2.5	0.2
PGII-83	**Fluorescein**	10:1	$EtOH/H_2O$ (1:1)	TEA	12.5	-
PGII-83	**Ir-PS**	5:1	H_2O/CH_3CN (1:1)	TEA (5%)	10	3.6 (2.5h)
						Hg => 4.6 (2h)
	″	1:5	″	″	″	0.04 (2.5h) (eq. to 0.2 vs PS)
	″	10:1	″	″	″	7.4 (3h)
	″	1:1	″	″	″	1.4 (3h)
	″	10:1	″	″	11	8.3 (1h)
	″	10:1	″	″	9	7.5 (3.5h)
	″	10:1	″	TEA (10%)	10	8.0 (2h)

We could obtain hydrogen when we employed the Ir-PS or fluorescein (20 TON). For control experiments with Hg, a drop of Hg was added to the solutions and irradiation was performed under vigorous stirring to investigate if metallic nanoparticles or colloids could be responsible for the observed H_2 evolution. When fluorescein is employed, activity is lost in presence of Hg, which suggests that catalytically active nanoparticles were present in the first test.

We thus decided to focus on the use of Ir-PS and since we used novel nickel complexes for hydrogen production, a systematic study of this system was necessary. Therefore, different pH, different TEA, dye and catalyst concentrations were examined in order to obtain the best hydrogen production of the photocatalytic system. The concentrations of the photosensitizer and the catalysts were selected based on the observations from previous work of our lab and previous publications where relative photocatalytic systems were used.

a) Effect of catalysts and photosensitizer concentration

In order to study the effect of catalyst and photosensitizer concentration in hydrogen production all different parameters were kept constant such as pH (pH =10), sacrificial electron donor (TEA 5% v/v) and the solution (acetonitrile/water 1/1). For the initial experiment Ir-PS was used in concentration 5×10^{-4} M and the catalyst in concentration 10^{-4}M and 12.5 TON were obtained for PGII-99 and 4.97 for PGII-83. We could observe for both catalysts that when we increased the concentration of the photosensitizer (10^{-3}M) keeping constant the concentration of the catalyst, the TON were increased and when we increased the concentration of the catalyst, (5×10^{-4} M) TON were decreased. These were also observed in other systems described in the literature. The best result was obtained using 5.0 x 10^{-4} M of photosensitizer giving 28 TON after 6 hours when 5.0 x 10^{-5} M of catalyst **PGII-99 (Fig. 32)** was used and 7.4 TON after 3 hours in the case of 5.0 x 10^{-5} M of catalyst **PGII-83 (Fig. 33).**

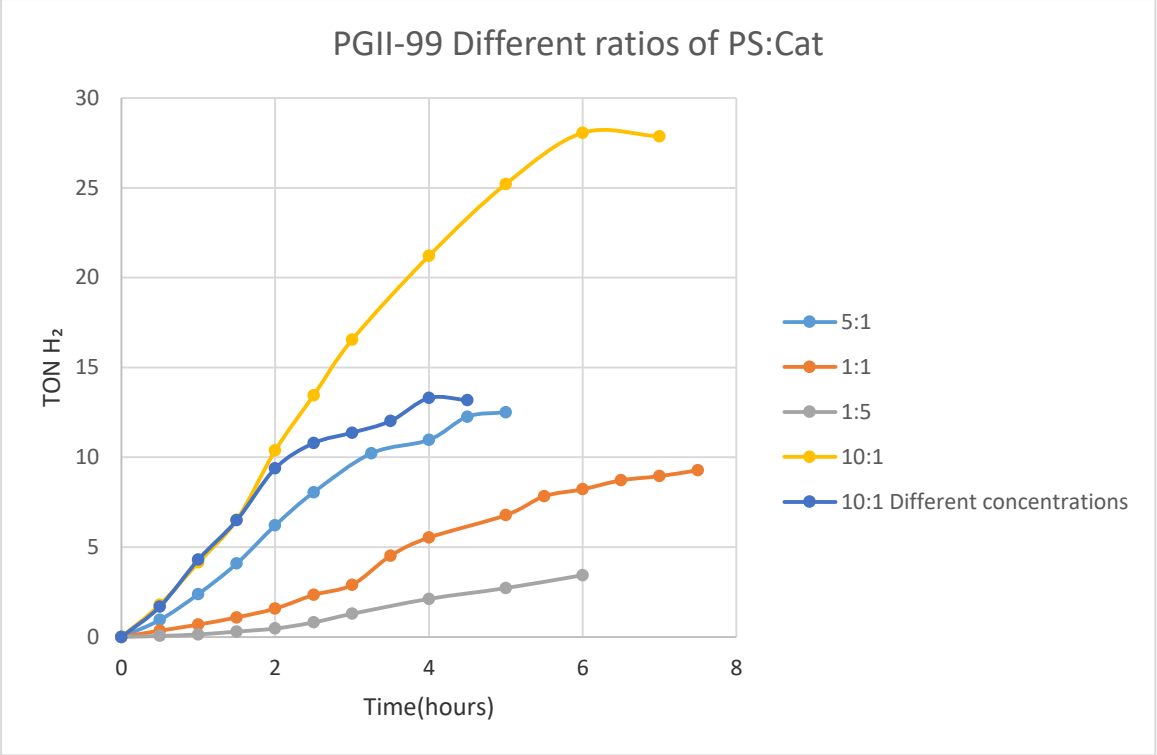

Fig. 32: Plot of hydrogen production upon irradiation of solutions (1:1 acetonitrile/water) containing different concentrations of **Ir-PS** and **PGII-99** and TEA 5% v/v at pH 10.

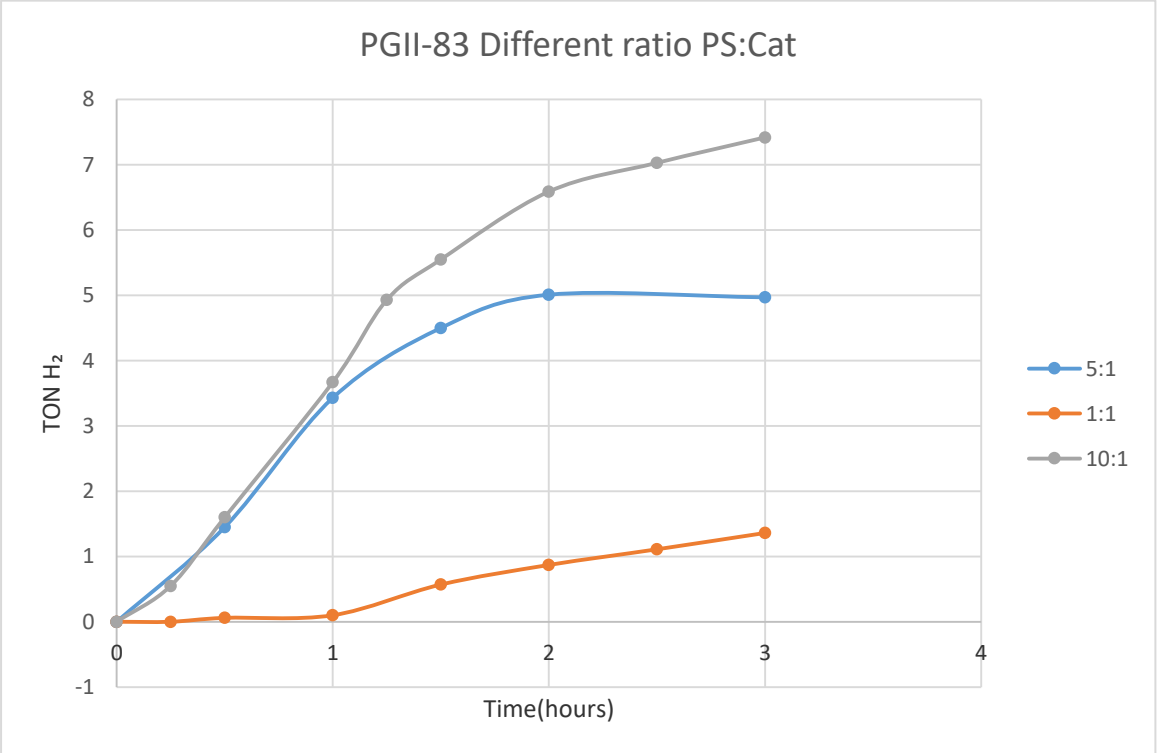

Fig. 33: Plot of hydrogen production upon irradiation of solutions (1:1 acetonitrile/water) containing different concentrations of **Ir-PS** and **PGII-83** and TEA 5% v/v at pH 10.

b) Effect of proton's concentration (pH)

One important parameter that we examined was the pH. More specifically the TON numbers were measured at pH 9, 10 and 11. The efficiency of the system depends on the concentration of the protonated and the non-protonated form of the sacrificial electron donor. It is known that the optimum pH value is often close to the pKa value of the sacrificial electron donor, in our case the pKa of TEA is 10.75. Therefore, at pH < pKa there is a low amount of SD that makes the quenching and regeneration of the photosensitizer less efficient. This could explain why the H_2 production at pH = 9 is less compared to pH = 10.

The optimum pH value for the PGII-99 (**Fig. 34**) is 10 reaching 28 TON after 6 hours of irradiation. At higher pH 11, less amount of hydrogen is detected, probably due to the fact that in more basic conditions there are less protons in order to be reduced and also it seems that the catalysts are not so stable under more basic conditions.

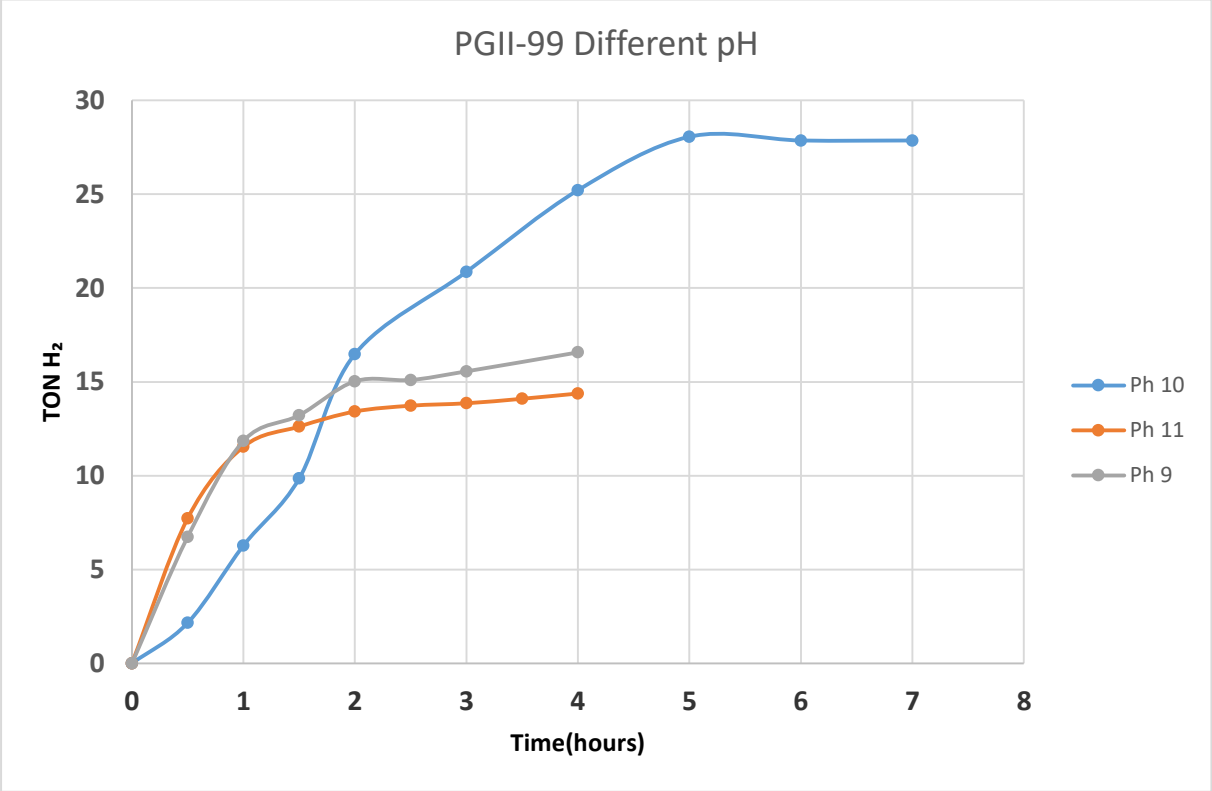

Fig. 34: Plot of hydrogen production upon irradiation of solutions (1:1 acetonitrile/water) containing **PS** (C_{PS} = 5.0 × 10^{-4} M), **catalyst PGII-99** (C_{cat} =5×10^{-5} M) and TEA 5% v/v at different pH.

The optimum pH value for the PGII-83 (**Fig. 35**) is 11 with TON of 8.3 after only 1 hour of irradiation. We could observe that the TON numbers in pH 11 is bigger compared to 7.4 TON in pH 10 but we could detect hydrogen only in the first hour of irradiation. The difference between the two nickel complexes may be explained by the presence of the hydroxyl groups although their effect is not clearly understood yet

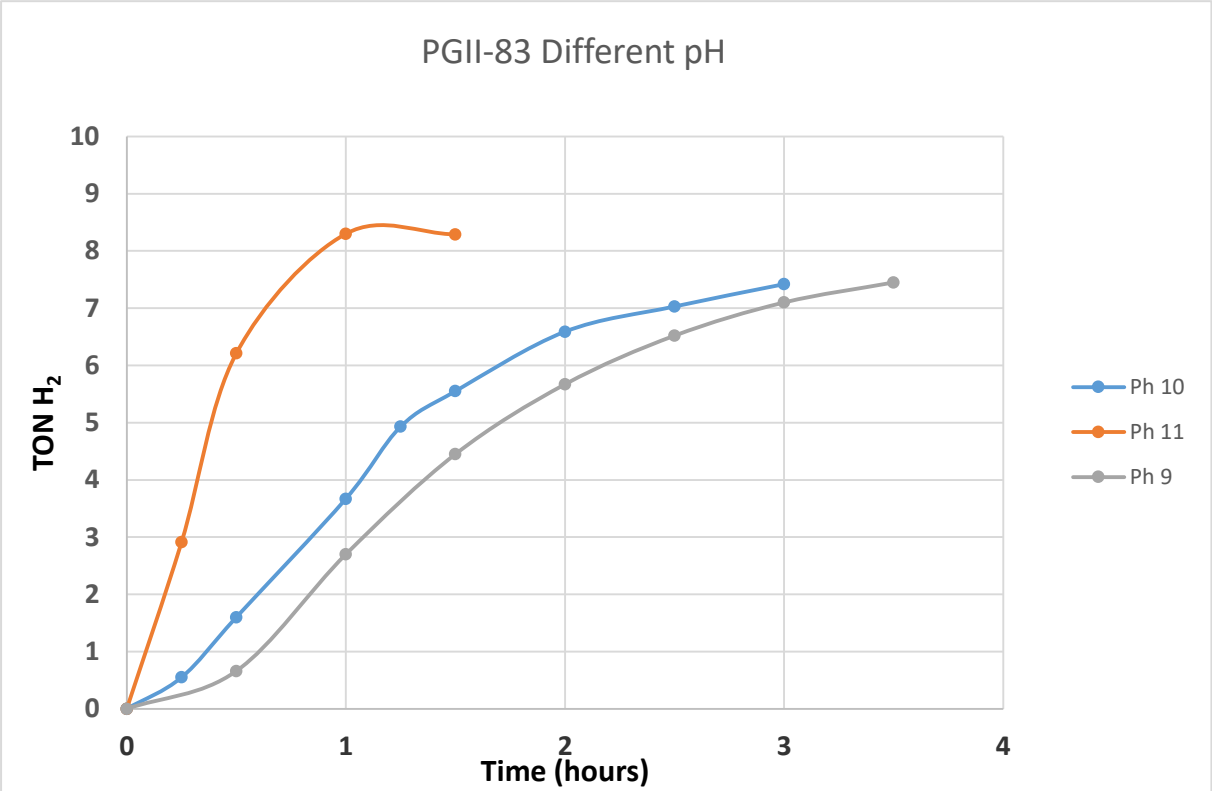

Fig. 35: Plot of hydrogen production upon irradiation of solutions (1:1 acetonitrile/water) containing **PS** (C_{PS} = 5.0 × 10^{-4} M), **catalyst PGII-83** (C_{cat} =5×10^{-5} M) and TEA 5% v/v at different pH.

c) Effect of the concentration of TEA

The light-driven hydrogen production catalysed by the nickel catalysts is also dependent on the amount of sacrificial electron donor. For instance, for PGII-99, the yield of hydrogen production is lower at higher TEA concentration (**Fig. 36**). Probably there are stability issues in the presence of a higher concentration of base.

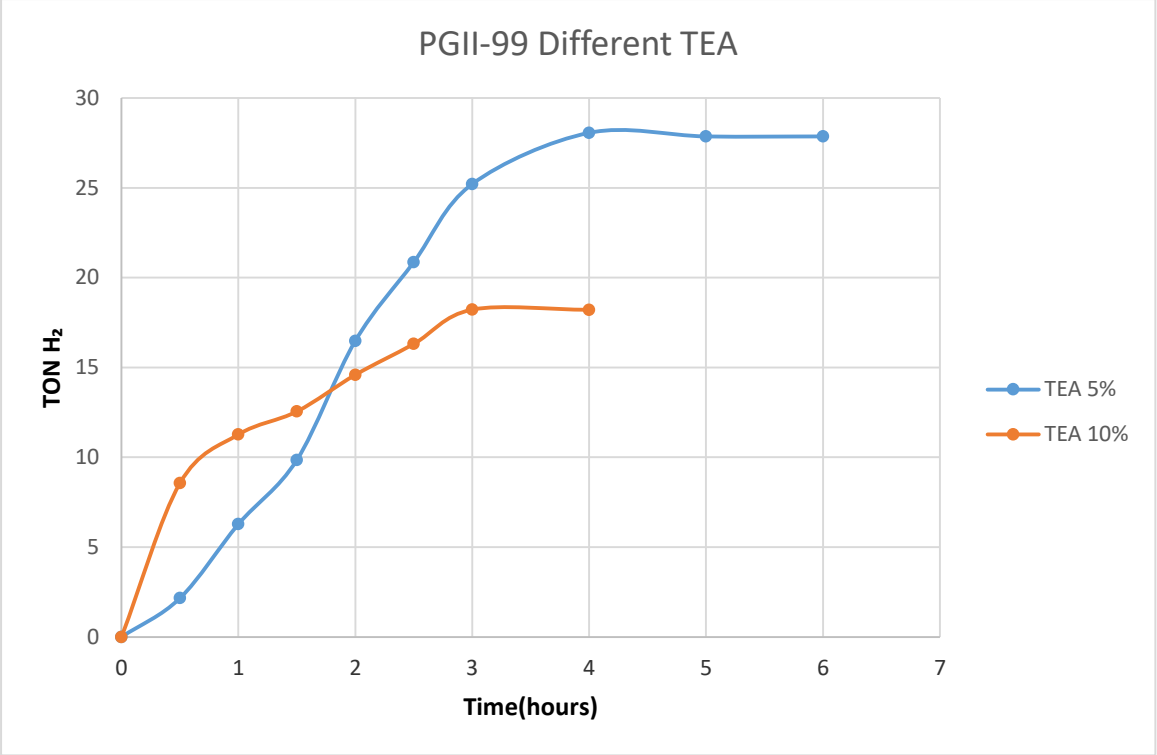

Fig. 36: Plot of hydrogen production upon irradiation of solutions (1:1 acetonitrile/water) containing **PS** (C_{PS} = 5.0 × 10^{-4} M), **catalyst PGII-99** (C_{cat} =5×10^{-5} M), pH 10 and different concentrations of TEA.

For PGII-83, again we could observe higher TON numbers (8.0 after 2 hours of irradiation) due to the presence of hydroxyl groups (**Fig. 37**).

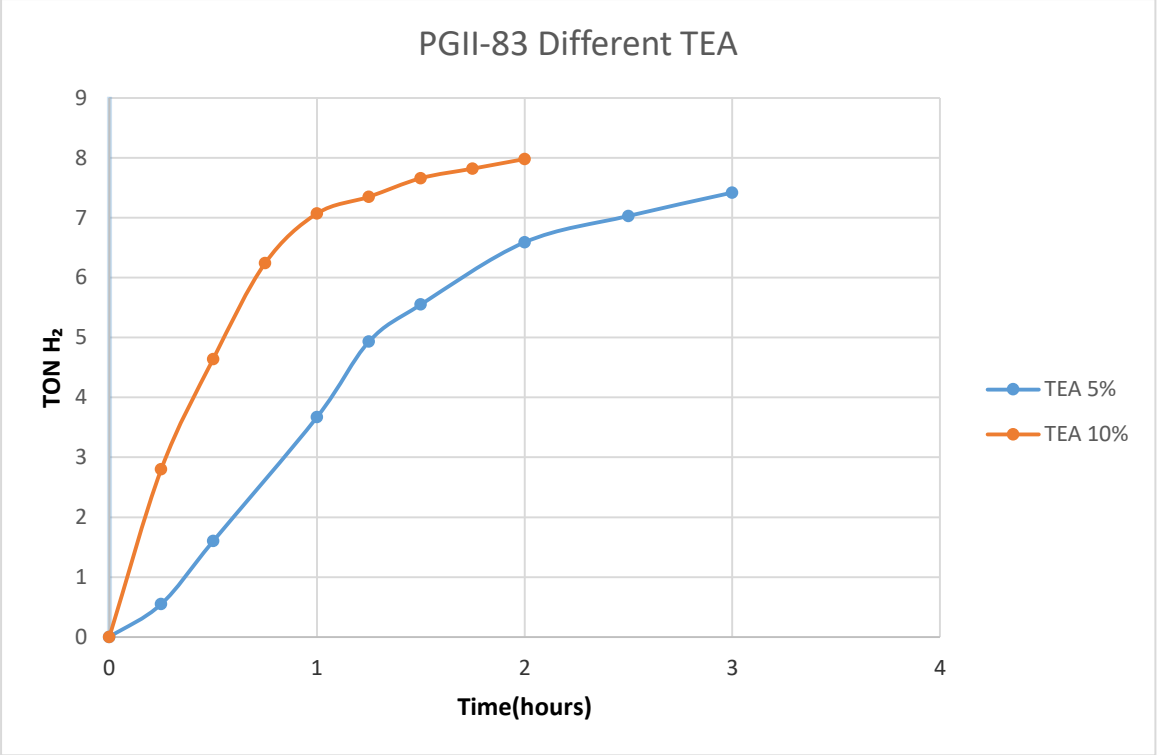

Fig. 37: Plot of hydrogen production upon irradiation of solutions (1:1 acetonitrile/water) containing **PS** (C_{PS} = 5.0 × 10^{-4} M), **catalyst PGII-83** (C_{cat} =5×10^{-5} M), pH 10 and different concentrations of TEA.

d) Mercury poisoning test

The mercury poisoning test was realised in order to investigate the effect of mercury during hydrogen production. More particularly, hydrogen production was not affected by the presence of mercury in the reaction mixture of PGII-99 (under the best conditions) indicating that metallic nickel particles are not formed during the experiment (**Fig. 38**). Metallic mercury remains shiny without forming an amalgam with nickel.

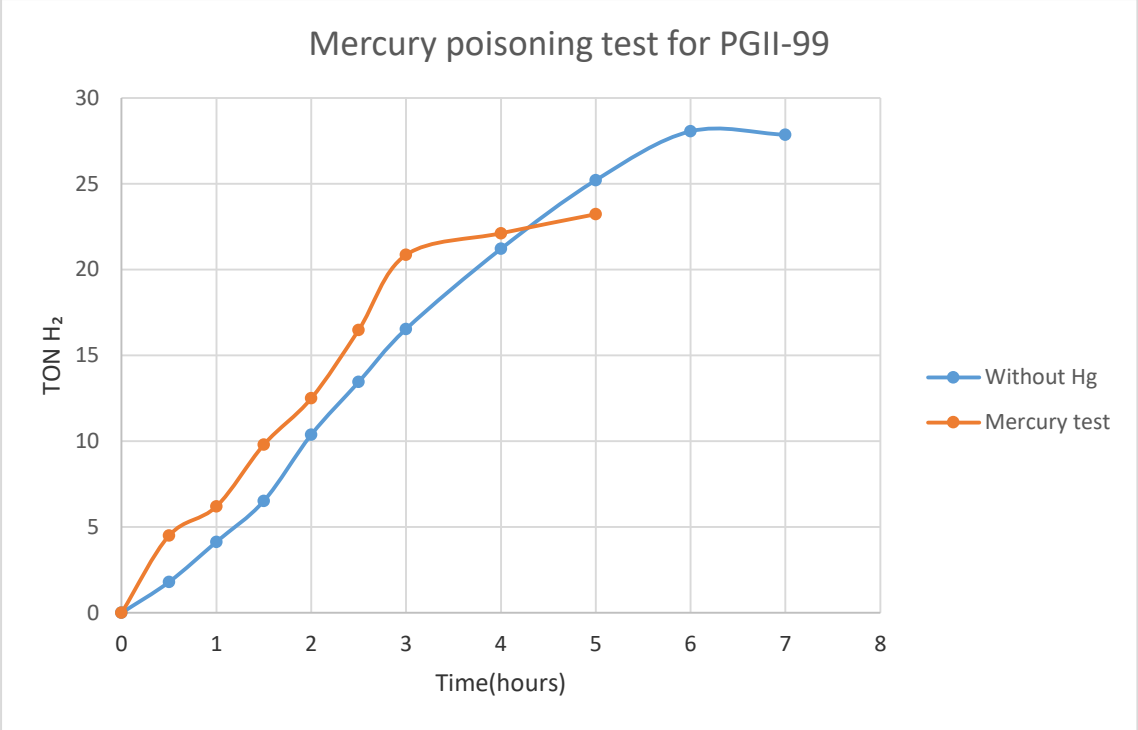

Fig. 38: Plot of hydrogen production upon irradiation of solutions (1:1 acetonitrile/water) containing **PS** (C_{PS} = 5.0 × 10^{-4} M), **catalyst PGII-99** (C_{cat} =5×10^{-5} M), pH 10 and TEA 5% v/v for normal test (blue line) and mercury poisoning test (orange line).

e) Comparison of the two coordination spheres

The goal was to examine whether the fluoroalcohol groups might act as proton relays. In the figure below, there are the plots of hydrogen for both systems under the best conditions (**Fig. 39**). We can observe that the complex with the fluoroalcohol groups is less active compared to the one without these groups. This could be attributed to the difficulty that faces a proton to reach a nitrogen atom due to the bulky fluoroalcohol groups. This protonation is a crucial step of the mechanism for the hydrogen production, based on previous publications.[69] Possible steric hindrance is a possible explanation for the lower activity of PGII-83. Also, we could imagine that the two hydroxyl arms can coordinate to the Ni center, thus slowing down the formation of the hydride.

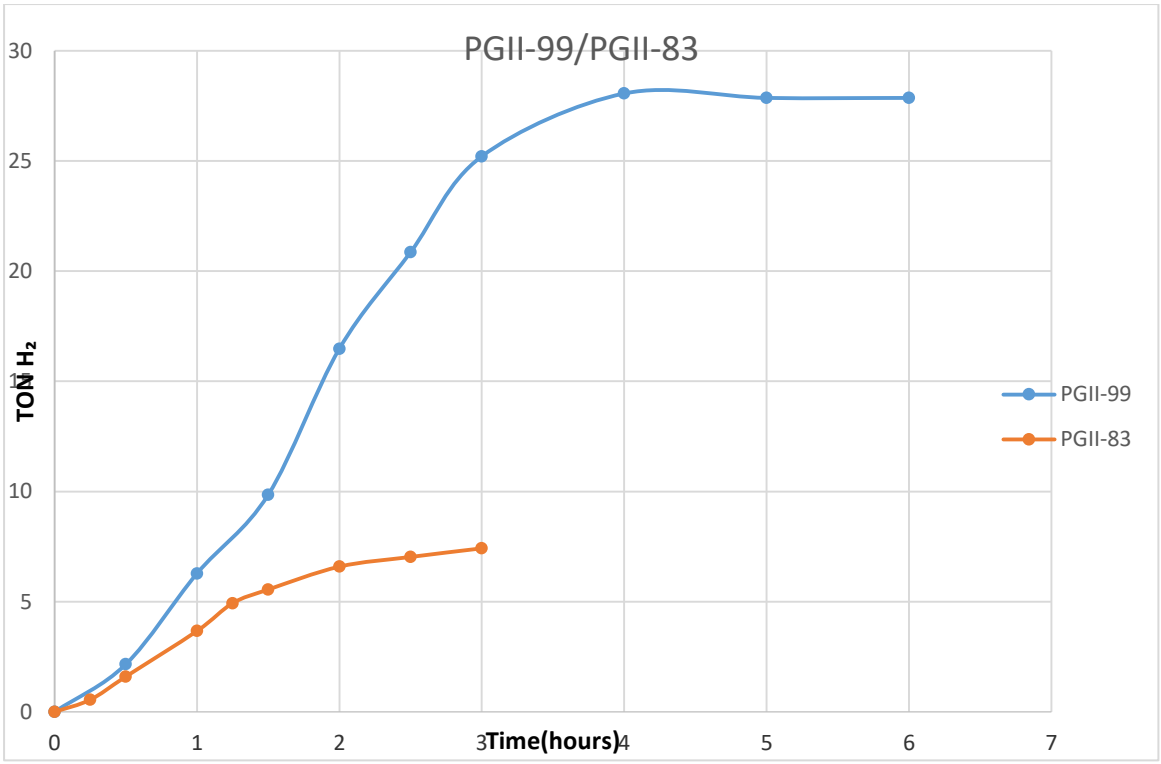

Fig. 39: Plot of hydrogen production upon irradiation of solutions (1:1 acetonitrile/water) containing **PS** (C_{PS} = 5.0 × 10^{-4} M), **catalysts** (C_{cat} =5×10^{-5} M) and TEA 5% v/v at pH 10.

2°) Photocatalytic activity assessment of the Co complexes

Based on previous publications,[84] we decided to test the same complexes with cobalt as central atom (**Fig. 40**) and make the comparison between them, because in similar photocatalytic systems the cobalt complexes are much more active.

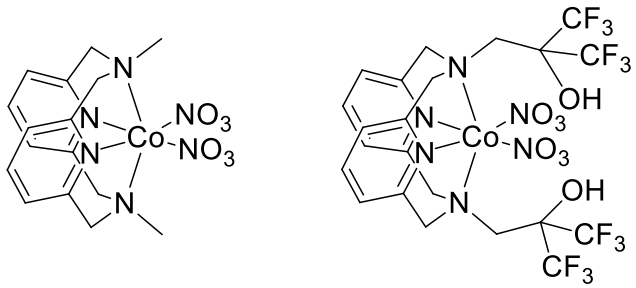

PGII-105 **PGII-104**

Fig. 40: The structure of the cobalt complexes used as catalysts.

In order to compare the cobalt complexes with nickel complexes, the first experiments were mimicking completely the previous experimental conditions. A detailed research

shown in the table below (**Table 3**) was made in order to find the best conditions for our systems.

Table 2: Experiments that have been done in order to assess the photocatalytic activity of the two novel nickel complexes

Catalyst	**PS**	**Ratio (PS/cat)**	**Solvents**	**SED**	**pH**	**TON vs Cat** (time when H_2 evolution stopped)
PGII-105	**Ir-PS**	5:1	**H_2O/CH_3CN (1:1)**	**TEA (5%)**	**10**	37.6 (6h)
	″	10:1	″	″	″	85.2 (6h)
	″	50:1	″	″	″	284.8 (6h) **Hg** + **Hg** => 324 (5h)
	″	100:1	″	″	″	384.0 (6h)
	″	50:1	″	TEA (10%)	″	820(5h)
	″	**50:1**	**″**	**″**	**11**	**1426.3 (4h)**
	″	50:1	″	″	12	431.2 (4.5h)
PGII-104	**Ir-PS**	5:1	H_2O/CH_3CN (1:1)	TEA (5%)	10	12.0 (5h)
	″	10:1	″	″	″	24.0(5h)
	″	50:1	″	″	″	187 (4.5h) **Hg** + **Hg** => 220.5 (4h)
	″	100:1	″	″	″	235.4 (7h)
	″	50:1	″	TEA (10%)	″	617.2 (5h)
	″	50:1	″	″	11	718.4 (4h)
	″	50:1	″	″	12	370.7 (4.5h)

a) Effect of catalysts and photosensitizer concentration

We had the same motif with the nickel complexes. For the initial experiment Ir-PS was used in concentration 5×10^{-4} M and the catalyst in concentration 10^{-4}M and 37.8 TON were obtained for PGII-105 and 11.8 for PGII-104. We could observe for both catalysts that when we increased the concentration of the photosensitizer keeping constant the concentration of the catalyst, the TON were increased. Also, when we decreased the concentration of the catalyst (5×10^{-5}M, 10^{-5}M) we had a tremendous increase of the TON for both catalysts. The best results were obtained using 10^{-3} M of photosensitizer (Ir-PS) giving 389 TON after 6 hours of irradiation when 10^{-5} M of catalyst **PGII-105 (Fig. 41)** was used and 235 TON after 7 hours in the case of 10^{-5} M of catalyst **PGII-104 (Fig. 42).**

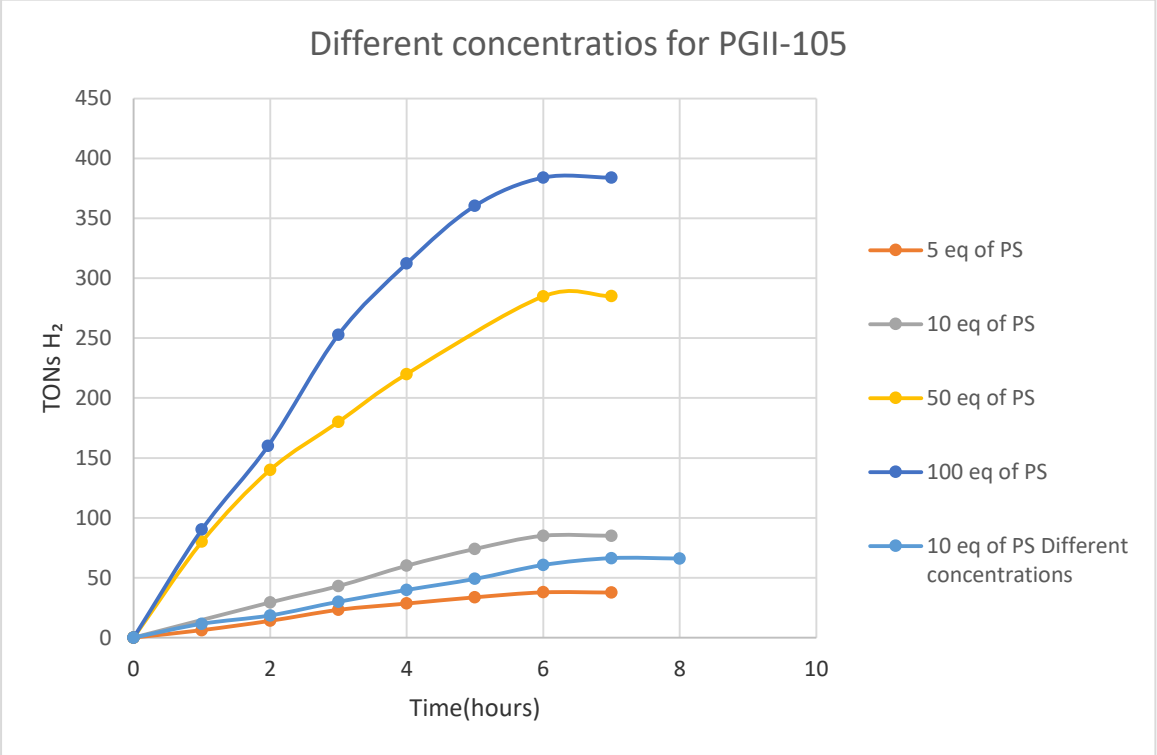

Fig. 41: Plot of hydrogen production upon irradiation of solutions (1:1 acetonitrile/water) containing different concentrations of **Ir-PS** and **PGII-105** and TEA 5% v/v at pH 10.

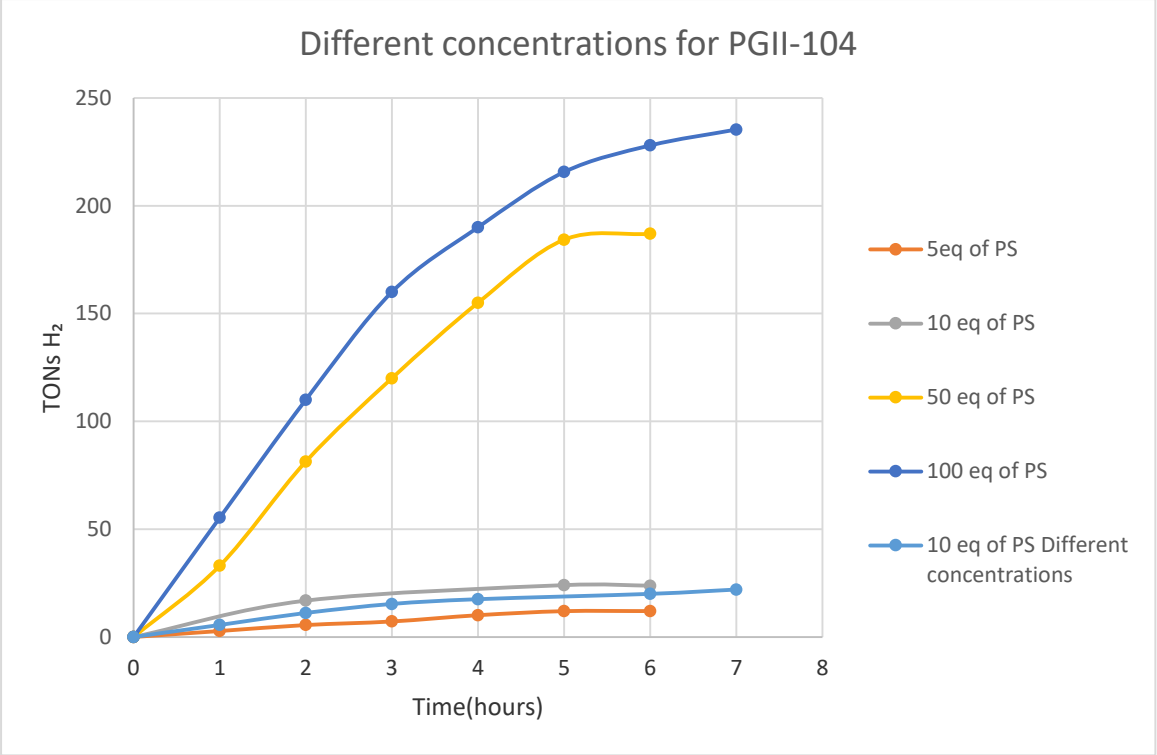

Fig. 42: Plot of hydrogen production upon irradiation of solutions (1:1 acetonitrile/water) containing different concentrations of **Ir-PS** and **PGII-104** and TEA 5% v/v at pH 10.

b) Effect of the concentration of TEA

When we increased the concentration of TEA, the TON numbers for both catalysts were increased significantly, reaching for PGII-105 (**Fig. 43**) 820 TON after 5 hours of irradiation and for PGII-104 (**Fig. 44**) 530 TON after 3 hours of irradiation. Both systems are more active in higher concentration of TEA.

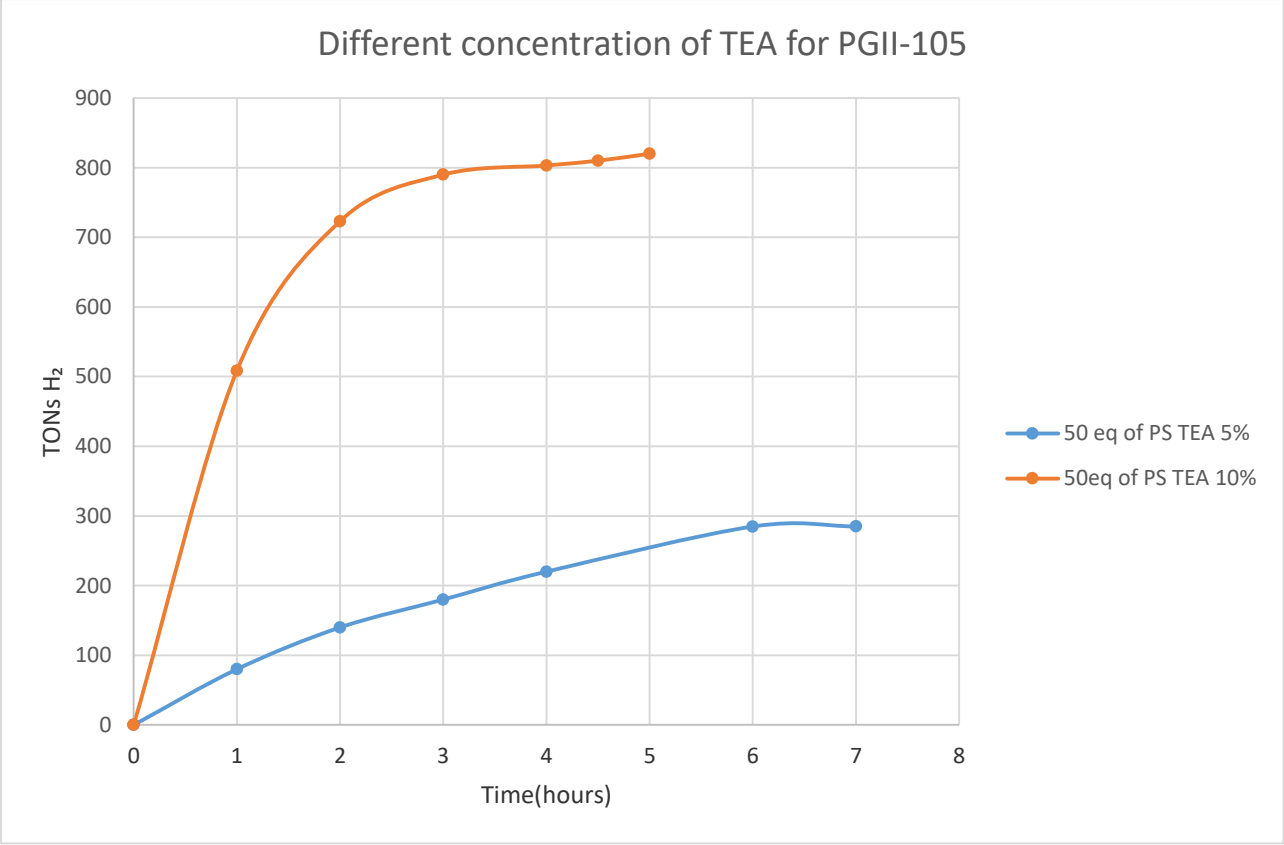

Fig. 43: Plot of hydrogen production upon irradiation of solutions (1:1 acetonitrile/water) containing **PS** (C_{PS} = 5.0 × 10^{-4} M), **catalyst PGII-105** (C_{cat} =10^{-5} M), pH 10 and different concentrations of TEA.

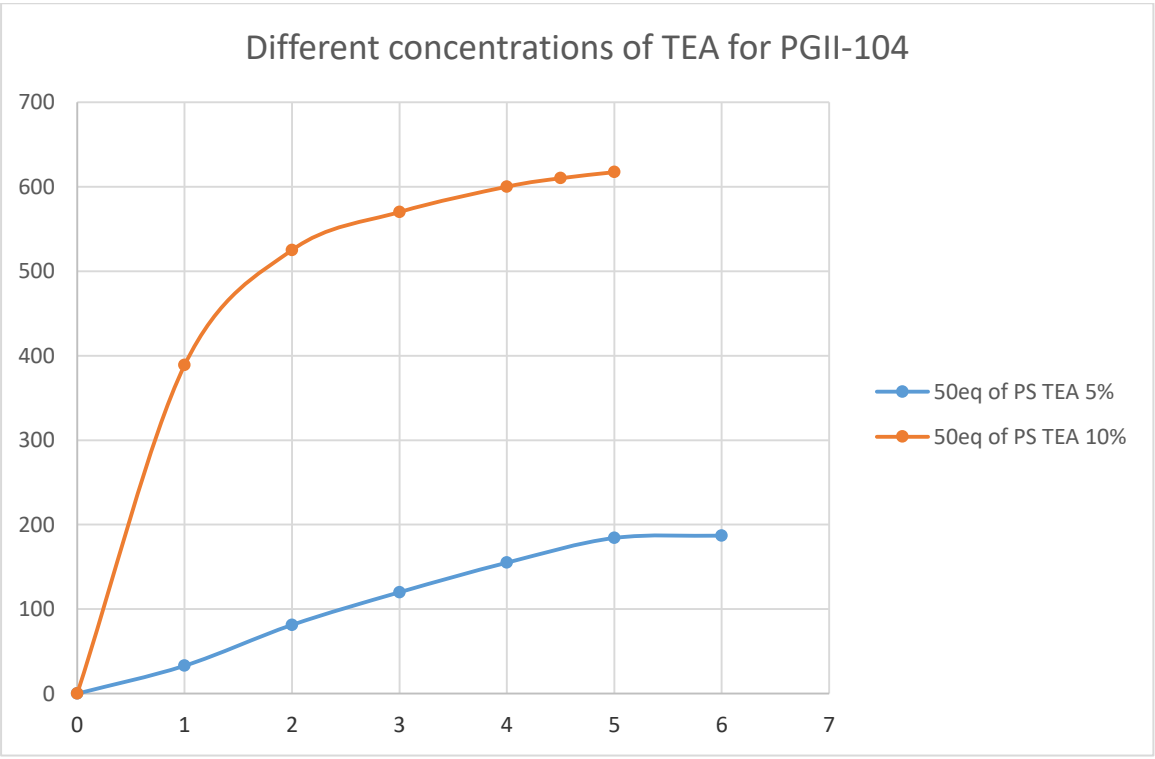

Fig. 44: Plot of hydrogen production upon irradiation of solutions (1:1 acetonitrile/water) containing **PS** (C_{PS} = 5.0 × 10^{-4} M), **catalyst PGII-104** (C_{cat} =10^{-5} M), pH 10 and different concentrations of TEA.

c) Effect of proton's concentration (pH)

In order to study the effect of pH in hydrogen production all different parameters were kept constant such as C_{PS} = 5.0 × 10^{-4} M, C_{cat} =10^{-5} M, sacrificial electron donor (TEA 10% v/v) and the solution (acetonitrile/water 1/1). We could observe for both catalysts that when we increased the pH 11, the activity of both systems was increased. For PGII-105 (**Fig. 45**), we could obtain 1426 TON numbers after 4 hours of irradiation and for the PGII-104 (**Fig. 46**) 718 TON after 4 hours of irradiation. It was already mentioned that the optimum pH is close to the pKa of the SED. For TEA, the pKa is 10.75 so it is reasonable for the system to work better at this pH value. When we increased the pH 12, the activity was decreased. This could be attributed to the low proton concentration in so basic conditions, slowing down the protonation steps at the catalytic center.

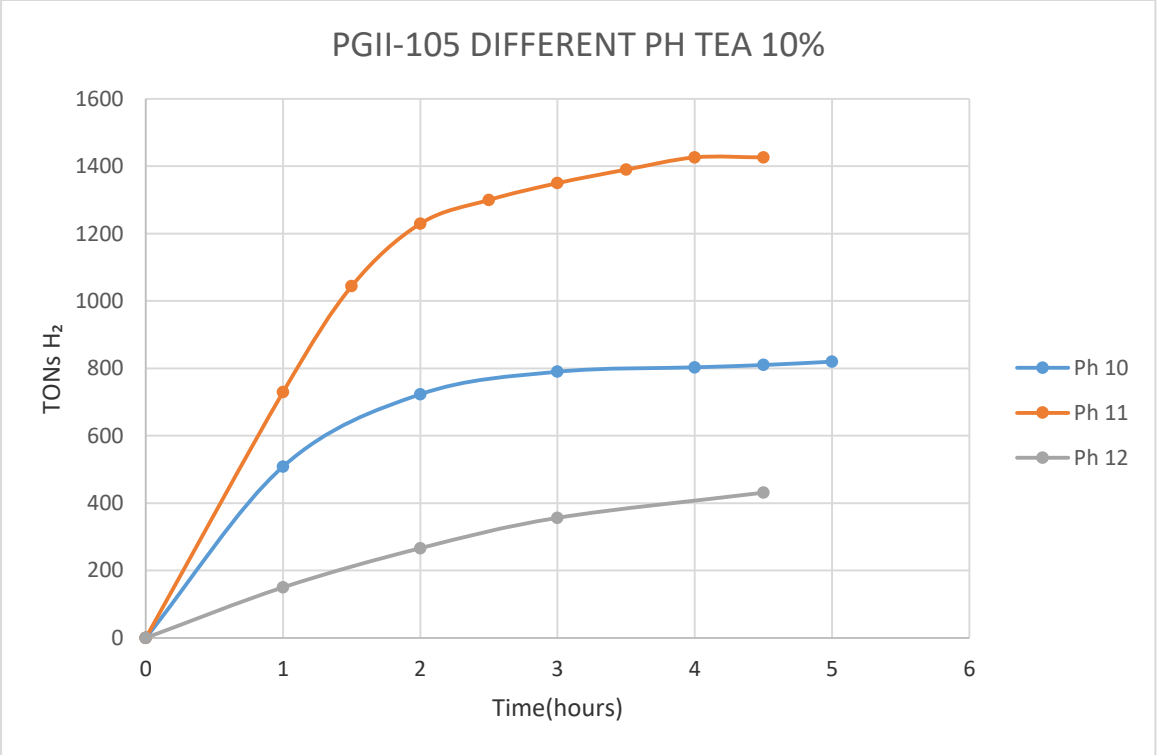

Fig. 45: Plot of hydrogen production upon irradiation of solutions (1:1 acetonitrile/water) containing **PS** (C_{PS} = 5.0 × 10^{-4} M), **catalyst PGII-105** (C_{cat} =10^{-5} M) and TEA 10% v/v at different pH.

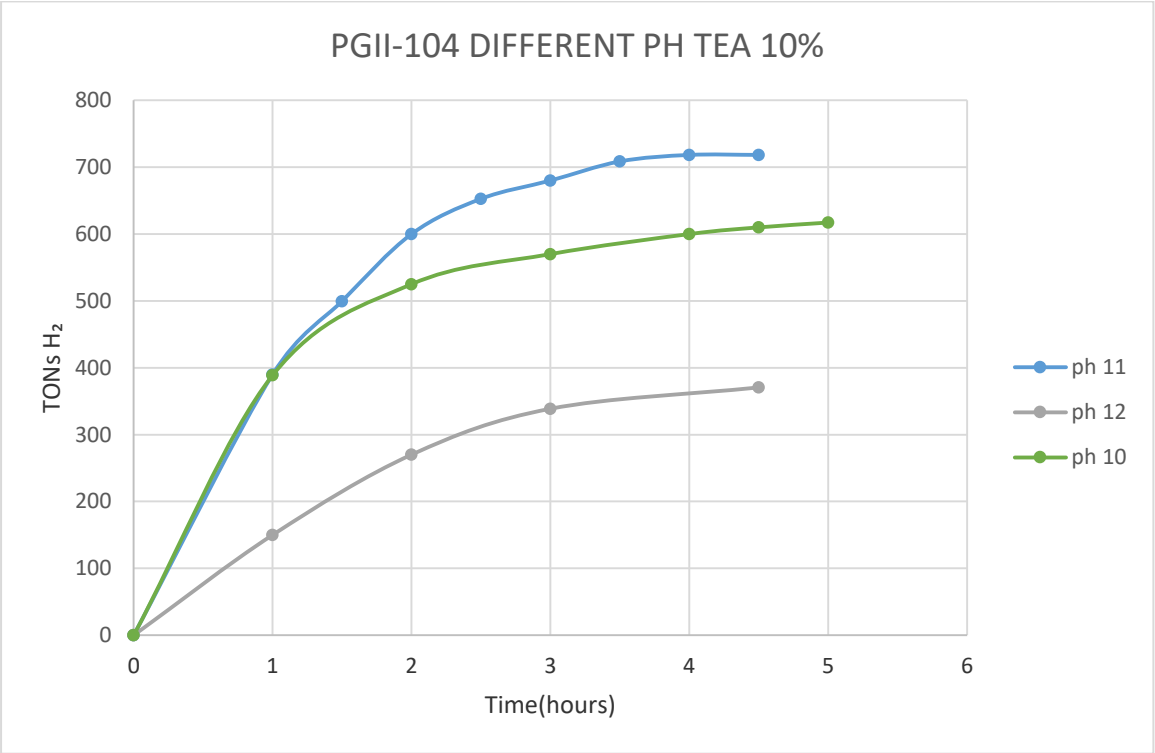

Fig. 46: Plot of hydrogen production upon irradiation of solutions (1:1 acetonitrile/water) containing **PS** (C_{PS} = 5.0 × 10^{-4} M), **catalyst PGII-104** (C_{cat} =10^{-5} M) and TEA 10% v/v at different pH.

d) Mercury poisoning test

The mercury poisoning test was realised in order to investigate the effect of mercury during hydrogen production. Again, hydrogen production was not affected by the presence of mercury in the reaction mixture of both catalysts, indicating that metallic cobalt particles are not formed during the experiment (**Fig. 47**). Metallic mercury remains shiny without forming an amalgam with cobalt.

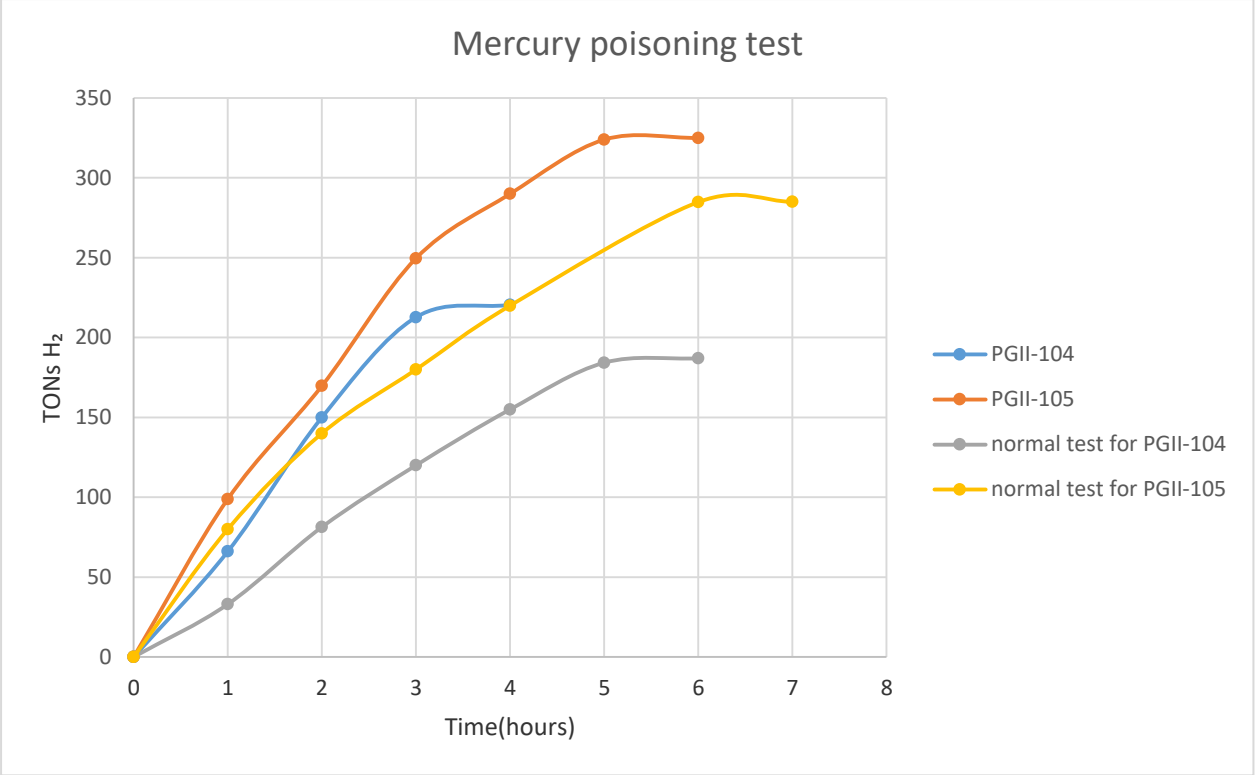

Fig. 47: Plot of hydrogen production upon irradiation of solutions (1:1 acetonitrile/water) containing **PS** ($C_{PS} = 5.0 \times 10^{-4}$ M), **catalyst PGII-105/104** ($C_{cat} = 10^{-5}$ M), pH 10 and TEA 5% v/v for normal tests and mercury poisoning tests.

e) Regeneration of the system

Due to the fact that the cobalt complexes were novel catalysts for hydrogen evolution, we tried to find if they are stable during the irradiation. We chose to regenerate the system, adding 1eq of PS. The addition of PS was sufficient to partially recover the hydrogen evolution (**Fig. 48**). This indicates that the catalyst doesn't decompose after 3 hours but is stable for almost 6 hours.

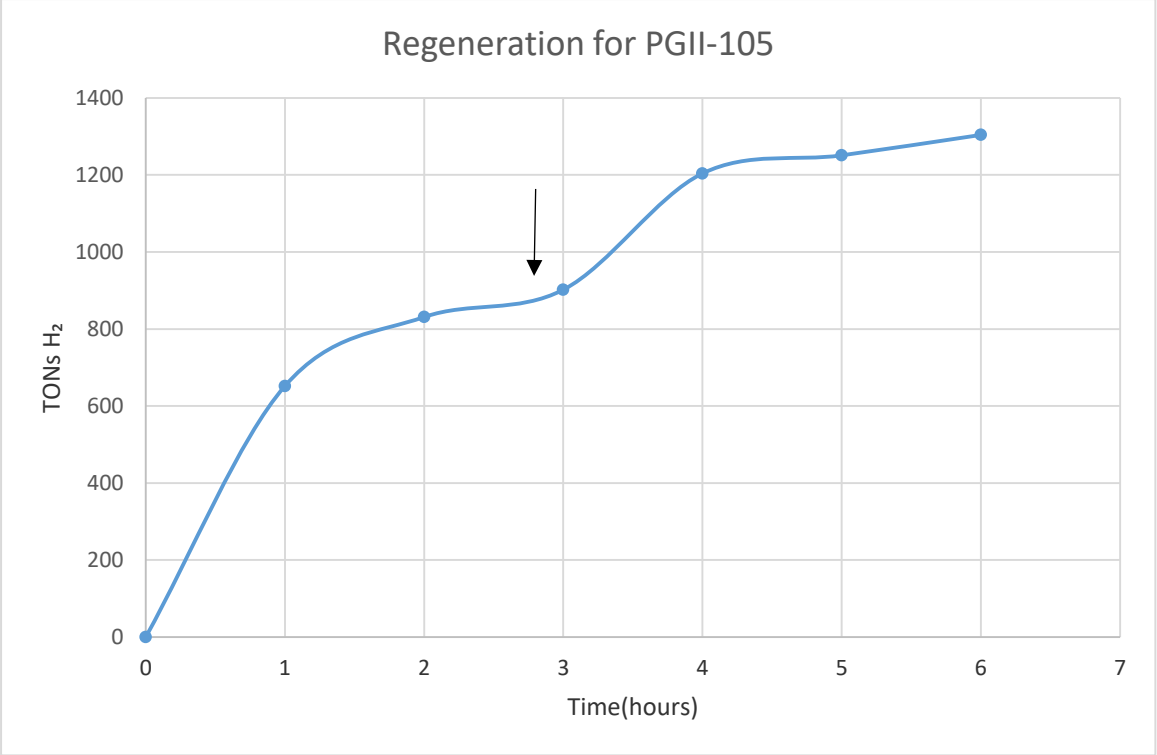

Fig. 48: Plot of hydrogen production upon irradiation of solutions (1:1 acetonitrile/water) containing **PS** (C_{PS} = 5.0 × 10^{-4} M), **catalyst PGII-105** (C_{cat} =10^{-5} M), TEA 10% v/v, pH 10 with the addition of 1eq of PS after 3 hours of photocatalytic activity.

f) Comparison between cobalt and nickel complexes

The final goal was to examine whether the cobalt or nickel catalyst are more active and whether the fluoroalcohol groups might act as proton relays. We can observe that for nickel and cobalt complexes the fluoroalcohol groups is less active compared to the one without these groups. This could be attributed to the difficulty that faces a proton to reach a nitrogen atom due to the bulky fluoroalcohol groups (steric hindrance). This protonation is a crucial step of the mechanism for the hydrogen production, based on previous publications.[69] Also, we could imagine that the two hydroxyl arms can coordinate to the Co center, thus slowing down the formation of the hydride. It is obvious that cobalt complexes are more active compared to the nickel ones. Also, the cobalt complexes are more active in more basic conditions and in greater concentration of TEA. On the contrary, for the nickel complexes only the catalyst with the fluoroalcohol groups shows a similar behavior.

CONCLUSIONS

In summary, photocatalytic systems consisting of 4 novel nickel and cobalt catalysts with Ir complex as photosensitizer, TEA as sacrificial electron donor at different pH in CH_3CN/H_2O (1:1) solution, were reported. Upon visible irradiation ($\lambda > 440$ nm) hydrogen production was detected with the best result obtained at pH 11 with $C_{ps} = 5.0 \times 10^{-4}$ M and the PGII-105 catalyst ($C_{cat} = 10^{-5}$ M) with a TON of 1426, after 4 hours of irradiation. The results clearly indicates that the activity of the cobalt complexes is higher compared to the nickel ones. The fluoroalchohol group does not act as an electron relay to these systems. To the contrary, it decreases the catalytic activity. Further investigations are necessary to shed light on the mechanism that takes place in these photocatalytic systems.

APPENDIX

In the following appendix there are some spectrum of characterization of the compounds that have been synthesized.

UV-Vis spectrum

UV-Vis spectrum of compound $SnTPP(COOMe)_4Cl_2$ in CH_2Cl_2

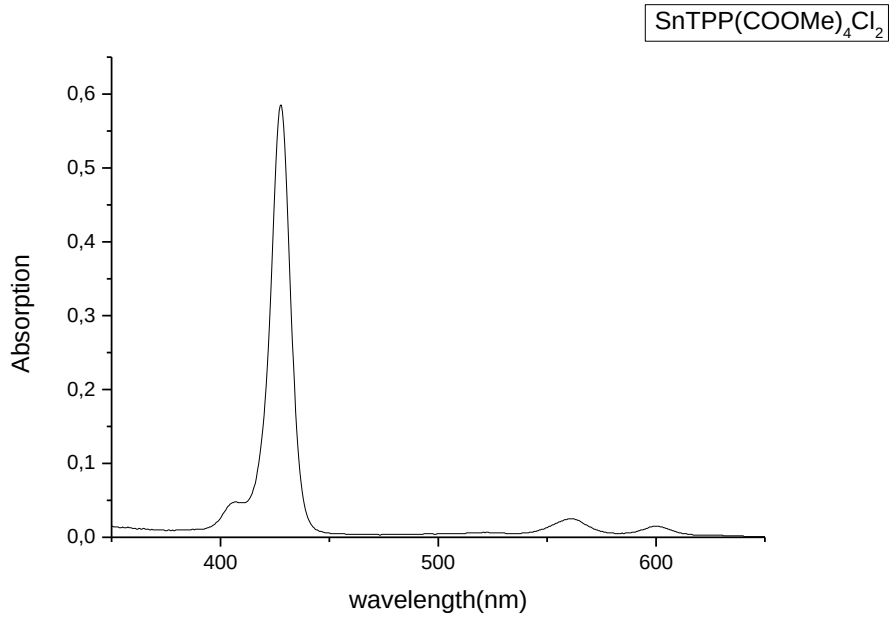

UV-Vis spectrum of compound $SnTPP(COOH)_4Cl_2$ in water

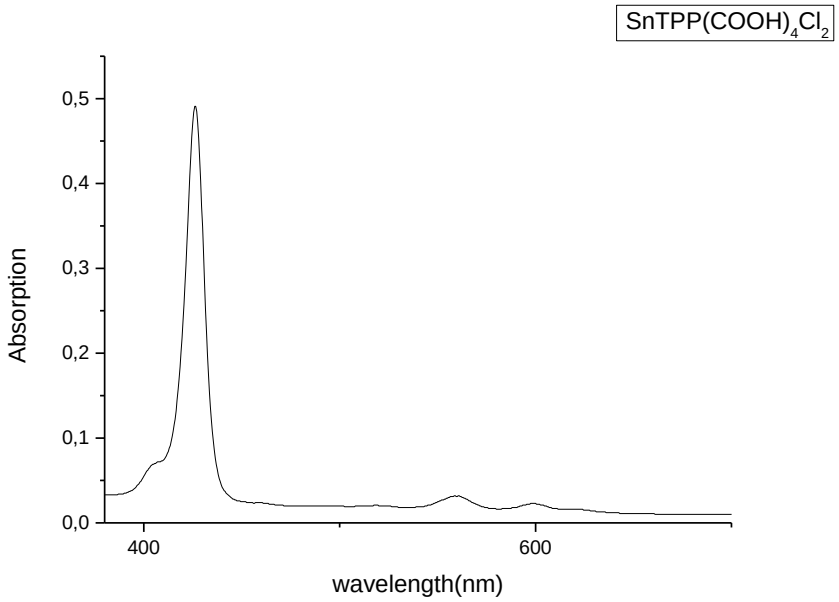

UV-Vis spectrum of compound SnTPP[(PO(OEt)$_2$]$_4$Cl$_2$ in CH$_2$Cl$_2$

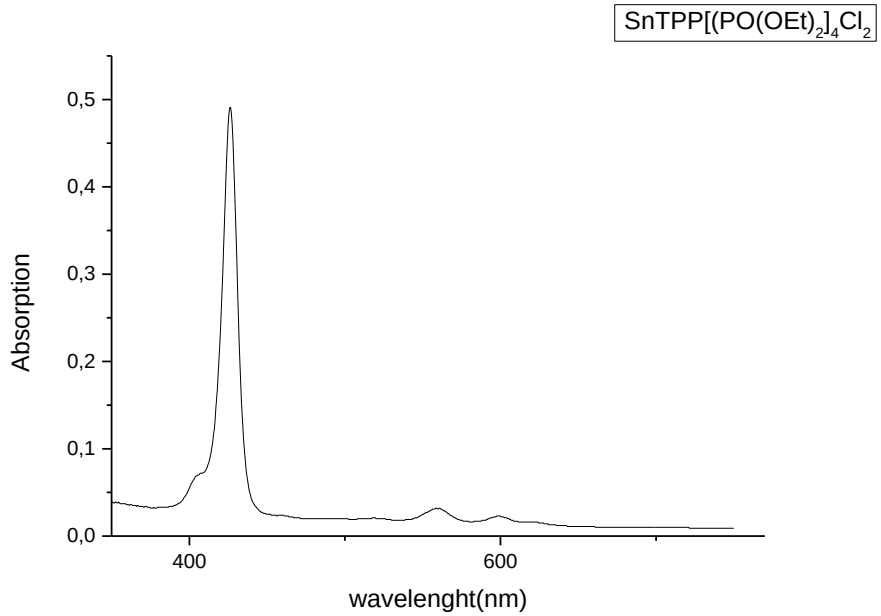

UV-Vis spectrum of compound ZnPCNCOOH in DMSO

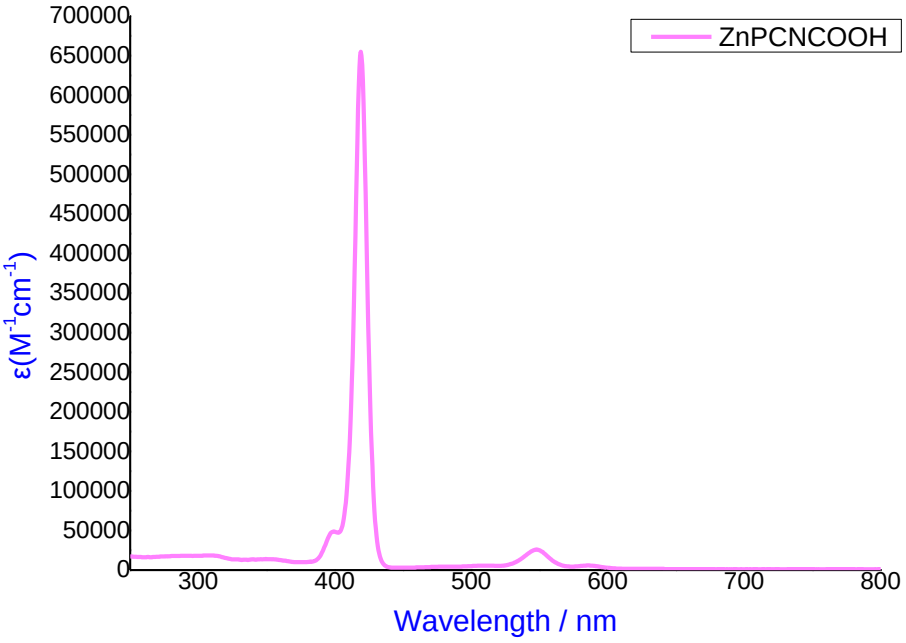

Emission spectrum

Emission spectrum of complex $SnTPP(COOMe)_4Cl_2$ in CH_2Cl_2

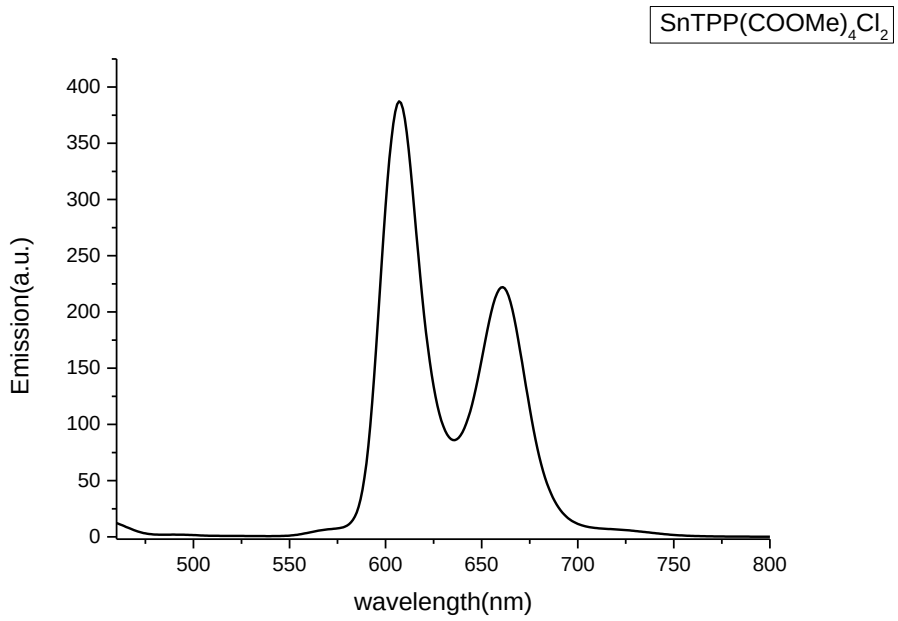

Emission spectrum of complex **ZnPCNCOOH** in DMSO

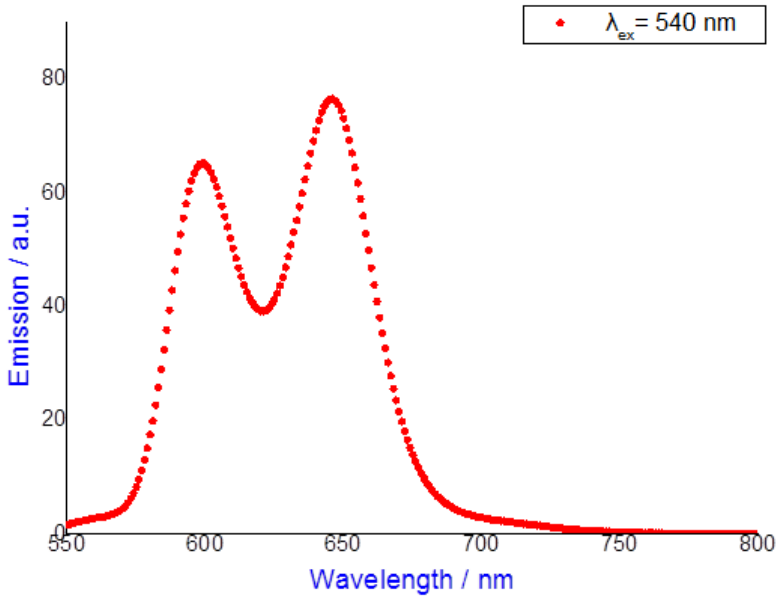

NMR spectrum

^{1}H NMR spectrum of compound ZnPCNCOOH in DMSO

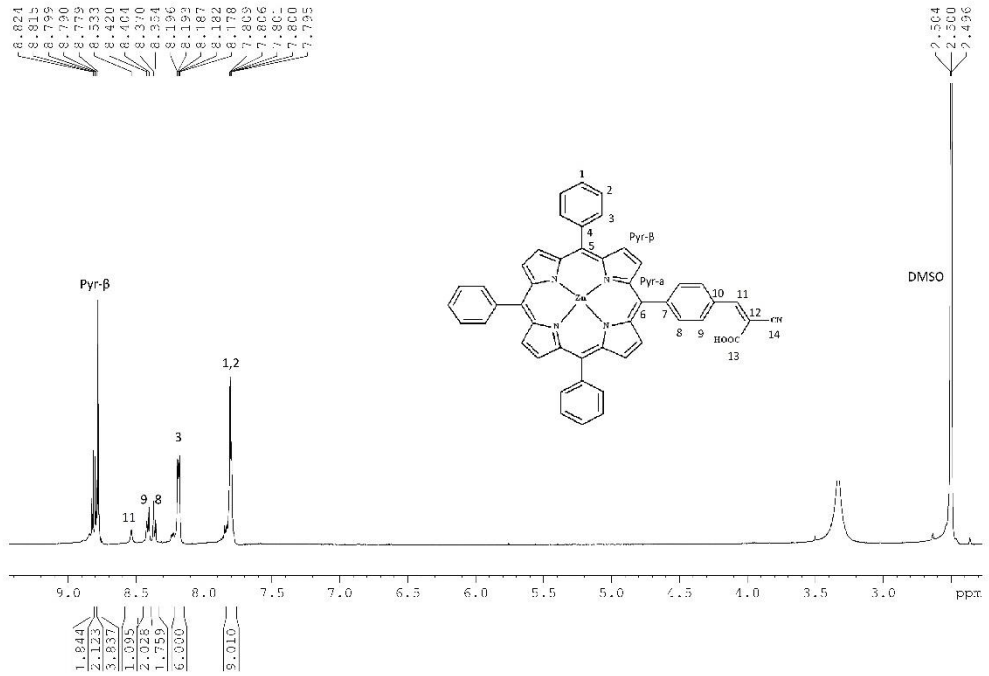

^{13}C NMR spectrum of compound ZnPCNCOOH in DMSO

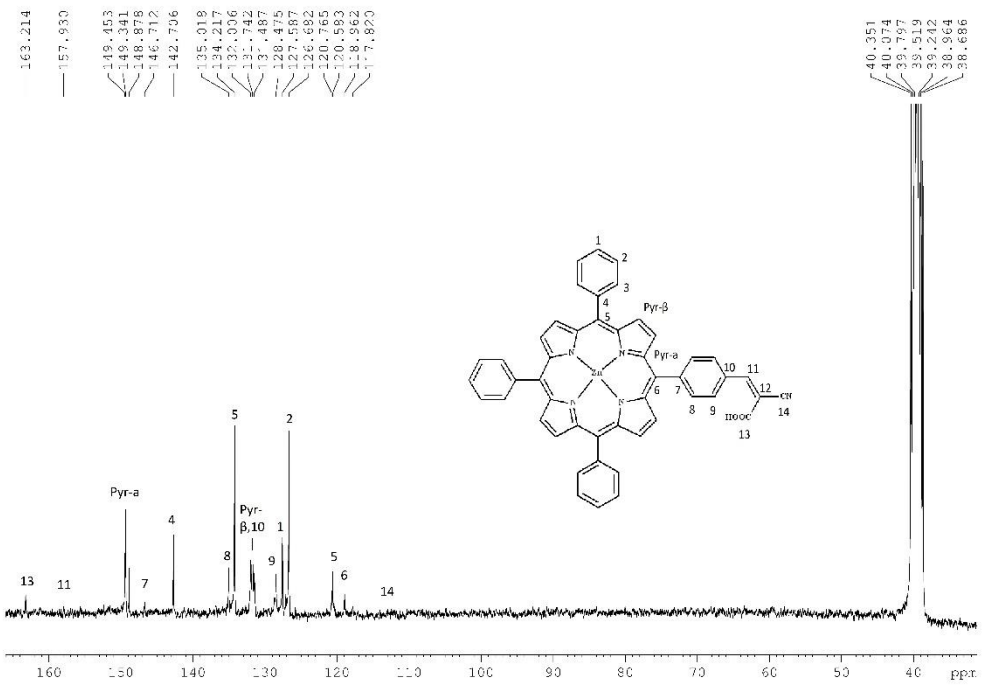

MALDI-TOF spectrum

MALDI-TOF spectrum of compound TPyP in DMSO

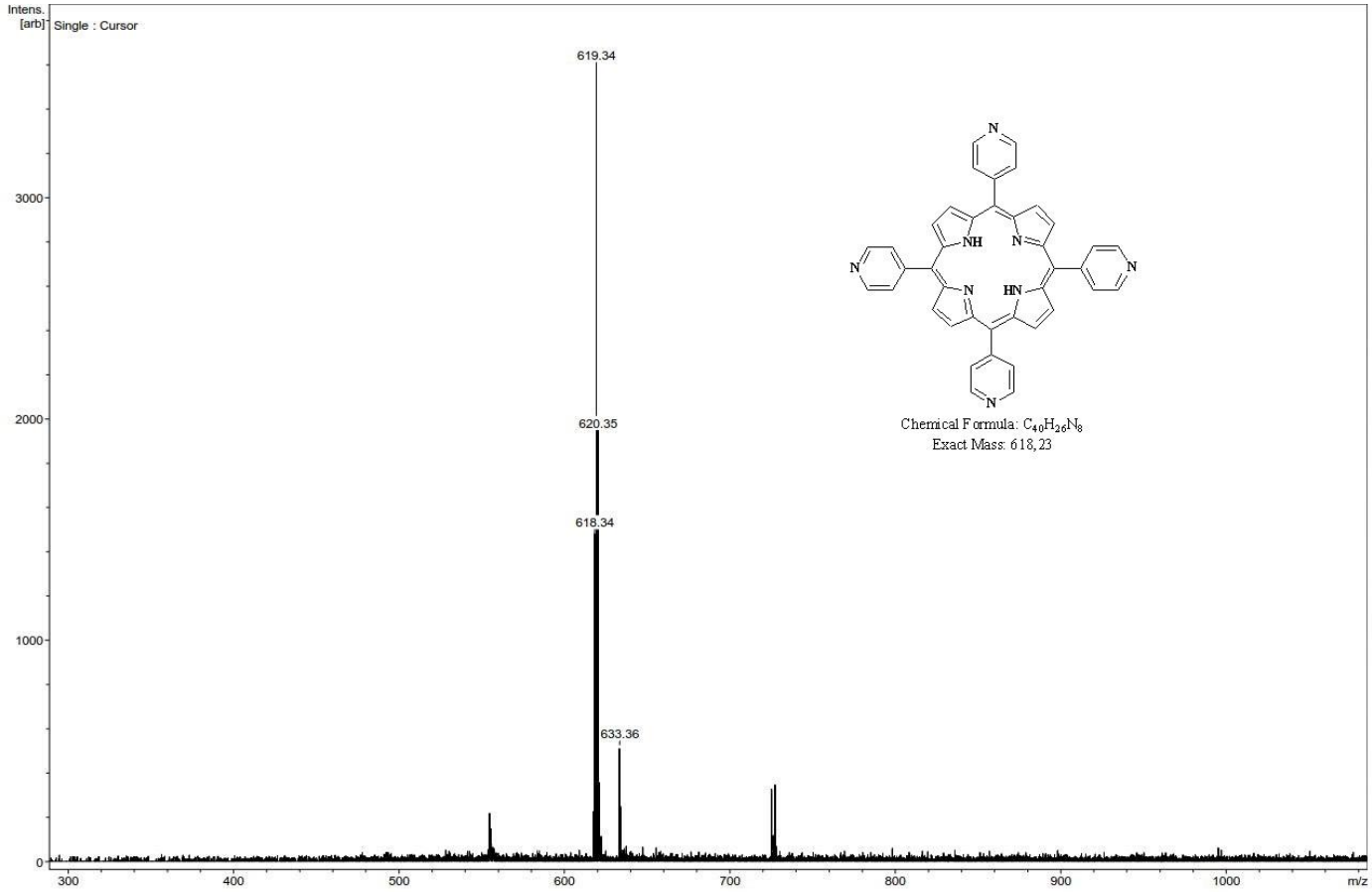

X-ray crystallography

ORTEP representation of the molecular structure of **PS1(**$SnTPP(COOMe)_4Cl_2$).
Crystal was obtained in dichloromethane/hexane.

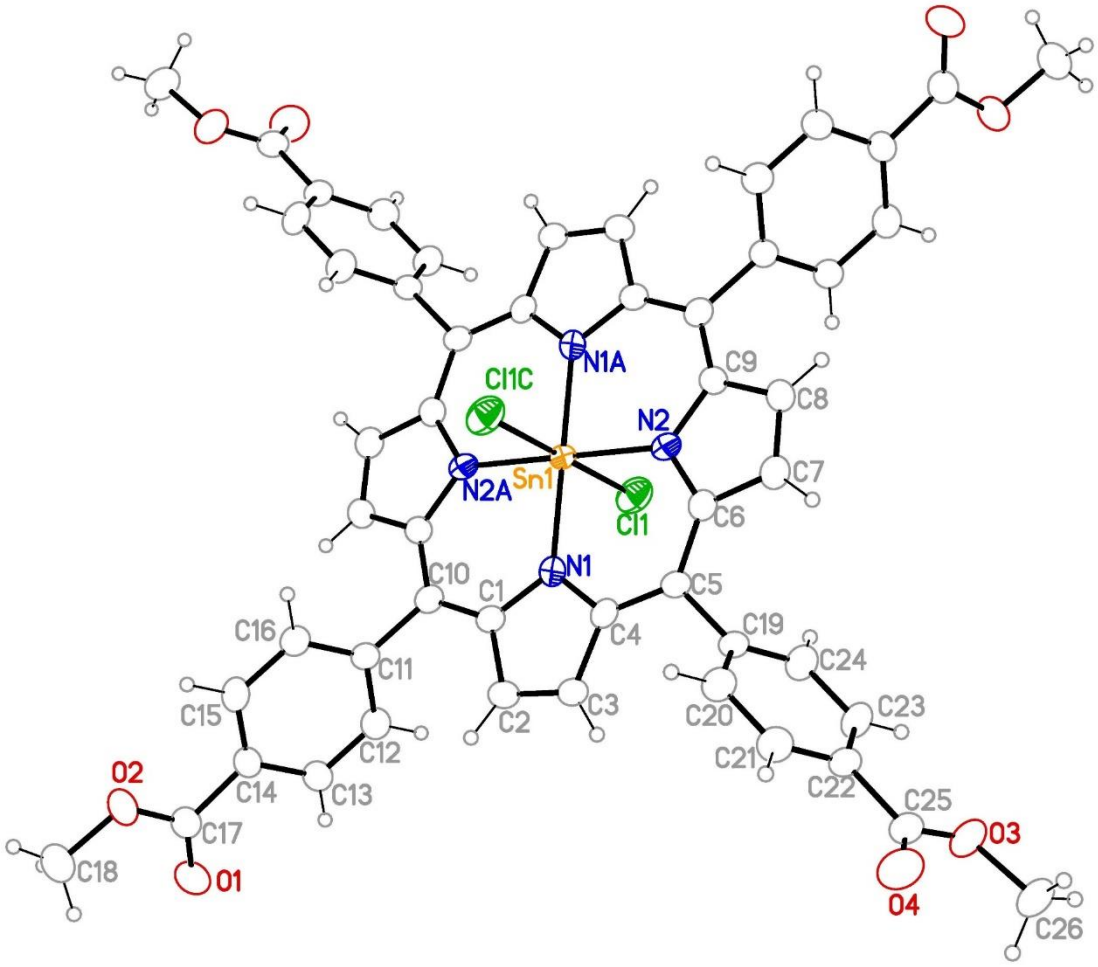

X-ray structure of PGII-105.

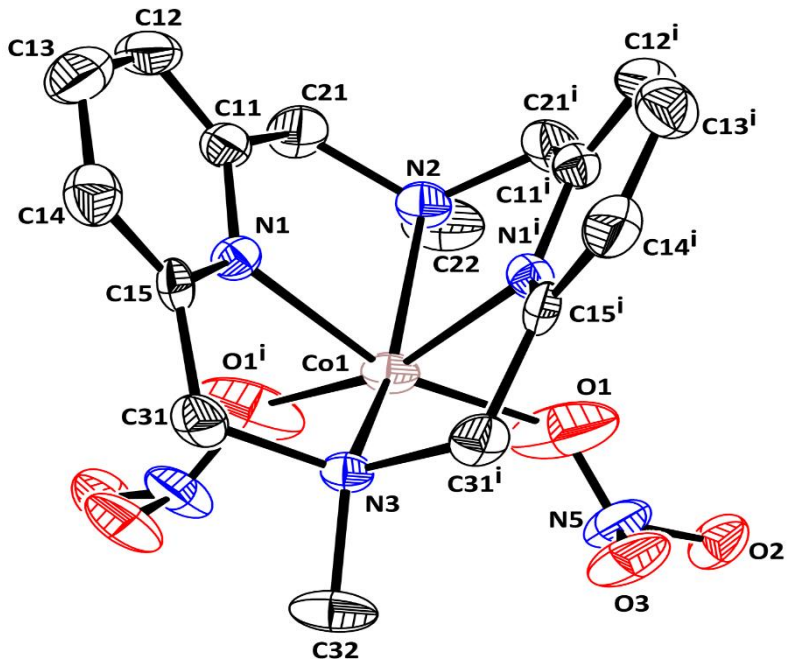

X-ray structure of PGII-104.

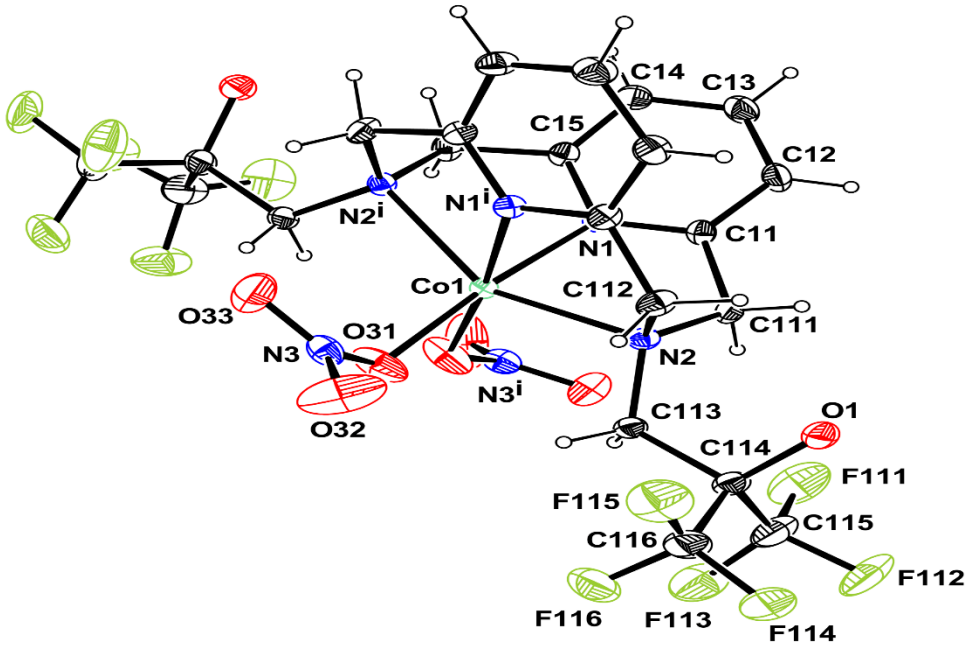

X-ray structure of PGII-83.

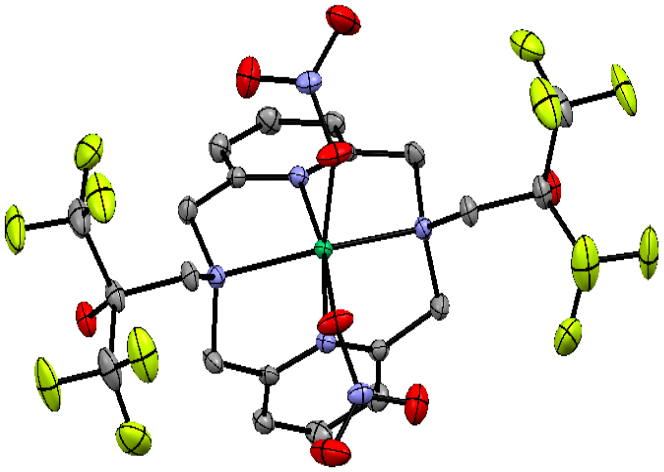

X-ray structure of PGII-99.

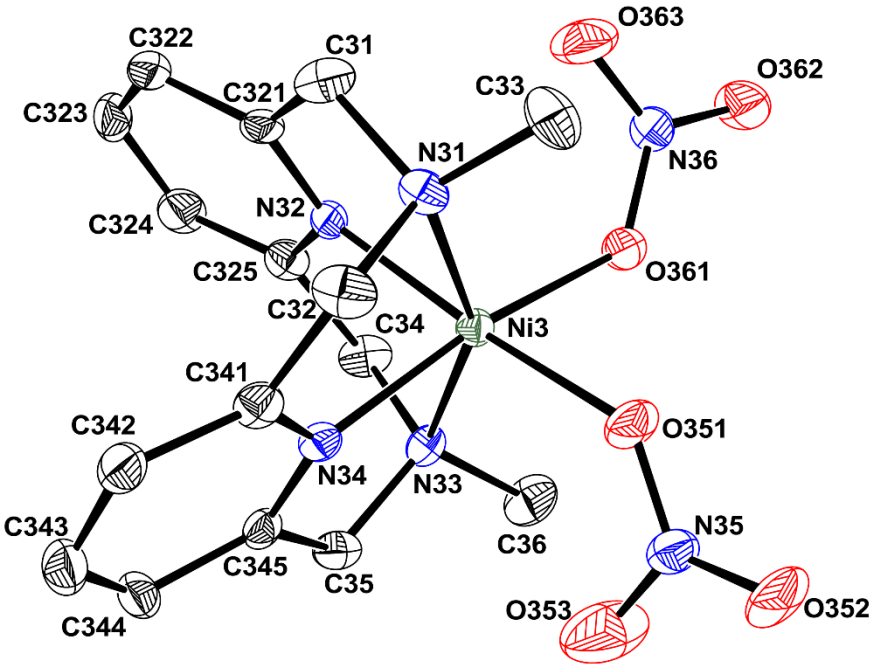

References

1 Palmer, D.*"Hydrogen in the Universe"*,**1997** NASA.

2 Armaroli, N.; Balzani, V. *Energy for a Sustainable World: From the Oil Age to a Sun-Powered Future*, **2010**.

3 Rifkin, J.; *The Hydrogen Economy: The Creation of the Worldwide Energy Web and the Redistribution of Power on Earth*, **2002**.

4 Momirlan, M.; Veziroglu, *T. N. International Journal of Hydrogen Energy* **2005**, 30, 795.

5 J.D. Holladay.; J. Hu,; D.L. King.; Y. Wang *An overview of hydrogen production technologies*, Pacific Northwest National Laboratory, 902 Battelle Blvd., Richland, WA 99352, USA

6 Trager, R. *Chem. World* **2009**, 9.

7 Dellantonio, A.; Fitz, W. J.; Repmann, F.; Wenzel, W. W. *Journal of Environmental Quality* **2010**, 39, 761

8 Luque, R.; Herrero-Davila, L.; Campelo, J. M.; Clark, J. H.; Hidalgo, J. M.; Luna, D.; Marinas, J. M.; Romero, A. A. *Energy and Environmental Science* **2008,** *1*, 542

9 Goldemberg, J. *Energy and Environmental Science* **2008**, *1*, 523

10 Gallezot, P. *ChemSusChem* **2008**, *1*, 734

11 Inderwildi, O. R.; King, D. A. *Energy and Environmental Science* **2009**, *2*, 343

12 Voith, M. *Chem. Eng. News* **2009**, *87*

13 Turner, J. A.; Williams, M. C.; Rajeshwar, K. *The Electrochemical Society Interface* **2004**, 24

14 Nakicenovic N, Swart R. Special report on emissions scenarios, pp. 48–55. Washington, DC: Intergovernmental Panel on Climate Change. **2000**

15 Shaheen, S.E.; Ginley, D.S.; Jabbour, G.E. *MRS Bull* **2005**, *30*, 10

16 Archer, M.D.; Barber, J. **2004** Photosynthesis and photoconversion. In Molecular to global photosynthesis (eds MD Archer, J Barber), pp. 1–41. *London, UK: Imperial College Press*

17 Volbeda, A.; Charon, M.H.; Piras, C.; Hatchikian, E.C.; Frey, M.; Fontecilla-Camps, J.C. Nature **1995**, *373*, 580

18 Peters, J.W.; Lanzilotta, W.N.; Lemon, B.J.; Seefeldt, L.C. *Science* **1998**, *282*, 1853

19 Nicolet, Y.; Piras, C.; Legrand, P.; Hatchikian, C.E.; Fontecilla-Camps, J.C. *Structure* **1999**, *7*, 13

20 Zirngibl, C.; Van Dongen, W.; Schworer, B.; Von Bunau, R.; Richter, M.; Klein, A.; Thauer, R.K. *Eur. J. Biochem.* **1992**, *208*, 511

21 Tard, C.D.; Pickett, C.J. *Chem. Rev.* **2009**, *109*, 2245

22 Wang, M.; Chen, L.; Sun, L. *Energy Environ. Sci.* **2012**, *5*, 6763

23 Du, P.; Eisenberg, R. *Energy Environ. Sci.* **2012**, 5, 6012

24 Artero, V.; Chavarot-Kerlidou, M.; Fontecave, M. *Angew. Chem. Int. Ed.* **2011**, 50, 7238

25 De Lacey, A.L.; Fernandez, V.M.; Rousset, M.; Cammack, R. *Chem. Rev.* **2007**, *107*, 4304

26 Bruschi, M.; Greco, C.; Kaukonen, M.; Fantucci, P.; Ryde, U.; De Gioia, L. *Angew. Chem. Int. Ed.* **2009**, 48, 3503

27 Fujishima, A.; Honda, K. *Nature* **1972**, *238*, 37

28 V.; Sara Thoi, Y.; Sun, J.R,; Long, C.J.; Chang, *Chem. Soc. Rev.* **2013**, 42, 2388
29 Ursua A., Gandia L. M., Sanchis P. Hydrogen production from water electrolysis: current status and future trends, in Proceedings of the IEEE (New York, NY: Electronics and Electrical Engineers, Inc.), **2012**, 410–426
30 Eckenhoff W.T,; Eisenberg R.; *Dalton Trans.,* **2012**, 41, 13004
31 Andreiadis E.S.; Chavarot-Kerlidou M.; Fontecave M.; Artero V.; *Photochemistry and Photobiology*, **2011,** 87, 946-964)
32 P. Schaeffer, R. Ocampo, H. J. Callot, P. Albrecht, *Nature* , **1993**, 364, 133-136
33 Kadish K. M., Smith K. M., Guilard R. Eds., *The porphyrin Handbook*, **2000-2003**, Vol. 1-20
34 P. Rothemund.; *"A New Porphyrin Synthesis. The Synthesis of Porphin". J. Am. Chem. Soc.*, **1936**, 58 *(4):* 625–627
35 A. D. Adler; F. R. Longo; J. D. Finarelli; J. Goldmacher; J. Assour; L. Korsakoff: "A simplified synthesis for meso-tetraphenylporphine". *J. Org. Chem.*, **1967**, 32 (2): 476–476
36 G. A. Spyroulias, A. Despotopoulos, C. P. Raptopoulou, A. Terzis, A. G. Coutsolelos, *Chem. Commun.*, **1997**, 783-784
37 W. K. Wong, L. Zhang, W. T. Wong, F. Xue, T. C. W. Mak, *J. Chem. Soc*., Dalton Trans., **1999**, 509-638
38 J. W. Buchler, M. Kihn-Botulinski, J. Löffler, B. Scharbert, *New J. Chem*., **1992**, 16, 545-553
39 Website : *pharmaxchange.info/press/2012/04/ultraviolet-visible-uv-vis spectroscopy-derivation-of-beer-lambert-law*. November **2015**
40 Soret J. L., *Compt. Rend.* **1883,** 97, 1267
41 Misra; Prabhakar; Dubinskii; Mark. (**2002**). *Ultraviolet Spectroscopy and UV Lasers*. New York: Marcel Dekker
42 Nelson, R.W.; Nedelkov, D.; Tubbs, K.A. *Anal. Chem.* **2000**, *72*, 405
43 Moyer, S.C.; Cotter, R.J. *Anal. Chem.* **2002**, *74*, 469
44 Mavromoustakos, A.; Matsoukas, I. NMR. *Use of Nuclear Magnetic Resonance in the Design and Synthesis of Pharmaceutical Molecules. National institution of Research*, Athens, **1998**
45 Pochapsky, T.; Pochapsky, S. *NMR for Physical and Biological Scientists*. Taylor & Francis, New York, **2005**
46 L. Stryer, Biochemistry, University of Crete, 3rd edition, 1, **1997**
47 Dempsey, J.L.; Brunschwig, B.S.; Winkler, J.R.; Gray, H.B. *Acc. Chem. Res.* **2009**, *42*, 1995
48 Du, P.; Schneider, J.; Luo, G.; Brennessel, W.W.; Eisenberg, R. *Inorg. Chem.* **2009**, *48*, 4952
49 McCrory, C.C.L.; Uyeda, C.; Peters, J.C. *J. Am. Chem. Soc.* **2012**, *134* 3164
50 Juris, A.; Balzani, V.; Barigelletti, F.; Campagna, S.; Belser, P.; von Zelewsky, A. *Coord. Chem. Rev.* **1988**, *84*, 85
51 Probst, B.; Guttentag, M.; Rodenberg, A.; Hamm, P.; Alberto, R. *Inorg. Chem.* **2011**, *50*, 3404
52 Juris, A.; Balzani, V.; Barigelletti, F.; Campagna, S.; Belser, P.; von Zelewsky, A. *Coord. Chem. Rev.* **1988**, *84*, 85
53 Probst, B.; Guttentag, M.; Rodenberg, A.; Hamm, P.; Alberto, R. *Inorg. Chem.* **2011**, *50*, 3404
54 Cline, E.D.; Adamson, S.E.; Bernhard, S. *Inorg. Chem.* **2008**, *47*, 10378
55 Lazarides, T.; McCormick, T.; Du, P.; Luo, G.; Lindley, B.; Eisenberg, R. *J. Am. Chem. Soc.* **2009**, *131*, 9192

56 McCormick, T.M.; Han, Z.;. Weinberg, D.J; Brennessel, W.W.; Holland, P.L.; Eisenberg, R. *Inorg. Chem.* **2011**, *50*, 10660
57 Krüger W and Fuhrhop JH. *Angew. Chem., Int.Ed. Engl.* **1982**; 21: 131-132
58 Hawecker, J.; Lehn, J.-M.; Ziessel, R., *New J. Chem.* **1983**, *7*, 271–277
59 Du, P.; Knowles, K.; Eisenberg, R. *J. Am. Chem. Soc*. **2008**, 130 (38), 12576–12577
60 Zhang P, Wang M, Dong J, Li X, Wang F, Wu L and Sun L. *J. Phys.Chem.C* **2010**; 114: 15868-15874
61 Fihri, A.; Artero, V.; Pereira, A.; Fontecave, M. *Dalton Trans.* **2008**, 5567–5569
62 Pellegrin Y.; Odobel F.; *C. R. Chimie*, **2016**, 1-13
63 Gross, M. A.; Reynal, A.; Durrant, J.R.; Reisner, E. *J. Am. Chem. Soc*. **2014**, 136, 356-366
64 Martindale, B.C.M,; Hutton, A. M.; Caputo, C. A.; Reisner, E. *J. Am. Chem. Soc.* **2015**, 137, 6018-6025
65 McLaughlin, M. P.; McCormick, T. M.; Eisenberg, R.; Holland, P. L. *Chem Commun,* **2011**, 47, 7989-7991
66 Kasap, H.; Caputo, C. A.; Martindale, C. M.; Godin, R.; Lau, V. W.; Lotsch, B. V.; Durrant, J. R.; Reisner, E. *J. Am. Chem. Soc.* **2016**, 138, 9183-9192
67 Martindale, B. C. M.; Joliat, E.; Bachmann, C.; Alberto, R.; Reisner, E. *Angew. Chem. Int. Ed*. **2016**, 55, 1-6
68 Hong-hua, C.; Jin-yun, W.; Ming-qiang, H.; Cheng-bing, M.; Hui-min, W.; Xiao-wei, S.; Chang-neng, C. *Dalton Trans*. **2013**, 42, 8684
69 Han, Z.; McNamara, W. R.; Eum, M.; Holland, P. L.; Eisenberg, R. *Angew. Chem. Int. Ed*. **2012**, 51, 1667-1670
70 Han, J.; Zhang, W.; Zhou, T.; Wang, X.; Xu, R. *RSC Adv*., **2012**, 2, 8293-8296
71 Zhang, W.; Hong, J.; Zheng, J.; Huang, Z.; Zhou, J. S.; Xu, R. *J. Am. Chem. Soc.* **2011**, 133, 20680-20683
72 Dong, J.; Wang, M.; Li, X.; Chen, L.; He, Y.; Sun, L. *ChemSusChem*, **2012**, 5, 2133-2138
73 Han, Z.; Shen, L.; Brennessel, W. W.; Holland, P. L.; Eisenberg, R. *J. Am. Chem. Soc.* **2013**, 135, 14659-14669
74 Han, Z.; Qiu, F.; Eisenberg, R.; Holland, P. L.; Krauss, T. D. *Science*, **2012**, 338, 1321
75 Panagiotopoulos, A.; Ladomenou, K.; Sun, D.; Artero, V.; and Coutsolelos, A.G. *Dalton Trans*, **2016**, 45, 6732-6738
76 Landrou, G.; Panagiotopoulos, A.; Ladomenou, K.; Coutsolelos, A.G. *JPP*, **2016**, 20, 534-541
77 Krüger, W.; Fuhrhop J.H. *Angew. Chem., Int.Ed. Engl.* **1982**, 21, 131-132
78 Arnold D.P.; Block J. *Coord. Chem. Rev.* **2004**, 248, 299-319
79 O'Regan, B. C.; López-Duarte, I.; Martínez-Díaz, M. V.; Forneli, A.; Albero, J.; Morandeira, A.; Palomares, E.; Torres, T.; Durrant, J. R. *Journal of the American Chemical Society* **2008**, *130*, 2906
80 Yu, Q.; Wang, Y.; Yi, Z.; Zu, N.; Zhang, J.; Zhang, M.; Wang, P. *ACS Nano* **2010**, *4*, 6032
81 Murray, L.J.; Lippard, S.J.; *Acc. Chem. Res.* **2007**, *40*, 466-474
82 Simmons, T.R.; Berggren, G.; Bacchi, M.; Fontecave, M.; Artero, V. *Coord. Chem. Rev.* **2014**, 270-271, 127-150
83 Guillo, P.; Daran, J.C.; Manoury, E.; Poli, R. *ChemistrySelect* **2017**, *2*, 2574-2577
84 Call, A.; Codol, Z.; Acuna-Pares, F.; Lloret-Fillol, J. Chem. Eur. J. **2014**, 20, 6171 – 6183